REFERENCE ONLY

UNIVERSITY OF LONDON THESIS

Degree Phd Year 2005 Name of Author FOGELSON, N.

Oscillations in the basal ganglia in Parkinson's disease patients and their influence on the cerebral cortex and behavioural performance

Noa Fogelson

Thesis submitted for the degree of
Doctor of Philosophy in Neurological Studies
University London

May 2005

Sobell Department of Motor Neuroscience
and Movement Disorders
Institute of Neurology
University College London
Queen Square
London WC1N 3BG

ProQuest LLC
789 East Eisenhower Parkway
P.O. Box 1346
Ann Arbor, MI 48106-1346

ABSTRACT

Oscillations in the basal ganglia in Parkinson's disease patients and their influence on the cerebral cortex and behavioural performance

Synchronised bursting of the basal ganglia, specifically at frequencies below 30 Hz, has been implicated to have a major role in the pathophysiology of Parkinson's disease (PD). The aim of this thesis is to further investigate the pathological role of low frequency activities in the subthalamic nucleus. These activities are characterised through exploration of their interactions with oscillatory cortical activities as well as with subthalamic prokinetic high frequency activities; and by determining their contribution to parkinsonian bradykinesia.

The present work shows a strong coupling between local field potential (LFP) activities recorded with macroelectrodes in the subthalamic area (SA) and cortical EEG, particularly in the alpha and upper beta bands, in the untreated parkinsonian patient. The presence of several functional sub-loops between the subthalamic area and cerebral cortical motor regions, distinguished by their frequency, cortical topography and temporal relationships, are demonstrated. In the treated parkinsonian patient, LFP activity in the 5-32 Hz band was significantly and selectively negatively correlated with that in the 65-85 Hz band. These correlations occurred around the time that peak plasma L-dopa levels would be expected, and were associated with concurrent dyskinesias. This raises the possibility that spontaneous fluctuations in the balance between low and high frequency activities may contribute to levodopa-induced dyskinesias. Finally, frequency-response curves to subthalamic deep brain stimulation in PD patients, demonstrated small local maxima and minima in kinesia

time at different frequencies over 5-30 Hz, corresponding to previously identified oscillatory activities in the basal ganglia. In addition, there was a differential effect of stimulation at the clinically effective frequency in the presence and absence of dopaminergic therapy. Thus, synchronisation of local neuronal activity in the SA may have some functional consequences that vary according to the frequency of synchronisation and are modulated according to the prevailing level of dopaminergic activity.

ACKNOWLEDGMENTS

I would especially like to thank:
First and foremost, my supervisor Prof. Peter Brown for his guidance, professional advice, encouragement and support. I am indebted to him for his time and efforts.

Andrea Kühn, Alek Pogosyan, Paul Silberstein, Lucy Strens and David Williams for their invaluable assistance and collaboration.

Peter Asselman for his assistance and support.

All the patients who participated in the studies.

GlaxoSmithKline for the financial support of this PhD.

My parents and brother for all their help and support.

I would also like to thank the following collaborators:
Marwan Hariz and Patricia Dowsey Limousin from the Sobell Department of Motor Neuroscience and Movement Disorders and Unit of Functional Neurosurgery, Institute of Neurology, London, UK.

Marina Tijssen, Gerard van Bruggen, Hans Speelman, Andries Bosch and Anne-Fleur van Rootselaar from the Department of Neurology, Academic Medical Centre, Amsterdam, Netherlands.

Andreas Kupsch and Thomas Trottenberg from the Department of Neurology, Charité Campus Virchow, Humboldt University Berlin, Berlin, Germany.

Angelo Quartarone, Angelo Insola, Paolo Mazzone and Vincenzo Di Lazzaro from the Institute of Neurological and Neurosurgical Sciences, University of Messina, Messina; the Operative Unit of Neurophysiology and the Operative Unit of Functional and Stereotactic Neurosurgery CTO "A. Alesini" Hospital, Institute of Neurology, Università Cattolica, Rome, Italy.

PUBLICATIONS

Work incorporated in this thesis:

Fogelson N, Kühn AA, Silberstein P, Dowsey Limousin P, Hariz M, Trottenberg T, Kupsch A, Brown P (2005) Frequency dependent effects of subthalamic nucleus stimulation in Parkinson's Disease. Neurosci Lett 382: 5-9.

Fogelson N, Pogosyan A, Kühn AA, Kupsch A, van Bruggen G, Speelman H, Tjissen M, Quartone A, Insola A, Mazzone P, Di Lazzaro V, Limousin P, Brown P (2005) Reciprocal interactions between oscillatory activities of different frequencies in the subthalmic region of patients with Parkinson's disease. Eur J Neurosci 22: 257-266.

Fogelson N, Williams D, Tijssen M, van Bruggen G, Speelman H, Brown P (2005) Different functional loops between cerebral cortex and the subthalamic area in Parkinson's disease. Cereb Cortex, doi:10.1093/cercor/bhi084.

Fogelson N, Kühn AA, Silberstein P, Dowsey Limousin P, Hariz M, Trottenberg T, Kupsch A, Brown P (2004) Differential effects of different frequencies of stimulation of the sub-thalamic nucleus in treated Parkinson's disease. Mov Disord 19 (Suppl 9): S298, Abstr. 864.

Additional published work during PhD programme:

Fogelson N, Loukas C, Brown J, Brown P (2004) A common N400 EEG component reflecting contextual integration irrespective of symbolic form. Clin Neurophysiol 115: 1349-1358.

Strens LHA, Fogelson N, Shanahan P, Rothwell JC, Brown P (2003) The ipsilateral human motor cortex can functionally compensate for acute contralateral motor cortex dysfunction. Curr Biol 13: 1201-1205.

Fogelson N, Loukas C, Brown J, Brown P (2003) N400 and detection of contextual anomalies regardless of representational form. Muscle Nerve Suppl 12: S77, Abstr. 218.

TABLE OF CONTENTS

Title page 1

Abstract 2

Acknowledgments 4

Publications 5

Table of contents 6

List of tables 11

List of figures 11

Abbreviations 13

Chapter 1: Introduction 15

1.1 Basal ganglia 15

1.1.1 Structure 15

1.1.2 Basal ganglia single unit activity 17

1.1.3 Synchrony inferred from local field potentials 19

1.1.4 The role of synchrony 21

1.1.5 Oscillations in the healthy basal ganglia 24

1.2 Motor Cortex 25

1.2.1 Motor areas 25

1.2.2 EEG 28

1.2.3 Mechanisms of EEG 29

1.2.4 EEG rhythms in healthy subjects 31

1.3 Interactions between the basal ganglia and motor cortex 35

1.3.1 Projections between basal ganglia and motor cortex 35

1.3.2 Indirect and direct pathways 36

1.3.3 Neurotransmitters 38

1.4 Parkinson's disease 39

1.4.1 Etiology and symptoms 39

1.4.2 PD and the basal ganglia circuitry model 41

1.4.3 Therapy 43

1.4.3.1 Medication 43

1.4.3.2 Deep Brain Stimulation 44

1.4.3.2.1 Mechanisms of DBS 46

1.5 Pathophysiological neurophysiology in PD 47
1.5.1 Problems with the basal ganglia circuitry model 47
1.5.2 Basal ganglia oscillations in the parkinsonian state 48
1.5.2.1 Animal models of PD 48
1.5.2.2 PD patients 50
1.5.3 EEG in PD 52
1.5.4 Basal ganglia – cortical coherence in PD 54
1.6 Objectives of the thesis 55

Chapter 2: Methods **56**
2.1 Subjects 56
2.1.1 Patients 56
2.1.2 Surgery 59
2.1.3 Confirmation of macroelectrode localization 62
2.2 Recordings 65
2.2.1 Sampling and filtering 65
2.2.2 EEG 66
2.2.3 LFPs 68
2.2.4 Montage 69
2.2.5 Artifacts 71
2.3 Analysis 72
2.3.1 Fast Fourier Transformation 72
2.3.2 Coherence 74
2.3.3 Partial coherence 75
2.3.4 Phase 76
2.3.5 Polarity reversal 77
2.3.6 Temporal correlations 78
2.3.7 Control charts 79
2.4 Clinical assessment 79
2.4.1 UPDRS 79
2.4.2 BRAIN TEST 80
2.5 Statistical analysis 81
2.5.1 Normal distribution 81
2.5.2 Z-score 81

2.5.3 Standard errors and confidence intervals 82
2.5.4 T-tests 82
2.5.5 ANOVA and Friedman's test 83
2.5.6 Fisher's exact test 84
2.5.7 Correlations 85

Chapter 3: Different functional loops between cerebral cortex and the subthalamic area in Parkinson's disease **86**
3.1 Introduction 86
3.2 Methods 87
3.2.1 Patients and surgery 87
3.2.2 Recordings 89
3.2.3 Analysis 90
3.2.3.1 Coherence 90
3.2.3.2 Partial coherence 92
3.2.3.3 Phase 94
3.2.3.4 Polarity reversal 94
3.3 Results 94
3.3.1 Spectral analysis 94
3.3.2 Differential topography of coherence in the STN area 97
3.3.3 Differential topography of coherence at the cortex 98
3.3.4 Partial coherence 103
3.3.5 Phase 108
3.3.6 Polarity reversal 110
3.4 Discussion 110
3.4.1 Experimental limitations 111
3.4.2 Is coherence between the subthalamic LFP and EEG in PD pathological or physiological? 113
3.4.3 Quantitative differences between subcortico-cortical coupling over different frequency ranges 114
3.4.4 Topography of subcortico-cortical coupling 116
3.4.5 Phase relationships between SA LFPs and cortical EEG 117
3.4.6 Multiple functionally distinct oscillatory subcortico-cortical loops 118
3.5 Summary of key points 120

Chapter 4: Reciprocal interactions between oscillatory activities of different frequencies in the subthalamic region of patients with Parkinson's disease 121

4.1 Introduction 121

4.2 Methods 122

4.2.1 Patients and surgery 122

4.2.2 Recordings 126

4.2.3 Analysis 126

4.3 Results 131

4.3.1 Average correlations 131

4.3.2 Individual correlations 134

4.3.3 Timing of negative correlations and their phenomenological associations 135

4.3.4 Negative correlations reflect changes over short-time periods 138

4.3.5 Focality of the 65-85 Hz spectral peak 139

4.4 Discussion 144

4.4.1 Experimental limitations 144

4.4.2 Relationship between dynamic oscillatory patterns and clinical state 146

4.4.3 Two reciprocal patterns of oscillatory synchronisation in the subthalamic area 147

4.5 Summary of key points 149

Chapter 5: Frequency dependent effects of stimulation in the region of the subthalamic nucleus in Parkinson's disease 150

5.1 Introduction 150

5.2 Methods 151

5.2.1 Patients and surgery 151

5.2.2 Protocol 152

5.2.3 Statistical analysis 155

5.3 Results 157

5.4 Discussion 163

5.4.1 Experimental limitations 163

5.4.2 Non-linearities in the response to SA stimulation at frequencies $\leq$ 30 Hz 167

5.4.3 Differences in the frequency-response curve off and on medication 168
5.5 Summary of key points 170

Chapter 6: Discussion **171**
6.1 Summary of results 171
6.1.1 Chapter 3 171
6.1.2 Chapter 4 172
6.1.3 Chapter 5 172
6.2 General experimental limitations 173
6.3 Low frequency activity at 4-32 Hz 174
6.4 Low frequency activity below 30 Hz – not a homogeneous band 174
6.5 High frequency activity at 65-85 Hz 176
6.6 Pathological or physiological exaggeration? 176
6.7 Pathological significance in PD 178
6.8 Circuit loops in the subthalamic area 180
6.9 Future directions 182

References **183**

LIST OF TABLES

Table 2.1 Patients participating in the studies 58

Table 3.1 Clinical details 88

Table 4.1 Clinical details 123

Table 5.1 Stimulation parameters at the time of evaluation 156

LIST OF FIGURES

Figure 1.1 Basal ganglia nuclei 16

Figure 1.2 Motor areas of the cerebral cortex 27

Figure 1.3 Motor circuit of the basal ganglia 36

Figure 1.4 Connections within the basal ganglia circuitry model 39

Figure 2.1 Localization of the macroelectrode 61

Figure 2.2 Post-operative MRI 62

Figure 2.3 The subthalamic nucleus and neighbouring structures 64

Figure 2.4 The standard placement of EEG recording electrodes 67

Figure 3.1 Raw signals and coherence peaks 96

Figure 3.2 Distribution of maximal coherence 97

Figure 3.3 Topography of coherence 100

Figure 3.4 Comparison of partial and standard mean transformed coherences 106

Figure 3.5 Topography of partial coherence 107

Figure 3.6 The distribution of phase across the four frequencies 109

Figure 4.1 LFP recorded from the right subthalamic area in case 9 130

Figure 4.2 Matrix of average negative and positive temporal correlation scores between spectral components of the LFP across 21 sides 133

Figure 4.3 Timing of peak dyskinesias with respect to significant correlations 137

Figure 4.4 Temporal evolution of spectral correlations for the frequencies of maximum negative correlation 139

Figure 4.5 Microelectrode LFP gamma activity is localized to STN 143

Figure 5.1 Timeline of experimental protocol 154

Figure 5.2 The effect of subthalamic area stimulation frequency on mean kinesia time after overnight withdrawal and after administration of antiparkinsonian medication 160

Figure 5.3 The effect of subthalamic area stimulation frequency on the percentage change in mean kinesia time normalised to unstimulated performance 161

Figure 5.4 Individual frequency response curves 162

ABBREVIATIONS

AC-PC	anterior commissure-posterior commissure
AL	ansa lenticularis
ANOVA	analysis of variance
CL	confidence limit
CP	cerebral peduncle
CT	computed topography
DBS	deep brain stimulation
EEG	electroencephalography
EMG	electromyography
EPSP	excitatory post-synaptic potential
ERD	event-related desynchronisation
ERS	event-related synchronisation
FF	Fields of Forel
FFT	Fast Fourier Transformation
FIR	finite impulse response
GABA	gamma-amino butyric acid
GP	globus pallidus
GPe	globus pallidus externa
GPi	globus pallidus interna
H1	H1 Field of Forel
HFS	high frequency stimulation
IC	internal capsule
IPSP	inhibitory post-synaptic potential
KT	kinesia time

L-DOPA	levodopa
LF	lenticular fasciculus
LFP	local field potential
M1	primary motor cortex
MII	premotor cortex
ME	macroelectrode
MPTP	1-methyl-4-phenyl-1,2,3,6-tetrahydropyridine
MRI	magnetic resonance imaging
6-OHDA	6-hydroxydopamine
PD	Parkinson's disease
PMC	premotor cortex
PPN	pedunclopontine nucleus
Put	putamen
S1	somatosensory cortex
SA	subthalamic area
SEM	standard error of mean
SMA	supplementary motor area
SN	substantia nigra
SNc	substantia nigra pars compacta
SNr	substantia nigra pars reticulate
STN	subthalamic nucleus
Thal	thalamus
UPDRS	Unified Parkinson's Disease Rating Scale
ZI	zona incerta

CHAPTER 1: Introduction

The basal ganglia have a major functional role in voluntary movement. As such, they are extensively linked with the motor areas of the cerebral cortex. One of the main methodologies of studying the function of the human brain is through the recording of its electrical activity, which is characterised by oscillatory rhythms. In the first part of the introduction, the structures and rhythmic activities of the basal ganglia and its cortical projection sites, will be described.

Impaired function of the basal ganglia is the hallmark of Parkinson's disease – a common neurological disease. Accumulating evidence of over a decade has implicated synchronised bursting of the basal ganglia as having a major role in the pathophysiology of Parkinson's disease. In the second part of the introduction, this evidence will be reviewed and put into context of the thesis.

1.1 Basal ganglia

1.1.1 Structure

The basal ganglia consist of five nuclei situated bilaterally in the white matter of the cerebral hemispheres. The nuclei are the caudate nucleus, putamen (together commonly referred to as the striatum), subthalamic nucleus, substantia nigra and the globus pallidus (Figure 1.1). The caudate nucleus and putamen are divided by the internal capsule, which is a mass of fibres connecting the neocortex and the thalamus. There is a further division of the globus pallidus (GP) into external (GPe) and internal (GPi) segments, at least in primates. The substantia nigra (SN), situated in the midbrain, is also divided into two zones – pars compacta (SNc) and pars reticulata

(SNr). The SNr is situated ventrally and consists of neurons similar to those in the globus pallidus. The subthalamic nucleus (STN) is situated between the thalamus and the midbrain and is connected anatomically with GP and SN. A separate nucleus, called the nucleus accumbens, is situated adjacent to the ventral striatum and is related to limbic structures. Activity of neuronal cells within the GP and STN of awake monkeys is related to limb movement (DeLong et al., 1985).

The basal ganglia link the thalamus and cerebral cortex through several parallel circuits. These functionally and anatomically segregated circuits are characterised by function, cortical origin and target, and include the motor, limbic, prefrontal and oculomotor loops (Alexander and Crutcher, 1990). This thesis will focus on the motor aspects of the basal ganglia function. The motor basal ganglia circuitry will be discussed in section 1.3.

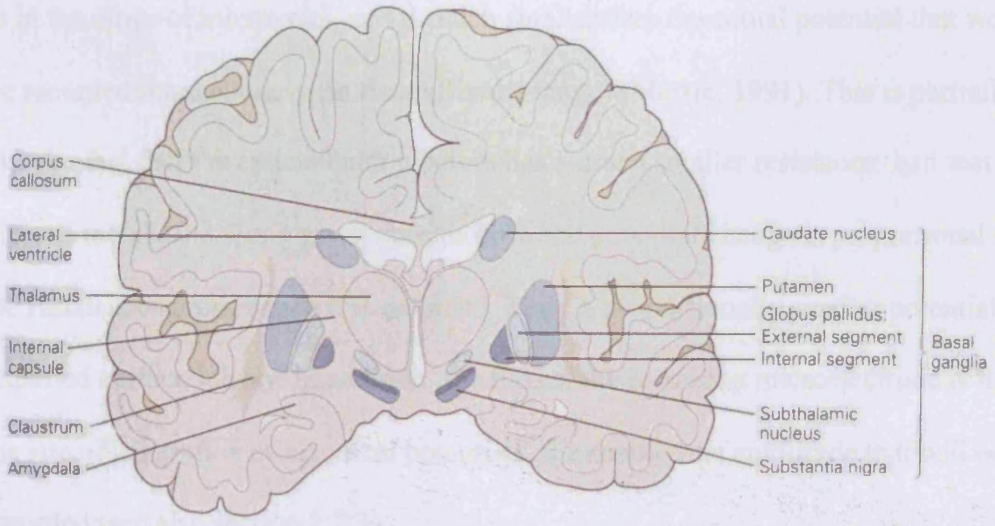

Figure 1.1 Basal ganglia nuclei (DeLong, 2000, p.855).

1.1.2 Basal ganglia single unit activity

Depth recordings from the basal ganglia are, broadly speaking, of two types – single unit and local field potential (LFP) recordings (see section 1.1.3). In this section I will discuss how synchronisation is determined from recordings of single neurons. Microelectrode recordings measure the electrical activity of neurons. Specifically, it is the recording of extracellular potentials, resulting from action potentials generated by a single neuron (Hutchison et al., 2003). Action potentials occur when the neuronal membrane potential reaches a certain threshold of depolarization (Spehlaman, 1981a), as a result of the summation of excitatory postsynaptic potentials (see section 1.2.3). The membrane then becomes freely permeable to sodium and potassium ions, which results in a brief reversal of the membrane potential. This potential change constitutes the action potential.

It is important to stress, that the extracellular potential, recorded by the microelectrode is in the range of microvolts, and is much smaller than the actual potential that would be recorded intracellularly (in the millivolts range) (Martin, 1991). This is partially due the fact that the extracellular medium has a much smaller resistance than that of the cell membrane. For a given current flow, the potential change is proportional to the resistance across which it is recorded. Thus, a proportionally smaller potential is recorded extracellularly. In addition, the further the recording microelectrode is from the site of generation of electrical potentials, the smaller the amplitude that will be recorded (see also section 1.2.3).

Single unit recordings provide a means of characterising neuronal activity by measuring their spike discharge rate (Hutchison et al., 2003; Abeles and Gerstein, 1988). When the discharge activity of a pair of neurons is recorded simultaneously it is also possible to determine the degree of synchrony or coupling between them, using cross-correlograms (Abeles and Gerstein, 1988; Bergman, 1998).

Cross-correlations describe the temporal relation between two signals. Cross-correlograms determine how the spikes of one neuron are distributed in time with respect to the spikes of another neuron. When the activity of the two neurons is correlated (i.e they fire in synchrony), a peak at zero time is observed in the cross-correlation function. On the other hand, a flat cross-correlogram, indicates that the pair of neurons do not interact with one another. A symmetrical peak or a periodic cross-correlogram, may indicate that the two neurons receive a common input (Knox, 1981; Bergman, 1998), while a trough can indicate reciprocal inputs or mutual inhibition between the two neurons (Knox, 1981). The auto-correlogram function of a single neuron can also indicate oscillatory activity, characterized by repetitive, equally spaced peaks. In general, correlation between a cell pair may indicate direct interactions between the cells, or a common input (Knox, 1981; Bergman, 1998; Singer, 1993).

There are a few disadvantages to single unit recordings. First, recordings are of a limited number of neurons, so that significant patterns may not be observed (Abeles and Gerstein, 1988). Second, if recordings are not performed over long periods, brief significant neuronal discharges may not be detected. On the other hand, long periods of recording may be non-stationary, so that neuronal activities, including frequency of

oscillation change over time. This also means that absence of a recorded oscillatory activity does not necessarily mean that there is no synchrony. The higher the frequency oscillation that is being recorded, the worse the sampling problems become (Buzsáki and Draguhn, 2004; Singer, 1993). Recording the activity of a large population of neurons gets round the sampling, and this is achieved by the simultaneous recordings of large arrays of units, or through local field potential recordings, as discussed in the next section.

1.1.3 Synchrony inferred from local field potentials

LFPs record the activity of a population of neurons, and therefore show plenty of oscillations as opposed to recordings of unit pairs. In this thesis the major interest is in the oscillatory nature of the basal ganglia and particularly in the STN as a system, and thus LFP recordings are more appropriate. The argument here is that LFPs are a surrogate marker of the activity of the local neuronal population. LFPs are essentially the summation of excitatory and inhibitory post-synaptic potentials (for further details see section 1.2.3) at the membranes of the local neuron population near to the recording electrode. The synchronised activity of these neurons result in extracellular currents and these are reflected by LFP fluctutions. LFPs would be very small or absent if the local neural activity was random. So LFPs have been defined as "the envelope of the probability of non-random coherence in the (local) neural ensembles " (John, 2002, p.4). Amplitude fluctuations, large enough to record through macroelectrodes, are an indication of synchronised rhythmic activity of a large number of neurons (Singer, 1993).

The neuronal laminar arrangement is also critical in determining the amplitude of the signal that is picked up by the recording electrode. As will be discussed in greater detail in section 1.2.3, an organised parallel laminar arrangement, as seen in the cortex, facilitates the summation of postsynaptic potentials, and as a result the generated signal is recorded with less attenuation (Martin, 1991). Considering the disorganised neuronal arrangement of the basal ganglia, it is surprising that a LFP is generated at all. In fact, the amplitude of basal ganglia LFPs are a third of those recorded from the cortex. However, the fact that we can record LFPs from the basal ganglia suggests that its neuronal structure is relatively 'open field' (see section 1.2.3), as supported by morphological studies from the STN and GP (Chang et al., 1983; Yelnik et al., 1984). So, oscillatory activity depends not only on the pacemaker properties of single neurons but also on the properties of the network architecture.

Further evidence that LFPs are a reflection of the local neuronal activity has been demonstrated in the following studies. *In vivo* recordings from rat nucleus accumbens have demonstrated that changes in LFP activity are due to synchronous membrane potential fluctuations (Goto and O'Donnell, 2001), while recordings from the rat subthalamic nucleus (STN) demonstrate a close correspondence between LFP activity and synchronized neuronal activity following cortical stimulation (Magill et al., 2004a). Furthermore, Berke et al. (2004) demonstrated LFPs from the rat striatum to "reflect local cellular and/or synaptic activity rather than volume-conduction from the overlying cortex". Spontaneous LFP oscillations are also synchronized with neuronal activity in the striatum of healthy or parkinsonian primates (Courtemanche et al., 2003) and in the STN of anesthetized rats (Magill et al., 2004b) and alert parkinsonian patients (Levy et al., 2002b). A close relationship between neuronal activity and basal

ganglia LFPs is also implied by the coherence with non-zero phase differences observed between different basal ganglia sites (Brown et al., 2001) and between these and cortical EEG (Marsden et al., 2001; Williams et al., 2002), as discussed in section 1.5.4.

1.1.4 The role of synchrony

It is widely accepted that synchrony has a functional role in the brain, and indeed oscillatory, synchronous activities are ubiquitous throughout the brain (Steriade et al., 1990). Broadly speaking low frequency activity below 8 Hz characterises different stages of sleep, whereas activities of higher frequencies (8-~100 Hz), characterise states of wakefulness and arousal. These different rhythmic activities will be discussed in greater detail in section 1.2.4. In general, oscillations of low frequencies synchronise activity of neurons in larger cortical areas, whereas those of higher frequencies are more focal and regionally restricted (Buzsáki and Draguhn, 2004; see also section 1.2.4).

Synchrony has been implicated to have a significant functional role in signal transmission and synaptic plasticity (Singer, 1993). In addition, neural synchrony at a high frequency range referred to as gamma (above 32 Hz), is considered to have a fundamental role in perceptual integration and categorization, memory, consciousness and learning (Singer, 1993; Malsburg, 1995; Engel et al., 2001; John, 2002; Miltner et al., 1999). These functions depend on the distribution of areas in the brain and also on a large amount of neurons (Singer, 1993). The temporal binding model was proposed as a possible mechanism for the integration of cortical processing (Singer, 1993;

Malsburg, 1995; Engel et al., 2001; John, 2002). This model is based on the temporal properties of neurons, so that neurons responding to the same stimulus are recruited through synchrony, thus enabling distant brain regions to be activated simultaneously (Singer, 1993; Malsburg, 1995). Thus, a representation of a stimulus consists of spatially distributed populations of simultaneously active neurons. In this way a single neuron can have many different representations, so that it is recruited at different times, in conjunction with different populations of co-active neurons, depending on the stimulus representation (Singer, 1993). This begs the question of how this neuron is 'labelled' as being recruited to the same assembly of co-active neuronal populations, for a particular response. The proposed mechanism was termed the temporal code, whereby neurons joining into a particular assembly must synchronise discharges on a millisecond time scale (Malsburg, 1995; Singer, 1993). This means that even if the activity of neurons overlap on a broad time scale, as long as their activity is correlated on a millisecond time scale with that of neurons of a particular assembly, they will be labelled as belonging to that assembly.

In relation to the binding theory, high frequency activity (gamma) is fast enough, in comparison to activities of lower frequency, to allow for an effective temporal code in the synchronisation of neural assemblies rapidly, over long enough distances (Singer, 1993). In this case, the temporal and spatial demands determine the lower and upper limits of the frequency range, respectively, with gamma frequency range being the best compromise. This is in line with the suggested function of gamma activity in information processing as stated in the beginning of this section.

However, recently the binding model has also been extended to lower frequencies, specifically in the beta range (see section 1.2.4). Scalp recordings in humans (Gerloff et al., 1998; Classen et al., 1998; Mima et al., 2000a), involving motor and visuomotor tasks, have demonstrated significant increases in interhemispheric coupling between primary and premotor areas (see section 1.2.1) in relation to movement. This suggests that lower frequencies may be important in the functional coupling of activities in large neuronal networks, and that this coupling may have a role in the integration of sensorimotor information.

Oscillations are also crucial for synchrony to exist (Singer, 1993), for two main reasons. First, the nature of oscillatory activity is such that it is repetitive and thus relatively predictable, which is necessary for synchrony. Second, synchronisation can be achieved through mediating oscillators (König and Schillen, 1991), which is essential when synchronizing the activity of distant areas. Having said that, synchrony can also result in oscillations. In any case, whether oscillations precede synchrony or vice versa, it is fair to say that oscillatory activity is an indicator of synchrony (Singer, 1993).

Bursting neurons can have oscillatory patterns even if isolated (Singer, 1993). These neurons have a firing pattern of alternating periods (on a multi-time scale) of fast repetitive spiking, or bursts, followed by a rest state. This synchronous repetitive bursting can facilitate temporal synchronisation of activity between local groups of neurons. In turn, the synchronised activity of the local population of neurons give rise to fluctuations of local field potentials, and thus of oscillatory activity of this population. On a larger scale of the neuronal network, when two spatially distant

assemblies of neurons are synchronised, and there is a correlation between two oscillatory signals – then it is appropriate to use the term coherence, as will be further discussed in section 1.5.4.

1.1.5 Oscillations in the healthy basal ganglia

Now that the different methods of subcortical recordings have been discussed (section 1.1.2 and 1.1.3), together with the potential significance of synchrony (section 1.1.4), I would like to review the evidence, albeit from animals (see section 1.5.2.1), of oscillatory activity in the healthy basal ganglia. Recordings from the basal ganglia of intact animals have shown uncorrelated activity of neurons in the striatum and GP of healthy alert primates (Raz et al., 2000, 2001; Bergman et al., 1998). There was also little or no oscillation in the GP and STN of healthy primates (Wichmann et al., 1994a; Nini et al., 1995; Raz et al., 2000). On the other hand, Courtemanche et al. (2003) have shown contradictory results of prominent 10-25 Hz oscillations, albeit in the caudate and putamen (i.e more anterior part of the basal ganglia) in awake primates, both at rest and during a visual task. However, in general the evidence suggests that the STN and GP do not exhibit prominent synchronisation between 1-30 Hz, in the awake state. As will be discussed later (section 1.5.2), this in contrast with the oscillatory activity observed in the parkinsonian state. The largely independent activity of GP neurons in the intact primates has been thought to be critical in the processing and extraction of cortical information (Bergman et al., 1998).

Recently, significant gamma power (46-70 Hz) was recorded from the STN of the intact rat (Brown et al., 2002a). It was suggested that this activity may be necessary

for voluntary movement, as it was increased during motor activity (Brown et al., 2002a). This activity may be similar in nature to the gamma activity associated with perceptual binding, as was discussed in section 1.1.4.

In addition, multi-second fluctuations (<0.5 Hz) have been noted in neuronal discharge rate from the GP, substantia nigra pars reticulata and STN, in the awake rodent (Ruskin et al., 1999; Allers et al., 2000; Ruskin et al., 2003). These slow fluctuations in discharge are highly correlated across units and basal ganglia nuclei (Ruskin et al., 2003) and are modulated by dopamine (Ruskin et al., 1999; Allers et al., 2000; Ruskin et al., 2003). There is a suggestion that the modulation of this activity may be involved in motor processing (Ruskin et al., 1999).

1.2 Motor cortex

There are several circuits associated with the basal ganglia, defined by the cortical area from which they originate (DeLong, 2000). These functionally and anatomically segregated circuits are the skeleto-motor, the oculomotor, the prefrontal and the limbic. Since the skeleto-motor circuit is most relevant in this thesis, I will focus on the motor areas of the cortex.

1.2.1 Motor areas

The cerebral cortex consists of two main motor areas (Greenstein B, and Greenstein A, 2000). The first is the primary motor cortex (M1). The second is the premotor area, which consists of the premotor cortex (MII) and the supplementary motor area (SMA).

The primary motor cortex receives direct projections from the premotor areas, the somatosensory cortex, and posterior parietal areas, as well as indirect projections from subcortical structures such as the basal ganglia and cerebellum. By integrating the information from these inputs, a descending signal for muscular activation is generated (Alexander and DeLong, 1992). The motor cortex also sends projections to the premotor cortex, SMA, somatosensory cortex as well as to subcortical structures such as the thalamus and basal ganglia.

The M1 is involved in motor control, especially related to dextrous movements, and is activated in the contralateral hemisphere during simple movements, such as the flexion and extension of the index finger (Roland et al., 1980; Gazzaniga et al., 1998).

The MII is involved in the motor control of proximal limbs and in the initial phases of motor preparation, specifically orientation towards a target (Moll and Kuypers, 1977; Alexander and DeLong, 1992). The premotor cortex receives inputs from the parietal cortex and the cerebellum, both of which are involved in visuomotor functions (Gazzaniga et al., 1998). This is in line with the hypothesis that the premotor cortex is involved in externally guided movements that rely on visual and somatosensory feedback.

The SMA is involved in complex motor functions and is activated bilaterally during the performance and imagination of complicated sequential finger movements (Roland et al., 1980). There is also evidence to suggest that it is involved in inter-limb co-ordination (Verheul and Geuze, 2004). The SMA is linked to internally guided movements (Jenkins et al., 2000).

The posterior parietal areas are involved in the integration of relevant sensory modalities, and thus have an important role in motor planning and movement coordination (Krakauer and Ghez, 2000; Gazzaniga et al., 1998).

The premotor areas also receive inputs from the prefrontal cortex. This is important in the integration of information stored in working memory that is required for motor planning, such as spatial orientation in space (Krakauer and Ghez, 2000).

The motor areas of the cerebral cortex are illustrated in Figure 1.2.

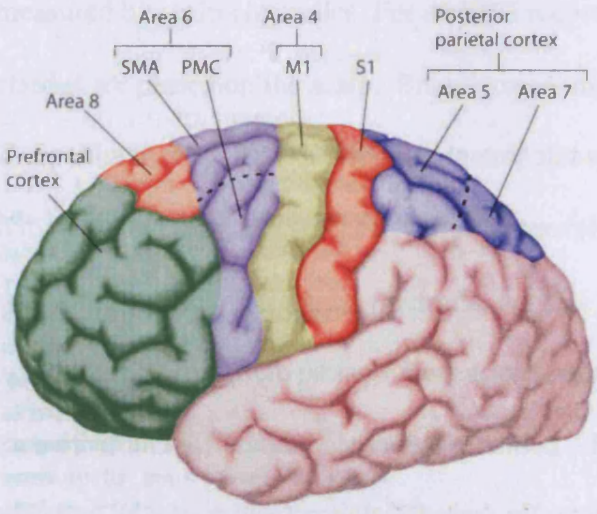

Figure 1.2 Motor areas of the cerebral cortex. M1 = primary motor cortex; SMA = supplementary motor area; PMC = premotor cortex; S1 = somatosensory cortex. (Gazzaniga, 1998, p.377).

1.2.2 EEG

Electroencephalography (EEG) is a one of the most efficient, non-invasive methods to record the electrical activity of the brain. It provides an attenuated measure of the overall electrical activity of the brain over a period of time. The principal source of EEG is the summated synaptic activity in the pyramidal cells – the major projection neurons in the cortex (Spehlman, 1981a). The net extracellular current flow as a result of this activity is picked up by the surface EEG electrode.

Populations of neurons that are active together generate electrical potentials that can be measured by scalp electrodes. For an EEG recording a set of standard locations of electrodes are placed on the scalp. Broadly speaking, two main arrangements can be used (Spehlman, 1981b). The first is a monopolar arrangement where the electrical activity recorded from electrodes at each site are relative to an electrode placed at a non-active distant site (reference electrode) such as the ear lobe. The second is a bipolar arrangement where pairs of electrodes at nearby recording sites are connected to each other and differential activity is recorded. Bipolar recording allows for better localization of activities/potentials, whereas referential recordings gives an "undistorted display" of potentials (Spehlman, 1981b) and are thus better suited for cortical wide spread activities. This will be discussed in more detail in section 2.2.4.

1.2.3 Mechanisms of EEG

Scalp electrodes record the summation of electrical potential changes of pyramidal cortical neurons (Spehlman, 1981a). These potential changes consist of excitatory and inhibitory post-synaptic potentials.

An excitatory post-synaptic potential (EPSP) is the result of the activation of an excitatory dendritic synapse. This increases the membrane permeability to ions in a non-selective manner, resulting in a transient current flow and depolarization of the cell membrane.

An inhibitory post-synaptic potential (IPSP) is the result of the activation of an inhibitory synapse on the cell body. This increases the membrane permeability to potassium (out of the cell) and chloride ions (into the cell), resulting in hyperpolarization and a decrease of current flow along the cell membrane.

The potential field that is generated as a result of an EPSP or IPSP can be modelled as an electrical dipole (Lopes da Silva and van Rotterdam 2005). An electrical dipole is a conductor with one positive and one negative end. When an electrical current is generated, a 'sink' is defined as the site of current inflow, whereas, the 'source' is the site of outward current flow. For example, an excitatory input received by a cortical pyramidal cell, resulting in an EPSP, will cause a current 'sink' (negative pole) at the dendrites, and a current 'source' (positive pole) near the soma. Thus, an EPSP or IPSP generated at the synapse of a pyramidal cell is essentially a dipole, and the summated potential fields of a population of pyramidal cells can be modelled as dipole layers

(Lopes da Silva and van Rotterdam 2005). The potential field that simple dipole layers produce is termed 'open field' (Lorento de No, 1947), where the arrangements of the sources and sinks allows for the spread of current, so that a potential difference is produced. This is in contrast to a 'closed field', which is radial in shape, so that the points along the circumference remain at zero potential (Niedermeyer, 2005).

In addition, there is direct evidence of a close relationship between scalp EEG and post-synaptic potentials of cortical cells, so that surface negativity is associated with EPSPs, while surface positivity with IPSPs (Creutzfeldt et al., 1966).

EPSPs and IPSPs are the major source of EEG signals due to their spatial and temporal properties. In comparison to the action potential, which does not contribute to recorded scalp EEG, these post-synaptic potentials are conducted over large areas of the cell membrane, and overlap temporally since they last longer (Lopes da Silva and van Rotterdam 2005).

Pyramidal neurons extend through nearly all the layers of the cortex (Spehlman, 1981a, Lopes da Silva and van Rotterdam 2005). These cells are the major contribution to the recorded EEG, in comparison to non-pyramidal cells, due to their dense parallel arrangement, with dendrites orientated perpendicularly to the surface of the cortex (Martin, 1991). This facilitates the summation of the flow of current in the extra-cellular space, and the resulting potential is recorded more efficiently since the 'sources' and 'sinks' are perpendicular to the scalp electrode. A fraction of the current produced by synaptic activity extends through the skull, resulting in different

potential levels at different areas of the scalp. The EEG signal is the recording of the difference between potential levels at two scalp electrodes.

The amplitude of surface EEG is in the order of microvolts, thousand times smaller than that of a single neuron, and the EEG signal is mainly from the activity of neurons in the proximity of the recording electrode. This is because the amplitude of a signal decreases by the square root of the distance from the site of generation (Martin, 1991; Lopes da Silva and van Rotterdam 2005). Therefore, surface EEG cannot record the activity of deep structures within the cortex such as the hippocampus, nor subcortical structures such as the thalamus, basal ganglia or the brain stem.

1.2.4 EEG rhythms in healthy subjects

Surface EEG patterns are characterised by their frequency and amplitude, which in the normal human EEG range from 1-100 Hz and 1-100 μV, respectively (Niedermeyer, 2005). There are five main activities that correlate with different stages of wakefulness. These oscillatory activities generally follow the rule of decreasing amplitude with increasing frequency of oscillation.

Delta (0.5-4 Hz) and theta (4-7 Hz) appear during early stages of sleep and drowsiness. The appearance of these low frequency, high amplitude activities during wakefulness is a sign of brain dysfunction. Delta activity is generated through pyramidal neurons and the thalamus (Steriade et al., 1993) and is suppressed upon arousal through the cholinergic input of cortical forebrain projections (Buzsaki et al., 1988). Theta waves are associated with the hippocampal formation in animals and

may facilitate in memory consolidation through long-term potentiation (Steriade et al., 1990).

Alpha activity (8-13 Hz) is characterised by moderate amplitude and appears over parietal and occipital sites during relaxed wakefulness. It is generated through the interaction of thalamocortical and cortico-cortical systems (Steriade et al., 1990; Lopes da Silva, 1991). Mu rhythm is characterised by the same frequency and amplitude as alpha activity, however, with very different topography. It is located centrally, can be recorded from electrodes C3 and C4 (see section 2.2.2), and is blocked by movement (Niedermeyer, 2005).

Beta activity (14-32 Hz) is characterised by low amplitude and appears over frontal areas and at times over central regions. This range can be further subdivided into lower (14-20) and upper beta bands (21-32 Hz). Lower beta activity (around 15 Hz) is most evident over the sensorimotor corticies and upper beta activity predominates over the mesial cortical regions, including the supplementary motor area (Pfurtscheller et al., 1997; 2003). Beta activity is associated with arousal, focused attention and intense mental activity (Steriade, 2005) and is thought to be generated through the interaction of cortico-cortical and thalamocortical loops (Llinás and Ribary, 1993; John, 2002).

Cortical gamma activity (above 32 Hz) is generally considered to be an induced activity in response to sensory stimuli (Singer, 1993). In the human, gamma activity has been recorded from the motor (Mima et al., 2000b), visual (Tallon-Baudry and Bertrand, 1999), and auditory cortex (Pantev et al., 1991). Gamma activity is

generally accepted to have a role in sensory perception in most modalities and is associated with attention (Herrman et al., 2004). In relation to the motor system it is thought to play a role in the temporal coding (see section 1.1.4) of the motor control system, facilitating cortico-muscular synchronisation (Mima et al., 2000b; Brown et al., 1998). In addition, gamma activity is considered to be a correlate of cognition, as it is observed both in the awake and dream state in humans (Llinás and Ribary, 1993).

Cortical neurons play a major role in the generation of fast rhythms above 20 Hz (Steriade, 2005). However, thalamocortical circuits and other subcortical structures including the basal ganglia, also generate fast rhythm oscillations, at the population level, as discussed in section 1.1.5.

As already mentioned in section 1.1.4, oscillations of low frequencies (e.g alpha) synchronise activity of neurons in larger cortical areas or distributed over different parts of the brain, whereas those of higher frequencies (e.g beta and gamma) are more focal and regionally restricted (Pfurtscheller and Lopes da Silva, 1999; Neuper and Pfurtscheller, 2001a; Buzsáki and Draguhn, 2004).

Oscillations in the alpha and beta frequency bands can display either an event-related blocking response or an event-related amplitude enhancement in humans. Event-related desynchronisation (ERD) is an event-related amplitude attenuation, associated with cortical areas involved in task-relevant processing and a state of maximal alertness and appears only during consciousness. Event-related synchronisation (ERS) on the other hand is an event-related amplitude enhancement, associated with cortical areas at rest or an 'idling' state (i.e not involved in sensory processing or motor preparation). Although, it has also been argued that ERS is a marker of

reduced cortical work or behavioural stillness rather than cortical inactivation (Mulholland, 1995). ERS appears both during consciousness and unconsciousness (Pfurtscheller, 1992).

There is evidence to suggest that ERD of lower alpha rhythm (8-10 Hz) is widespread and a functional correlate of attentional processes, while ERD of activity in the upper alpha (10-12 Hz) and lower beta range is spatially restricted and task-specific (Pfurtscheller, 1992; Klimesch et al., 1998; Neuper and Pfurtsceller, 2001a). In relation to the motor system, ERD of upper alpha and lower beta is detected 2 seconds prior to voluntary movement over the sensorimotor area, contralateral to the moving side, and bilaterally immediately before execution (Pfurtscheller, 1989). Within 1 second post-movement a beta ERS appears over the corresponding sensorimotor area (Neuper and Pfurtsceller, 2001b), and may be an indication of the recovery of the primary motor cortex after the movement (Pfurtscheller et al., 1998; Pfurtscheller and Lopes da Silva, 1999). In addition, there is a pattern of antagonistic ERD/ERS pattern over the relevant active motor area and over unactivated surrounding areas, respectively (Neuper and Pfurtsceller, 2001a; Pfurtscheller and Lopes da Silva, 1999). Together this evidence has led to the understanding of the ERD as a correlate of activated underlying cortical areas involved in processing of relevant information and motor behaviour, and the ERS as a correlate of deactivated coherent cortical neurons, thus unable to process information (Pfurtscheller and Lopes da Silva, 1999; Neuper and Pfurtsceller, 2001a). The hypothesis is that the activated state is reached through 'active' thalamo-cortical projections, which allow cortical areas to be ready for processing, while a thalamo-cortical disengagement, deactivates cortical networks that are not engaged in the task, at the same time (Neuper and Pfurtsceller, 2001a).

In addition, there is also evidence of ERS of low gamma (40 Hz) cortical activity before and during movement in humans with a prerequisite of alpha ERD (Salenius et al., 1996; Pfurtscheller and Lopes da Silva, 1999). This ERS may be an indication of active information processing and motor preparation (Singer, 1993; see section 1.1.4).

However, ERD and ERS are not phenomena that are exclusive to the cortex. Beta ERD and ERS have also been observed in the 'healthy' putamen, in relation to movement (Sochurkova and Rektor, 2003), so that there may be a parallel activation of both cortical and subcortical structures with movement.

1.3 Interactions between the basal ganglia and motor cortex

1.3.1 Projections between basal ganglia and motor cortex

The basal ganglia and the cerebral motor cortex are inter-connected extensively (Alexander and Crutcher, 1990; Figure 1.3). The motor circuit of the basal ganglia is illustrated in figure 1.3. The basal ganglia receive somatotopically- arranged information through inputs from the areas of the cerebral cortex that are involved in motor control i.e. SMA, MII, M1, somatosensory cortex, and superior parietal lobule (Côté and Crutcher, 1991; Alexander and DeLong, 1992). In addition it receives dopaminergic inputs from the midbrain. In turn the basal ganglia project back to the SMA and premotor cortex via the thalamus, specifically the ventral lateral and centromedian nuclei. The basal ganglia also have an output to the brain stem, specifically the pedunclopontine nuclei (PPN). The cerebral cortex projects mainly to the ipsilateral basal ganglia, which ultimately influence the contralateral side of the

body. The striatum receives most of the inputs from the cortex, thalamus and brain stem, whereas the globus pallidus and the substantia nigra are the origin of the major output projections from the basal ganglia. Specifically, the motor areas project to the central and caudal putamen (Alexander and Crutcher, 1990).

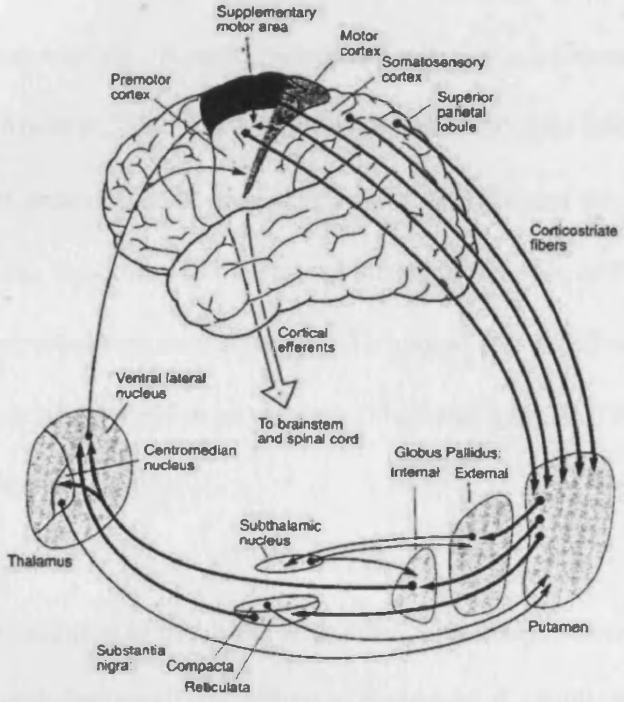

Figure 1.3 Motor circuit of the basal ganglia (Côté and Crutcher, 1991, p. 651).

1.3.2 Indirect and direct pathways

The classical model of basal ganglia circuitry is based on two parallel systems – the direct and indirect pathways (Alexander and Crutcher, 1990). The direct pathway is excitatory in essence, facilitating signal transmission from the basal ganglia to the cortex through disinhibition of the thalamus and thus excitation of the cortex. The indirect pathway on the other hand is inhibitory, in the sense that the projections from

the basal ganglia inhibit the thalamus, and in turn there is a decrease of excitatory signals to the cortex. The direct pathway projects from the striatum inhibiting the output nuclei (SN and GPi), which in turn disinhibit the thalamus. The indirect pathway projects from the striatum inhibiting the GPe first, which disinhibits the STN. The STN then excites the output nuclei, which inhibit the thalamus. The net result of the direct and indirect pathways are facilitation and inhibition of movement, respectively. Normal movement relies on a balance between the two pathways. However, this model is oversimplified and does not address the following issues. The existence of back projections from the GPe and the STN to the striatum, projections from the cortex to the striatal interneurons, role of GABAergic and cholinergic interneurons (see section 1.3.3), axonal collateralization between the circuits, and the role of the PPN as an output of the basal ganglia (Obeso et al., 2000; Bergman and Deuschl, 2002).

In addition to the direct and indirect pathways, there is a 'hyperdirect' cortico-subthalamo-pallidal pathway (Nambu et al., 2000; Parent and Hazrati, 1995). This pathway is faster in signal conduction than the direct and indirect patways (Nambu et al., 2000). The function of the hyperdirect pathway is explained in terms of the 'centre-surround' model (Mink, 1996). During preparation of a voluntary movement the cortex activates the GPi extensively through the hyperdirect pathway, thus inhibiting the thalamus. At the same time, specific neuronal populations in the GPi are inhibited through the direct pathway, which disinhibit specific targets in the thalamus. The net result is the execution of selected motor programmes and cancellation of other competing programmes.

1.3.3 Neurotransmitters

The basal ganglia receive excitatory glutaminergic inputs from the cortex and the intralaminar nuclei of the thalamus, dopaminergic inputs from the brain stem and serotonin from the raphe nuclei. However, within the basal ganglia nuclei 90-95% of the cells are GABAergic (gamma-amino butyric acid) medium-spiny projection neurons (Gerfen, 1995). In fact, the projections from the STN are the only excitatory connections within the basal ganglia. Large cholinergic local inhibitory inter-neurons also exist. Their role is to reduce the activity of the striatal output neurons.

80% of the dopamine in the brain is localised in the basal ganglia (Carlsson, 1959). Specifically it is localised within the SNc dopaminergic cells that also contain the pigment neuromelanin, which gives them their characteristic dark discoloration. The dopaminergic projections from the SNc affect the direct and indirect pathways differentially through two types of receptors in the striatum. D1 dopamine receptors facilitate transmission, while D2 dopamine receptors inhibit transmission (DeLong, 2000).

There is further modulation of the direct and indirect pathways by dopamine through synapses in the GP, STN, SN, and cortex (DeLong, 2000).

Degeneration of the dopaminergic nigrostriatal pathway as it occurs in Parkinson's disease and the depletion of dopamine seem to result in the increased activity of the output nuclei which increases inhibition of the thalamo-cortical pathways, resulting in impairment of movement (Albin et al., 1989; DeLong, 1990).

The connections within the basal ganglia, including the direct and indirect pathways, and the participating neurotransmitters are illustrated in figure 1.4

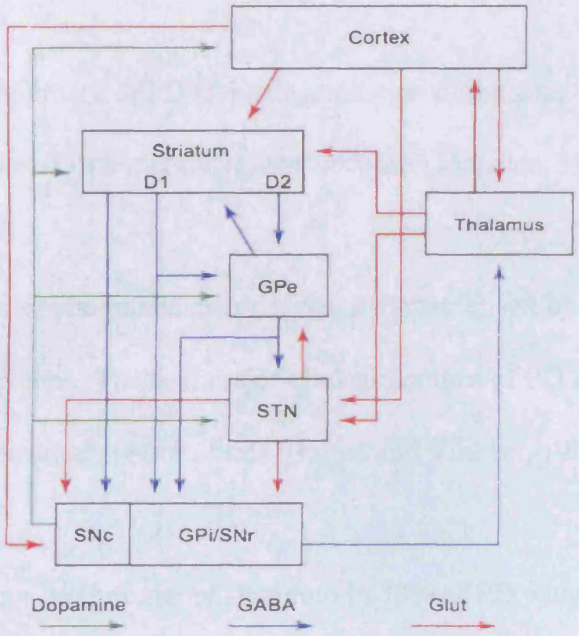

Figure 1.4 Connections within the basal ganglia circuitry model (Gurney et al., 2004, p.454). GPe = globus pallidus externus; GPi = globus pallidus internus; SNc = substantia nigra pars compacta; SNr = substantia nigra pars reticulate; STN= subthalamic nucleus.

1.4 Parkinson's disease

1.4.1 Etiology and symptoms

Parkinson's disease (PD) is one of the most common disabling neurological diseases of the basal ganglia, with an incidence of 19/100,000 per year and a lifetime prevalence rate of 2/1000 in the UK (MacDonald et al., 2000). It was first described

by James Parkinson in 1817. PD appears in the middle and late life, usually between the ages of 50 and 65 years, although there is also a rare juvenile form. The clinical profile is that of a slow, gradual, progression.

The hallmark of PD is the degeneration of the zona compacta of the substania nigra and a loss of dopaminergic projections (Marsden, 1992; Côté and Crutcher, 1991).

PD is a hypokinetic disorder, i.e. it characterised by poverty and slowness of movement. The four major clinical features of PD are tremor, bradykinesia, rigidity and postural abnormalities (Bernat and Vincent, 1987b; Marsden, 1992).

Tremor is a prominent symptom in 70% of PD patients and occurs distally more than proximally (Bernat and Vincent, 1987a). Tremor at frequencies of 4-7 Hz is observed when the patient is not moving actively and is therefore called resting tremor. It decreases once the patient intiates a voluntary movement, is absent during sleep and increases with anxiety and stress. Action tremor, at frequencies of 7-12 Hz, also appear in many PD patients during postural movements. Clinically rest and action tremor are associated ipsilaterally (Louis et al., 2001) but there is also evidence to suggest that there is no harmonic relationship between the two and there is no gradual increase of frequency from rest to action tremor (Lance et al., 1963).

Bradykinesia is one of the most disabling symptoms of PD as it prolongs routine daily activities. It is characterised by slowness of movement so that initiation of voluntary movement is delayed and the execution of the movement is prolonged (Marsden, 1992). Thus, patients have difficulties performing complex, repetitive movements. In

addition, patients also exhibit poverty of spontaneous movements (hypokinesia), apparent also in the characteristic 'frozen' expression. Bradykinesia can progress to a state of akinesia in which patients are unable to move.

Rigidity is characterised by constant muscle stiffness and is present in almost all PD patients. It is a result of the simultaneous activation of agonist and antagonist muscles. Cogwheel rigidity is the alternation between relaxation and resistance to passive movement of the extremities and may be caused due to an increased tonic stretch reflex (Marsden, 1992; Bernat and Vincent, 1987b).

Postural abnormalities in PD affect the limbs, neck and trunk. Flexion of trunk, elbows and knees, and the stooped posture due to rigidity all result in a loss of postural stability and a forward displaced centre of gravity (Bernat and Vincent, 1987b). The gait of PD patients is also characterised by difficulty to initiate steps. Once initiated these steps are small and result in 'shuffling'.

In addition to these motor manifestations, autonomic signs (e.g bladder dysfunction) and cognitive decline (dementia) may also develop in PD patients.

1.4.2 PD and the basal ganglia circuitry model

As discussed in section 1.3.2, in order for the basal ganglia to exhibit appropriate modulation on the cortical motor areas, a balance between the direct and indirect pathways is essential. Degeneration of the dopaminergic nigrostriatal pathway as it occurs in Parkinson's disease and the depletion of dopamine result in an imbalance of

these pathways so that there is increased conduction through the indirect pathway and reduced activity by the direct pathway (DeLong, 1990). According to the Albin-DeLong model, depletion of dopamine results in the increased striatal inhibition of the GPe, which in turn leads to a decrease in inhibition of the STN and thus to an increased activity of the STN activity and of the basal ganglia output nuclei (GPi and SNr) which increases inhibition of the thalamo-cortical pathways (Albin et al., 1989; DeLong, 1990). Similarly reduced inhibitory input from the putamen to the two output nuclei, through the direct pathway results in increased thalamic inhibition (DeLong, 1990). This is manifested as an impairment in movement and the typical hypokinetic symptoms of PD.

In contrast, hyperkinetic disorders involving the basal ganglia, including L-dopa induced dyskinesias, Huntington's disease chorea and hemiballismus, are explained by a reduction of the basal ganglia output, and thus disinhibition of the thalamocortical pathways (Wichmann and DeLong, 1996; Obeso et al., 1997). These disorders are characterised by excessive, involuntary movements – the opposite of the symptom manifestation in PD. In hemiballismus, the involuntary movements are a result of a vascular lesion in the STN, thus leading to reduced excitatory input to the GPi/SNr, and disinhibition of the thalamus. While in Huntington's chorea, the selective loss of GABAergic neurons in the striatum (DeLong, 2000), is suggested to result in reduced activity through the indirect pathway, as well as excessive inhibition of the output nuclei via the direct pathway (DeLong, 1990). Dyskinesias, induced as a result of dopaminergic treatment (see section 1.4.3.1), are thought to have a similar mechanism to chorea with regards to the Albin-DeLong model (DeLong, 1990; Obeso et al., 1997; Wichmann and DeLong, 1996). However, as will be discussed in section

1.5.1, paradoxical clinical observations of dyskinesias have also revealed the model's major shortcomings.

Studies of the basal ganglia of parkinsonian monkeys (see section 1.5.2.1) have supported the model, by showing increased neuronal activity of the STN and GPi (Wichmann et al., 1994b; Bergman et al., 1994). Increased STN neuronal activity is now considered the functional hallmark of PD (Wichmann and DeLong, 1996; Obeso et al., 1997). However, this model is problematic as discussed in section 1.5.1.

1.4.3 Therapy

1.4.3.1. Medication

In the 1950s low levels of dopamine were observed in postmortem examinations of brains of PD patients (Hornykiewicz, 1966). In addition, there is a degeneration of up to 90% of dopaminergic neurons in the substantia nigra (Côté and Crutcher, 1991). Since PD is a result of decreased levels of dopamine in the basal ganglia, it was proposed that restoration of dopamine in PD patients may ameliorate their symptoms (Birkmayer and Hornykiewicz, 1976). Thus, the administration of the dopamine precursor levodopa (L-3-4-hydroxyphenylalanine), which unlike dopamine, crosses the blood-brain barrier, was introduced (Birkmayer and Hornykiewicz, 1976; Côté and Crutcher, 1991).

There are three possible strategies of drug therapy in PD. First, dopamine replacement to the basal ganglia and substantia nigra. Second, stimulation of intact dopamine receptors. Third, restoration of the balance between dopaminergic and cholinergic systems by blocking acetylcholine. Benztropine and artane are examples

of anticholinergic drugs. Levodopa (L-dopa) is a presynaptic dopaminergic drug. While, bromocriptine and pergolide are examples of postsynaptic dopaminergic drugs (Bernat and Vincent, 1987b). Carbidopa, a dopa-decarboxylase inhibitor is often taken in conjunction with L-dopa. This increases the amount of L-dopa that reaches the brain, and also has the advantage of reducing peripheral L-dopa induced side effects such as nausea, vomiting and cardiac arrythmias (Bernat and Vincent, 1987b). So far, L-dopa has proven to be the greatest advance in the therapy of parkinsonian motor symptoms. However, most patients receive a combination of the three categories of medication mentioned above in order to obtain optimal amelioration of the symptoms.

Side effects of L-dopa include abnormal involuntary movements (dyskinesias), which are dose related and are associated with administration of high doses over a prolonged period. It is suggested that the prolonged period of administration causes alteration of gene expression, as well as receptor upregulation and increased sensitivity, which result in the dyskinetic symptoms (DeLong, 2000). In addition, oral antiparkinsonian medication is associated with fluctuations in the severity of motor symptoms over the course of a day, so that a patient without symptoms (ON medication) can suddenly turn OFF with a reoccurrence of parkinsonian symptoms. These side-effects increase over time.

1.4.3.2 Deep Brain Stimulation

The 1990s have seen a resurgence of surgery as potential therapy in PD. This was due to the limitations of dopaminergic medication, including dyskinesias and motor fluctuations, advances in surgical techniques including high frequency stimulation

(HFS), and the increasing understanding of basal ganglia circuitry, which was important in the selection of the surgical target.

There are three types of approaches to surgery in PD patients: ablative, deep brain stimulation and restorative (transplantation of foetal cells). The latter approach is still experimental and limited, so the main focus of this section will be on the first two approaches, which are more widely used.

The main subcortical targets in PD are the GPi and STN, with STN the preferred target for surgery (Starr et al., 1998). The rationale was that since the STN affects both output nuclei (GPi and SNr), disruption of its excessive activity in PD may ameliorate symptoms more so than disruption of GPi activity alone. This was first tested in 1- methyl-4-phenyl-1,2,3,6-tetrahydropyridine (MPTP) monkeys, in which lesioning and HFS of the STN reduced motor disturbances including rigidity and bradykinesia (Bergman et al., 1990; Aziz et al., 1991; Benazzouz et al., 1993). Another advantage of the STN as a surgical target is that it is anatomically and physiologically well delineated (Ashkan et al., 2004).

High frequency deep brain stimulation (DBS) has the same behavioral effects to those of lesioning (Starr et al., 1998) but has the advantage that it is reversible and adjustable so that parameters of stimulation can be modified for optimal effectiveness in each individual patient.

Bilateral STN stimulation is now considered to be highly effective therapy for severe parkinsonian patients, as there is a risk with surgical therapy of $\geq 5\%$ (Limousin et al.,

1995). Patients that are considered for surgery are mentally intact with a consistent history of idiopathic PD, who have had a beneficial response to L-dopa and who have a significant motor disability so that medication is no longer efficient enough to control the motor symptopms. An improvement in motor function by at least 50% and a significant reduction of L-dopa intake is observed in patients who have undergone bilateral STN DBS (Limousin et al., 1995; Starr et al., 1998; Lozano, 2001; Ashkan et al., 2004; Esselnik et al., 2004). The improvement in motor symptoms is observed in tremor, rigidity, akinesia and also gait (Limousin et al., 1995; Ashkan et al., 2004). The reduction of L-dopa intake is significant with 30% of patients stopping altogether (Ashkan et al., 2004) and as a result peak-dose induced dyskinesias were directly improved (Limousin et al., 1995; Starr et al., 1998; Ashkan et al., 20004). In addition, there is a long-lasting therapeutic effect, as there was no evidence of tolerance to the treatment after a five year follow up (Ashkan et al., 2004).

1.4.3.2.1 Mechanisms of DBS

Although high frequency STN DBS has similar behavioral effects to that of lesioning, the mechanism is much more complex and still largely not understood. STN HFS induces a deactivation of GPi and SNr (Benazzouz and Hallet, 2000). Several theories have been put forward as to what is being stimulated. The first is that stimulation directly inhibits STN neurons. Secondly, stimulation results in the antidromic activation of GPe-STN projections that send out inhibitory collaterals to the BG output nuclei. Thirdly, stimulation may directly affect axons near to the site of electrical stimulation (Lozano, 2001; Dostrovsky and Lozano, 2002) such as the pallidothalamic or nigrothalamic pathways, both of which pass close to the STN.

Limousin et al. (1997) have shown that STN stimulation significantly affects non-primary motor areas, including the dorsolateral prefrontal cortex and the SMA, but that these areas are not affected by GPi stimulation. This supports the hypothesis that STN stimulation directly affects the nigrothalamocortical pathways that do not involve the GPi.

In addition, there are also several possible mechanisms that lead to inhibition as a result of high frequency stimulation. The first, is the silencing of STN neurons through a depolarization block, so that the membrane is unable to produce an action potential (Magarinos-Ascone et al., 2002). The second, is that inhibition is due to membrane hyperpolarization (Dostrovsky and Lozano, 2002). A third possibility is inhibition through neuronal 'jamming'. The hypothesis here is that the additional impulses generated by HFS disrupt an already abnormal network (Benabid et al., 2002; Ashkan et al., 2004).

1.5 Pathological neurophysiology in PD

1.5.1 Problems with the basal ganglia circuitry model

Surgical interventions such as lesioning and deep brain stimulation in PD have resulted in clinical observations, which could not be explained by the classical Albin-DeLong model. Lesioning and stimulation of the GPi do not induce dyskinesias as predicted by the model and in fact improved L-dopa-induced dyskinesias (Marsden and Obeso, 1994; Obeso et al., 1997; Brown, 2003). In addition, lesioning of the thalamus does not worsen bradykinesia (Marsden and Obeso, 1994) and in

parkinsonian primates (see section 1.5.2.1), GPe lesioning does not reduce L-dopa induced dyskinesias (Blanchet et al., 1994).

In the primate parkinsonian model, excessive synchronisation, in addition to alterations in mean rates of firing were observed in the STN and GPi (Bergman et al., 1994; Filion and Tremblay, 1991). This raised the possibility that the pattern of neuronal discharge, with a tendency to discharge in bursts, and for the discharge between neighbouring neurons to be more synchronised, was as important if not more so, in determining the pathophysiology of the basal ganglia (Starr et al., 1998; Brown, 2003). This could explain the effects of lesioning and HFS, in terms of disruption of the abnormal synchronised activity of the GPi, so that no activity is preferable to a noisy output (Marsden and Obeso, 1994; Brown, 2003).

Excessive synchronisation of the basal ganglia is now seen to have a major role in the pathophysiology of PD as will be discussed in section 1.5.2. In addition, deep brain stimulation in PD patients, provides a rare opportunity to record the activity of the parkinsonian basal ganglia, specifically the STN, via the implanted macroelectrodes.

1.5.2 Basal ganglia oscillations in the parkinsonian state

1.5.2.1 Animal models of PD

The most important animal model of PD is the 1- methyl-4-phenyl-1,2,3,6-tetrahydropyridine (MPTP) – treated primate. MPTP is a toxin, which crosses the blood-brain barrier, and is then converted and accumulated in dopaminergic neurons, leading to neuronal death. In primates, administration of MPTP, causes irreversible,

severe parkinsonian symptoms, including rigidity, bradykinesia and tremor, which are L-dopa responsive (Shimohama et al., 2003).

Recordings from the GP and STN of MPTP primates have shown excessive synchronisation and bursting in the frequency range of rest and action tremor, i.e in the theta and alpha frequency range (Bergman et al., 1994; Nini et al., 1995; Raz et al., 2000, 2001; Goldberg et al., 2002). This activity has been shown to be correlated with clinical tremor in the primate model (Bergman et al., 1994; Raz et al., 2000).

In addition, there is abnormal synchronisation and bursting at the lower end of the so-called beta band (14-30 Hz) in the GP and striatum of MPTP treated primates (Raz et al., 1996, 2001; Bergman et al., 1998). In general, the basal ganglia in the MPTP PD model, seem to display a dominance of abnormal low frequency oscillatory activity. This implies that there are changes at the network level, in the parkinsonian state. In contrast to the independent activity of GP neurons, in the healthy primate (discussed in section 1.1.5), these neurons are now dominated by the common input from the striatum, in the dopamine depleted state, and exhibit synchronous activity.

Another animal model for PD is the 6-hydroxydopamine (6-OHDA) lesioned rat. In this model 6-OHDA is injected into the substantia nigra, leading to cell death within a few days. The advantage of this model is that the motor deficit can be quantified by measuring the rate of apomorphine-induced rotation of the rat. (Shimohama et al., 2003). So far, only one study has shown excessive beta synchronisation in the STN of 6-OHDA-lesioned rat, in support of the data from the MPTP treated primate (Sharott et al., 2005).

1.5.2.2 PD patients

Deep brain stimulation provided the opportunity to record the activity of the GP and STN in PD patients. The human parkinsonian basal ganglia showed similar oscillatory activity to that exhibited in the MPTP model. First, there was excessive synchronisation in the frequency range of rest and action tremor in the GP (Silberstein et al., 2003; Hutchison et al., 1997; Magnin et al., 2000; Levy 2001, 2002b) and the STN (Magarinos-Ascone et al., 2000; Priori et al., 2004). Second, there was abnormal synchronisation in the beta band (14-30 Hz) both in the GP (Priori et al., 2002; Brown et al., 2001, 2002b; Levy et al., 2002a; Silberstein et al., 2003) and the STN (Hutchison et al., 1998; Levy et al., 2000, 2001, 2002a,b; Marsden et al., 2001; Brown et al., 2001; Cassidy et al., 2002; Priori et al., 2002, 2004) of the parkinsonian human.

The tremor-related oscillatory frequencies may be related to clinical tremor. Several studies have shown synchronisation at frequencies below 10 Hz within the basal ganglia to be correlated with rest tremor (Hutchison et al., 1997; Brown et al., 2001; Levy et al., 2002). Furthermore, Taha et al. (1997) suggest that in pallidotomy of Parkinsonian patients, there is better tremor control when tremor-synchronous cells are included in the lesion. In addition, limb tremor has been associated with 15-30 Hz synchronous activity in the STN and GP of parkinsonian patients (Levy et al., 2000; 2002b). However, there are studies to suggest that the relationship between basal ganglia low frequency oscillations and peripheral tremor does not exist (Levy et al., 2001; Silberstein et al., 2003) or that the coupling is only transient and fluctuates over time (Hurtado et al., 1999).

There is no direct evidence of the relationship between basal ganglia low frequency activity and other parkinsonian symptoms. However, both tremor related and beta band synchronisation have been hypothesised to contribute to bradykinesia in PD (Volkmann et al., 1996; Brown et al., 2001; Moro et al., 2002; Timmermann et al., 2003; Timmermann et al., 2004). There is also evidence that beta activity in the STN is suppressed before and during movement (Levy et al., 2002a; Cassidy et al., 2002; Brown et al., 2002b; Williams et al., 2003, Kühn et al., 2004).

In contrast, after dopaminergic treatment, some PD patients develop a new activity around 70 Hz in the GP and STN, the so called gamma activity (Brown et al., 2001; Cassidy et al., 2002; Williams et al., 2002; Brown, 2003). This subcortical high frequency activity is observed at rest and is increased with movement (Cassidy et al., 2002; Brown et al., 2002b) and may therefore have some similarities to cortical gamma activity, which has been implicated in the planning of movement (Crone et al., 1998). Activity at 200-350 Hz has also been recorded after L-dopa administration, but this has only been shown in one study (Foffani et al., 2003).

This body of evidence has lead to the hypothesis that low frequency oscillations in the basal ganglia are primarly antikinetic in nature, and may therefore underlie the clinical symptoms of PD, whereas high frequency oscillations are prokinetic in nature (Brown and Marsden, 1998; Brown, 2003).

1.5.3 EEG in PD

EEG in PD is usually normal, however, a mild slowing of background activity is associated with more severe motor disability in mentally intact PD patients (Neufeld et al., 1988, 1994). Slowing of background activity is characterised by an increase in theta activity as compared to age-matched controls (Soikkeli et al., 1991; Neufeld et al., 1994).

As discussed in section 1.2.4, alpha and beta ERD and ERS in relation to movement, are markers of activation and deactivation of cortical regions involved in motor programming, respectively.

PD patients have reduced alpha and beta ERD over contralateral central motor areas before and during movement (Magnani et al., 1998; Brown and Marsden, 1999; Wang et al., 1999; Devos et al., 2004) and in contrast increased ERD over bilateral frontocentral regions (Devos et al., 2004). Alpha and beta attenuation is also delayed, with decreased latency, during motor preparation over the contralateral motor areas, in comparison to age-matched controls (Magnani et al., 1998; Devos et al., 2004). In addition, post-movement beta ERS is reduced, topographically focused and delayed in PD patients (Pfurtscheller et al., 1998; Devos et al., 2003; Pfurtscheller and Lopes da Silva, 1999). Impaired post-movement beta ERS may be an indication of impaired recovery of the motor cortex after a movement (Pfurtscheller et al., 1998).

L-dopa and STN DBS are both effective in restoring ERD/ERS abnormalities. The latency and amplitude of alpha and beta pre-movement ERD, over contralateral

central regions, are increased after treatment and stimulation (Brown and Marsden, 1999; Wang et al., 1999; Devos et al., 2004), while ERD latency decreased significantly over bilateral frontocentral regions in comparison to the non-treated condition (Devos et al., 2004). During movement there is also significant increase in latency over bilateral central regions, although these still remained shorter in comparison to controls (Devos et al., 2004).

Post-movement beta ERS significantly increased over the contralateral premotor and primary motor cortex, after STN DBS and L-dopa treatment (Devos et al., 2003). Improvements in ERD/ERS were correlated with improvement in bradykinesia (Brown and Marsden, 1999; Wang et al., 1999; Devos et al., 2003, 2004).

STN DBS and L-dopa, seem to change the abnormal cortical activity in PD patients by decreasing the abnormal spreading of ERD over frontal regions, by increasing the cortical activity of the primary sensorimotor cortex before and during movement, and by restoring motor cortical recovery after a movement.

These studies suggest that the basal ganglia have a major role in the release of relevant cortical areas from idling rhythms during voluntary movement (Brown and Marsden, 1999; Rothwell, 2003), so that when the function of the basal ganglia is impaired in PD, these rhythms predominate (Brown and Marsden , 1998).

1.5.4 Basal ganglia – cortical coherence in PD

Now that the predominate oscillatory activities of the basal ganglia and motor cortex in PD patients have been discussed separately, the question arises whether the activities in these functionally and anatomically related areas correlate. In PD patients undergoing deep brain stimulation, there is the opportunity to record from the externalised macroelectrode, in the interval after the operation but before the connection to the subcutaneous stimulator. This also allows for simultaneous EEG recordings. Coherence, which is defined as the correlation between two signals in the frequency domain, can thus be calculated. There are only a few studies that have performed these recordings, and these have shown evidence of coherence between the activities of the motor cortex and the STN and GPi at frequencies below 30 Hz, when the patients were off their antiparkinsonian medication (Brown et al., 2001; Marsden et al., 2001; Cassidy et al., 2002; Williams et al., 2002). This coherence was strongest with midline EEG, corresponding to the SMA, which as discussed in section 1.3.1, is closely connected to the STN. Marsden et al. (2001) have also shown that cortical midline - STN coherence in the beta frequency range correlated with the contact of most effective clinical efficacy during stimulation (Marsden et al., 2001). This is further supported by the attenuation of this low frequency coherence after the adminstration of dopaminergic medication (Brown et al., 2001; Cassidy et al., 2002; Williams et al., 2002). In the dopaminergic state, a high frequency coherence at ~70 Hz predominates between the cortex and the STN and GPi (Brown et al., 2001; Cassidy et al., 2002; Williams et al., 2002) which is also increased with movement (Cassidy et al., 2002). These studies suggest that cortico-subcortical coherence has functional significance, and as it is L-dopa responsive, may also have a major role in

the pathophysiology of PD (Brown, 2003). Perhaps, pathological levels of low frequency oscillations, lock the cortex and basal ganglia in slow idling rhythms, thus contributing to the clinical symptoms of hypokinesia.

1.6 Objectives of the thesis

The aim of this thesis is to further investigate the pathophysiology of PD patients. Specifically, the pathological role of low frequency activities in the STN will be further explored. This thesis attempts to characterize subthalamic low frequency activities by investigating their interactions with oscillatory cortical activities as well as with subthalamic prokinetic high frequency activities; and by determining their contribution to parkinsonian bradykinesia.

The main objectives of the thesis are:

- The characterization of low frequency cortical-subthalamic activities in terms of frequency, cortical topography and drive, in the parkinsonian state (chapter 3).
- To investigate the relationship between low and high frequency activities in the STN in the dopaminergic state (chapter 4).
- To determine the bradykinetic effects of STN electrical stimulation at different frequencies and dopaminergic levels (chapter 5).

CHAPTER 2: Methods

In the following chapter I will start by describing the patients who participated in the studies, followed by the recording techniques and clinical assessments. I will then move on to discuss the various quantitative analyses of the recorded data and the statistical tools used in this thesis.

2.1 Subjects

2.1.1 Patients

All the patients participating in the experiments in this thesis are Parkinson's disease patients, who had undergone bilateral implantation of subthalamic nucleus macroelectrodes for treatment of their parkinsonism, by high frequency stimulation. The patients in experimental chapters 3 and 4 were recorded a few days after the operation, when the electrode leads were still externalised, and before they were connected to the subcutaneous stimulator. Patients in chapter 5 participated in the study at least 3 months after the operation.

In chapters 3 and 4, EEG and/or LFP recordings were performed in subjects who were supine or seated and recorded while at rest. In chapter 5 patients performed a task which will be discussed in detail in section 2.4.2.

In all the studies, OFF medication refers to recordings that were performed after an overnight withdrawal of anti-parkinsonian medication, although it is acknowledged that patients were only likely to have been partially withdrawn from the effects of dopaminergic therapy after overnight abstinence. This is particulary relevant in the

case of dopamine agonists such as pergolide and cabergoline that have longer half-lives than L-dopa, of up to 21 and 65 hours, respectively (Blin, 2003; Rinne et al., 1997).

ON medication refers to recordings performed in subjects who under went overnight withdrawal of antiparkinsonian medication and were then recorded following administration of levodopa (200 mg in a soluble preparation with peripheral decarboxylase inhibitor).

All patients (Table 2.1), from five different centres, gave informed consent to take part in this study, which was approved by the joint ethics committee of the National Hospital for Neurology and Neurosurgery and the Institute of Neurology, London, and the ethics committees of King's College Hospital, London, the Charité, Berlin, the CTO "A. Alesini" Hospital, Rome, the Amsterdam Medical Centre, Amsterdam and the Policlinico Universitario, Messina in accordance with The Code of Ethics of the World Medical Association (Declaration of Helsinki, 1967).

In section 4.3.5 an additional group of patients from the Charité, Berlin (not mentioned in table 2.1), undergoing bilateral implantation of deep brain electrodes in the STN, were studied intra-operatively, after an overnight withdrawal of antiparkinsonian medication. Microelectrode LFP recordings were performed in the patients when they were awake and at rest.

There were no post-operative complications such as intracranial hemorrhage or infection in the patients participating in the studies.

Table 2.1 Patients participating in the studies.

Patient	Chapter no. (case no.)	Surgical Centre
1	3 (1)	Amsterdam
2	3 (2)	Amsterdam
3	3 (3)	Amsterdam
4	3 (4); 4 (12)	Amsterdam
5	3 (5); 4 (13)	Amsterdam
6	3 (6)	Amsterdam
7	3 (7); 4 (1)	Amsterdam
8	3 (8)	Amsterdam
9	3 (9)	Amsterdam
10	4 (2)	Rome
11	4 (3)	Messina
12	4 (4)	Rome
13	4 (5)	London
14	4 (6)	Rome
15	4 (7)	London
16	4 (8)	Berlin
17	4 (9); 5 (4)	London
18	4 (10)	London
19	4 (11)	London
20	4 (14)	Rome
21	4 (15)	Berlin
22	4 (16)	London
23	5 (1)	London
24	5 (2)	London
25	5 (3)	London
26	5 (5)	Berlin
27	5 (6)	Berlin
28	5 (7)	Berlin
29	5 (8)	Berlin
30	5 (9)	Berlin
31	5 (10)	Berlin
32	5 (11)	Berlin
33	5 (12)	Berlin
34	5 (13)	Berlin
35	5 (14)	Berlin
36	5 (15)	Berlin
37	5 (16)	Berlin
38	5 (17)	Berlin

2.1.2 Surgery

In essence, the surgery consists of the insertion of a pair of macroelectrodes (MEs) into the subthalamic nucleus. The ME that is used (model 3389, Medtronic Neurological Division, Mineapolis, USA) consists of four platinum-iridium cylindrical surfaces (1.27 mm diameter and 1.5 mm length) and a centre to centre separation of 2 mm. There are four contacts, with contact 0 the most caudal and contact 3 the most rostral (figure 2.1).

Before the surgery, the target, which is the STN, is identified by ventriculography and/or preoperative magnetic resonance imaging (MRI). The coordinates of the STN are then established. In the cases studied in this thesis, the intended coordinates for contact 1 were 10-13 mm from the midline, 0-3 mm behind the midcommissural point and 4-6 mm below the AC-PC (anterior commissure-posterior commissure) line.

Electrode localization is also tested intra-operatively by evaluating the effects of macro-stimulation on parkinsonian symptoms, especially rigidity and tremor of the limbs.

Intra-operative microelectrode recordings can also be used for localization by identifying characteristic bursting patterns of STN and bordering cells (Hutchison et al., 2003; Kühn et al., 2005). Bordering cells of low-density in the zona incerta and Field of Forel (see figure 2.3), approximately 1-3 mm rostral to the STN are characterised by high amplitude activity, while the high cell density of the STN is characterised by high background activity and high-amplitude, irregular single-unit discharges at frequencies between 25-70 Hz (Kühn et al., 2005). In section 4.3.5 intraoperative microelectrode LFP recordings were made with the TREC scanner

electrophysiological neuronavigation system using a tetrode (Thomas RECORDING, Giessen, Germany). The low impedance tetrode combined four platinum/tungsten fibres in a glass insulation electrode of outer diameter 100 μm with four circular contacts. Recording were made at different depths along a parasagittal trajectory (Kühn et al., 2005).

Usually within a week of the ME implantation, the electrode leads are internalised and are connected to a subcutaneous battery-operated stimulator.

In the months following the operation, the ME contact that has the best therapeutic effect, in terms of control of parkinsonian symptoms, is chosen for each side. The parameters of stimulation are adjusted until optimal clinical effectiveness is reached. The parameters of stimulation are pulse width (60-120 μs), amplitude (1-4 V), and frequency (130-180 Hz). Contacts can be stimulated using a monopolar or bipolar configuration (Starr et al., 1998). In the monopolar configuration, the contact of stimulation is the cathode, and the anode is the pulse generator. This type of stimulation is usually more widespread. The bipolar stimulation mode, where one contact is the cathode and the other the anode, allows for more local stimulation, and is usually used to control side effects that can result from the more widespread monopolar stimulation.

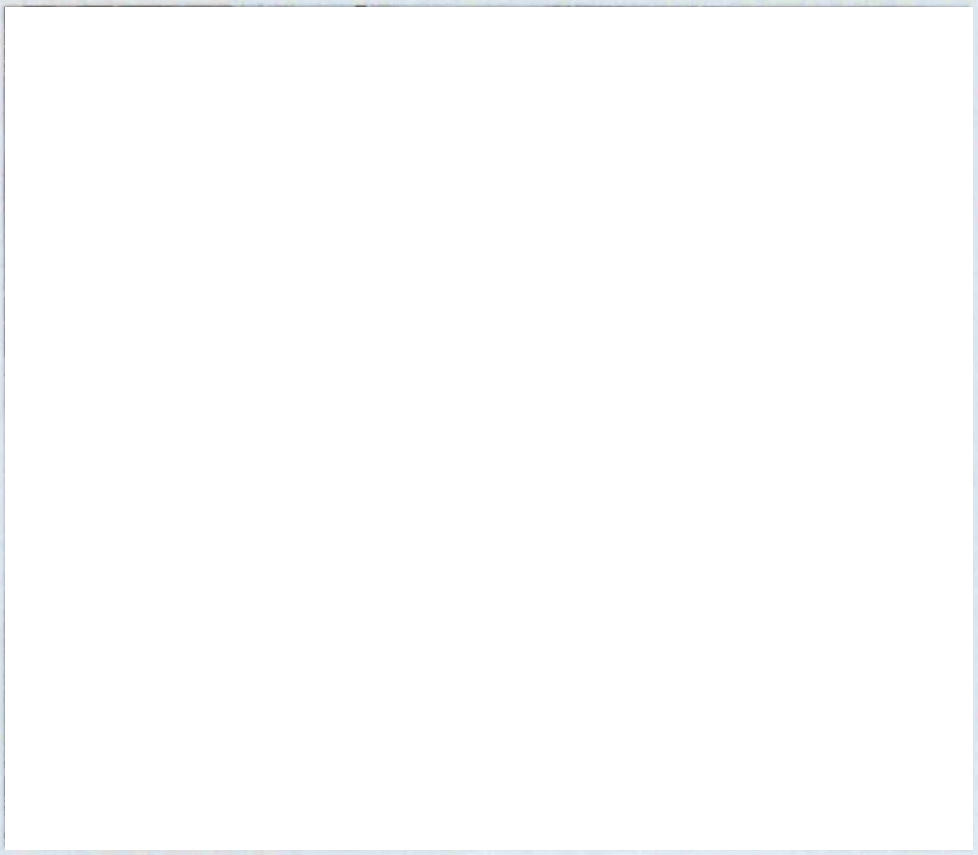

Figure 2.1 Localization of the macroelectrode. Coronal section of subthalmic nucleus (indicated by white arrow) and a cartoon of the intended position of the macroelectrode drawn to scale, with the four contacts, contact 0 being the most caudal and contact 3 the most rostral (adapted from picture provided by Marwan Hariz). GP = globus pallidus, Put = putamen.

2.1.3 Confirmation of macroelectrode localization

After the operation it is important to obtain further evidence of satisfactory targeting, even though the surgical intended coordinates were those of the STN. This can be achieved through several approaches. The first and most reliable method is post-operative imaging, including MRI or computed topography (CT) head. Ideally, at least one macroelectrode contact should be localized in the STN (a representative example is illustrated in figure 2.2). Post-operative imaging was used in all the centres except in patients operated on in Amsterdam.

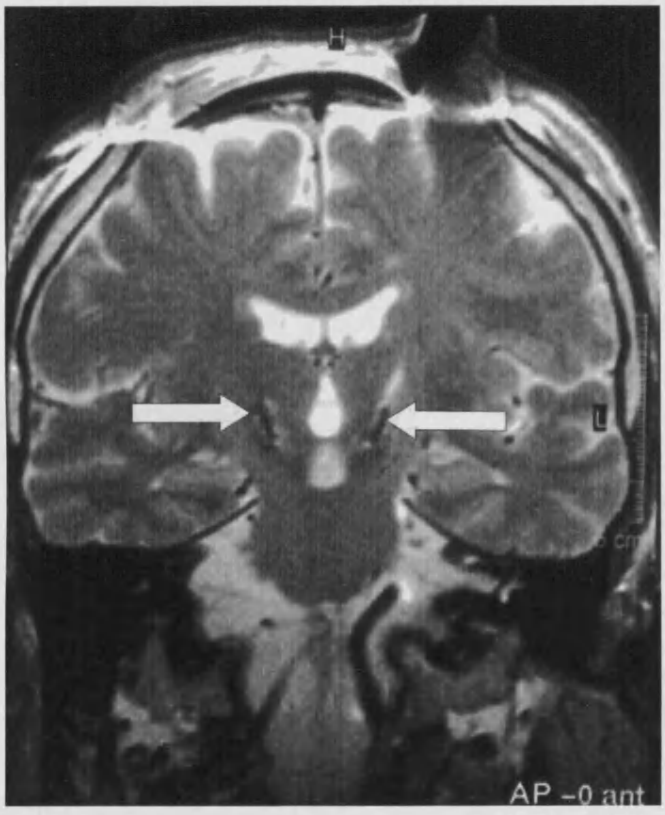

Figure 2.2 Post-operative MRI. Illustration of the localization of macroelectrodes in the post-operative T2-weighted MRI of case 15 in chapter 5. Arrows point to the macroelectrode artifacts.

The second approach is by assessing the clinical efficacy of high frequency DBS. The improvement in parkinsonian symptoms can be evaluated by comparing post-operative on and off bilateral stimulation and OFF medication pre-operative scores (using UPDRS; see section 2.4.1). The therapeutic effect of stimulation can also be assessed by evaluating the reduction in antiparkinsonian medication post-operatively (see section 1.4.3.2). However, there is dispute whether therapeutic effects involve stimulation of the sensorimotor STN or the area slightly dorsal to the STN, which includes the Field of Forel, the zona incerta and prelemniscal radiations (figure 2.3), but the presence of the stimulation target within the subthalamic area (SA) is not in dispute (Saint-Cyr et al., 2002; Voges et al., 2002). This method was used in all the patients participating in the studies.

With regards to studies of the bipolar LFP recordings in this thesis, the argument as to whether stimulation effects in the SA involve nuclear effects or white matter bundles is irrelevant, since LFPs are likely to be the product of synchronized EPSPs and IPSPs (see section 1.1.3), and not due to spontaneous activity in white matter (Magill et al., 2004a,b).

However, it is important to stress that ultimately, without histological verification of electrode site, placement of the macroelectrodes in the target STN should be considered presumptive. In addition, given the small size of the STN, it is unlikely that that all the macroelectrode contacts are situated within it.

Finally, patients were drawn from several surgical centres so that there may have been minor differences in surgical techniques and placement. Thus, the conservative term subthalamic area/region (SA) is used to refer to the positioning of the macroelectrode

contacts in the STN and adjacent areas, such as the Field of Forel, zona incerta, and prelemniscal radiations (see figure 2.3).

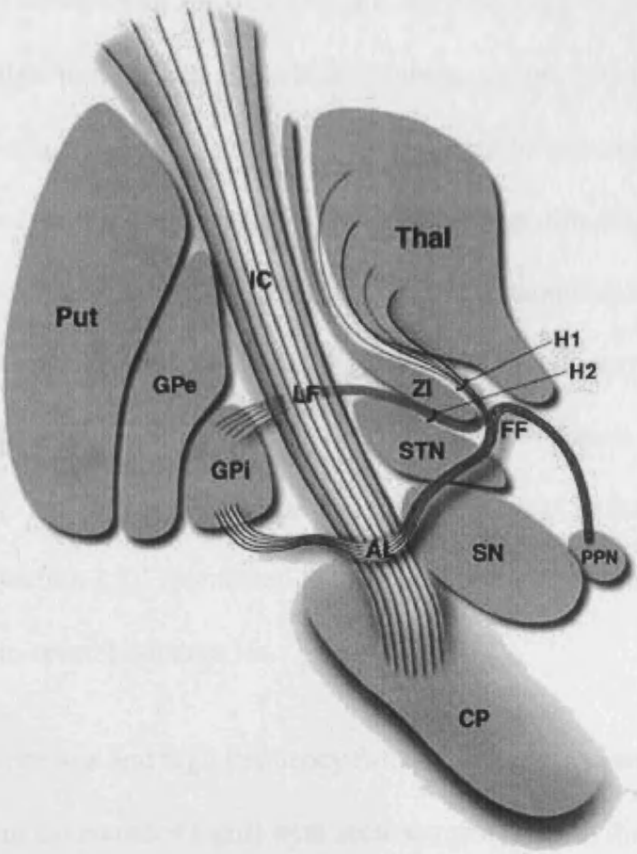

Figure 2.3 The subthalmic nucleus and neighbouring structures (Hamani et al., 2004; p.5). The subthalmic region includes the subthalmic nuclei, zona incerta, and the nuclei of the fields of Forel. Fibres passing through this region include the AL, LF (Forel's field H2) and H1. The AL contains fibres projecting to both the thalamus and the PPN. Prelemniscal radiations are not mentioned in this figure but consist of the posterior and inferior portion of the ZI (Plaha et al., 2004). AL = ansa lenticularis; CP = cerebral peduncle; FF = Fields of Forel; GPe = globus pallidus externus; GPi = globus pallidus internus; H1 = H1 Field of Forel (thalamic fasciculus); IC = internal capsule; LF = lenticular fasciculus (H2); PPN = pedunculopontine; Put = putamen; SN = substantia nigra; STN = subthalamic nucleus; Thal = thalamus; ZI = zona incerta.

2.2 Recordings

2.2.1 Sampling and filtering

To convert an analog EEG/LFP signal to a digital one, the voltage is amplified and then transformed into whole numbers at short time intervals. In order for the conversion to be accurate, it is important for the sampling rate to be at least twice that of the highest frequency contained in the analog signal (Gotman, 1990). In other words, frequencies exceeding half of the sampling rate are not represented. This is critical, since a sampling rate that is too low (longer time intervals) results in "aliasing". This means that high frequencies appear as aliased frequencies in the examined range of frequencies. This is crucial in the case of muscle artifacts (see section 2.2.5) contained in the signal, which are composed of high frequencies of up to several hundred Hz.

The low and high frequency filters determine the range of frequency that will appear in the recorded signal with accuracy and without distortion (Reilly, 2005). High frequency filters reduce or attenuate the amplitude of signals above the specified frequency, while passing low frequency activity without significant distortion. Low frequency filters on the other hand, attenuates low frequency activity, below a specified level. Low and high pass filters are independent and do not affect each other. Band pass filtering, attenuates all frequencies below and above two defined frequencies.

Filters introduce a time delay to the output signal, since the input signal cannot be processed instantaneously. Phase shifts change the timing of the signals and can modify the relationship of waves to each other. Practical filters also have a transition

zone, which is the region where the signal transmission shifts from pass-band to stop-band or vice versa. The filter's order is the relative steepness of the transition zone. The higher the order the narrower the transition zone, but the filtering process is more complex. In addition, practical filters deviate from the ideal values of the pass band and stop-band. The maximum and minimum deviations are referred to as ripple factors. The gap between the bands determines the extent of ripple in the band. The smaller the gap between the bands, the larger the ripple.

Band pass filtering of signals was performed using finite impulse response (FIR) digital filters in Spike2 v4.0. FIR digital filters allow the use of steep slopes with minimal phase distortion of the signal. In chapter 3 and 4, band pass filtering was adjusted in each subject individually, to minimise signal distortion. However, all time series from a single subject were subjected to the same filtering parameters.

2.2.2 EEG

The standard positions of the surface EEG electrodes are determined using the international 10-20 system (Fig 2.4). The electrodes are named according to area – frontopolar (Fp), frontal (F), central (C), temporal (T), parietal (P), and occipital (O); and according to laterality – left hemisphere (odd numbers), midline (z), and right hemisphere (even numbers). In the context of the motor system, the primary motor cortices approximately underly electrodes C3 and C4; the SMA is between Cz and Fz.

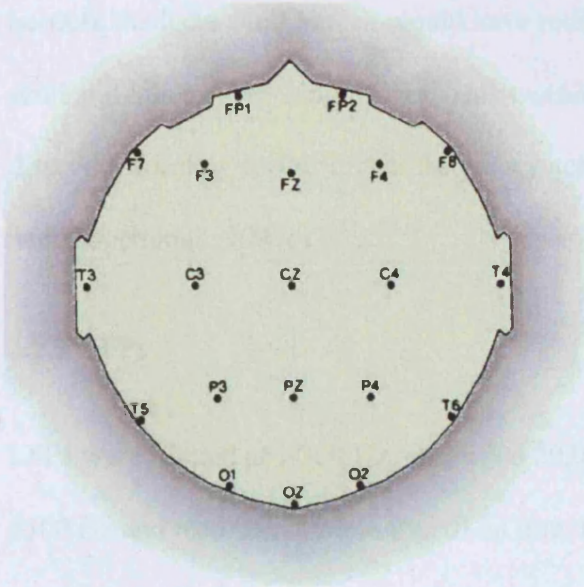

Figure 2.4 The standard placement of EEG recording electrodes. Fp, frontopolar; F, frontal; C, central; T, temporal; P, parietal, O, occipital; Z, vertex; even numbers, right hemisphere; odd numbers, left hemisphere.

EEG was picked up from Ag-AgCl electrodes, which were applied to the scalp with an electrolyte paste, according to the 10/20 system. Linked ears were used as reference. An electrode on the forehead was used as ground. Electrode impedance was less than 5 kΩ. EEG signals were filtered at 1-300 Hz, amplified 20,000 times, sampled at either 500 or 1000 Hz and recorded and monitored on-line. Amplification, filtering and recording were performed using the Schwartzer 34 amplifier system (Schwartzer GmbH, Medical Diagnostic Equipment, Munich, Germany) and Brainlab software (OSG bvba, Rumst, Belgium).

The positions of electrodes C3 and C4 had to be adjusted according to the position of the burr holes required for surgical implantation, to a maximum of 1 cm anterior to their accurate 10/20 positions. Burr holes were sited posterior to C3/C4. The possible effect on the EEG signal would be to increase the voltage over these areas. This is

because the local skull breech would have reduced the local filtering effects of the skull and other interposing tissues. This would have been expected to disproportionately favour higher frequency activities, such as those in the upper beta band (Spehlman, 1981c).

2.2.3 LFPs

LFPs were filtered at 1-300 Hz, amplified 20,000 -100,000 times, sampled at 500 - 2500 Hz and recorded and monitored on line. Linked ears were used as reference. An electrode on the forehead was used as ground. Amplification, filtering and recording were performed using the Schwartzer 34 amplifier system (Schwartzer GmbH, Medical Diagnostic Equipment, Munich, Germany) and Brainlab software (OSG bvba, Rumst, Belgium) in Amsterdam and a Nicolet Viking IIe and data capture through an A-D card (PCM-DAS12, ComputerBoards, Middleboro, MA 02346, U.S.A.) onto a portable computer using custom written software in Rome. Signals were amplified and filtered using a custom-made, 9V battery-operated portable high impedance amplifier (which had as its front end input stage the INA128 instrumentation amplifier, Texas Instruments Incorporated 12500 TI Boulevard Dallas Texas, USA) in Berlin and a D150 amplifier (Digitimer Ltd, Welwyn Garden City, Hertfordshire, UK) in Messina and London, before data capture through a 1401 A-D converter (Cambridge Electronic Design, Cambridge, UK) onto a portable computer using Spike2 software (Cambridge Electronic Design).

In chapter 4 all LFP signals were resampled to a common sampling rate of 200 Hz (see section 4.2.3), to enable the comparison of signals recorded with the different systems in each surgical center.

In section 4.3.5 intraoperative microelectrode LFPs, made from one of the four tetrode contacts, were amplified 4000-20,000, filtered at 1-141 Hz, and sampled at 25 kHz. The LFP signal was thereafter downsampled by 1 in 10 to an effective sampling rate of 2500 Hz. The contacts were referenced to the stainless steel guide tube of the tetrode.

Transient local edema following surgery could have changed the nature of LFPs. However, this seems unlikely, as oscillatory LFPs of similar character have been recorded in STN using microelectrodes, before implantation with a macroelectrode (Levy et al., 2002b). If anything, the most likely change would have been a reduction in LFP amplitude with any edema associated with macroelectrode implantation. As long as significant peaks in coherence and power are observed this should not be a consideration.

2.2.4 Montage

There were two categories of montages used in the recording of EEG/LFP signals in this thesis. The first is a monopolar montage, where the potential measured is the difference between the scalp electrodes/ME contact and a reference. The second is a bipolar montage, where the difference between a pair of electrodes/contacts is measured.

In chapters 3 and 4, LFP and EEG signals were originally recorded referenced to linked ears but later the following bipolar electrodes were derived and analysed off-line: left and right STN-ME 0-1, 1-2, 2-3 and Cz-Fz, Pz-Cz, C3-F3, P3-C3, C4-F4, P4-C4.

In EEG, a monopolar montage is better suited for recordings of widespread potentials. Its main disadvantage is that the reference potential is never completely inactive, and is thus a possible source of signal contamination. Bipolar recordings on the other hand, are better suited for the localization of potentials. This is often achieved by identifying a phase reversal (a marked change in polarity) at a common electrode.

In LFP recordings, it has been suggested that the depth potentials recorded with monopolar electrodes may be contaminated by cerebral cortical activities (Wennberg et al., 2002; Wennberg and Lozano, 2003). However, the use of bipolar recordings from the macroelectrode contacts, is a way to avoid a common scalp reference that may contaminate depth signals with cortical EEG. In addition, there is evidence from several studies that the LFP oscillations recorded with bipolar electrodes are locally generated rather than being the product of volume conduction. Polarity reversals (see section 2.3.6) are common in the beta band and there is a clear gradient of LFP power across bipolar contacts presumed to be in the STN in patients with PD (Kühn et al, 2004; Doyle et al., 2005). In addition, LFPs recorded with bipolar electrodes demonstrate clear spectral phase differences (see section 2.3.5) across a wide range of frequencies with respect to LFP activity recorded in nearby globus pallidus interna (Brown et al., 2001) and EEG activity picked up over mesial cortical areas (Marsden et al., 2001; Williams et al., 2002; Brown, 2003; Kühn et al., 2004). This in itself suggests that subthalamic LFPs are at least partly associated with synchronised pre-synaptic and/or post-synaptic effects at connected sites (Marsden et al., 2001; Brown et al., 2001; Williams et al., 2002) and would not be expected in the case of volume conduction of either cortical EEG (chapter 3) or dyskinetic electromyographic activity (chapter 4).

Although bipolar recordings were selected to ensure focality, this approach precludes any direct correlation with clinical variables, such as the possible site of contacts on post-operative imaging or the choice of contacts used for chronic stimulation. This is because of the non-linear relationship between proximity to the source and LFP oscillation amplitude that paradoxically arises when bipolar macroelectrode contacts are well positioned. For example, if the generator of a certain activity band lay midway between two adjacent contacts, power at corresponding frequencies would be negligible. In contrast, if the generator lay under one contact, the potential difference between this and adjacent contacts would be maximal.

2.2.5 Artifacts

Recordings can be contaminated by three major types of artifacts - eye movements, movement and muscle artifact, and 50 Hz noise.

Vertical eye movements and blinking appear as high amplitude random slow waves in the EEG signal from anterior electrodes. EEG sections including oculographic artifacts can be identified visually and excluded in the off-line analysis of the data. However, it is recognized that more subtle artifacts such as slow rolling eye movements may remain unidentified.

Muscle artifacts can contaminate the signal with electromyographic activity (EMG). These artifacts are composed of high frequencies of up to several hundred Hz, and can therefore be avoided if the signal is correctly filtered. Similarly, the cardiac pulsation artifact is of relatively low frequency and can also be avoided if filtered correctly. Movement artifacts such as movement of the head can interfere with signal recording and can be monitored on-line, or excluded in the off line-analysis.

50 Hz noise from surrounding electronic equipment or an ineffective ground electrode is a common source of contamination of EEG and LFP signals. This artifact can be reduced by lowering electrode impedance, coiling the electrode wires, and avoiding possible sources. It may also be filtered off-line using a digital 50 Hz band pass filter.

2.3 Analysis

Recorded activity was analysed in Spike2 v4.0 (Cambridge Electronic Design, Cambridge, UK).

2.3.1 Fast Fourier Transformation

In order to make quantitative measurements of the frequency content of EEG/LFP sections, the recorded data undergoes spectral analysis using an algorithm called the Fast Fourier Transformation (FFT). Spectral decomposition of the signal using FFT, results in a separation of different rhythms that constitute the signal, and allows for the estimation of their frequency independently of one another. The amplitude in each frequency band is quantified through the transformation, which converts the signal from the dimension of amplitude (μV) versus time, to the dimension of power (μV^2) at each frequency (Hz).

Ideally, sections analysed with FFT should have stationary statistical properties, if the spectrum is to reliably represent the frequency content of this section (Gotman, 1990). In general, a stationary section should not contain periodic activity or abrupt changes such as blinking, eyes closure or drowsiness.

Records are usually long lasting (more than 60 seconds) and are divided into a series of short (1-4 seconds) discrete sections of equal duration. The spectra are then estimated by averaging across these disjoint sections (Halliday et al., 1995).

There are three stages in the computation of the spectra (Gotman, 1990). First, a window filter is used, which ensures that the spectrum is largest at the specified frequency, and the values of neighbouring frequencies are tapered to zero. A Hanning window filter was used for all spectral analyses in this thesis. Second, for the FFT, the number of samples or points (N) needs to be a power of 2. The Fourier coefficient that is calculated for N points, is essentially N/2 pairs of numbers, per frequency. This pair of numbers are the two components of the coefficient, and are also referred to as the real (sine) and imaginary (cosine) components. In the third stage, the two components of each coefficient are squared and added for each frequency. The power at each frequency is therefore a positive number.

The frequency resolution can be determined by dividing the sampling resolution by the number of points (N) used in the FFT. Segment lengths of 1024 points were used, giving a frequency resolution of 1 Hz in chapters 3 and 4.

The log-transformation of the power spectrum is calculated, in order to normalise values for further statistical analysis.

2.3.2 Coherence

Coherence is a measure of the correlation between two signals in the frequency domain. Here it is based on the power spectra obtained from the FFT algorithm (section 2.3.1). In chapter 3 coherence between signals from scalp EEG and STN macroelectrode (ME) LFP was calculated. The EEG, denoted by $_A$, and LFP, denoted by $_B$, were assumed to be stationary. In the frequency domain estimates of the autospectrum of the EEG, $f_{AA}(\lambda)$, and LFP, $f_{BB}(\lambda)$, as well as of coherence, $|R_{AB}(\lambda)|^2$, were given by

$$|R_{AB}(\lambda)|^2 = \frac{|f_{AB}(\lambda)|^2}{f_{AA}(\lambda) f_{BB}(\lambda)},$$

where λ denotes the frequency and $f_{AB}(\lambda)$ is the cross spectrum between the signals. The cross-spectrum is the product of the FFT of one signal, and the complex conjugate of the FFT of a second signal (Gotman, 1990). The complex conjugate has the same amplitude but opposite phase as the complex number. Thus, the cross spectrum provides information about the amplitude and phase at different frequencies, as a measure of the interaction between the two signals.

Coherence is a measure of the degree to which one can linearly predict change in one signal given a change in another signal (Brillinger 1981; Halliday et al. 1995; Rosenberg et al. 1989). It is without units and it ranges from 0 to 1, with a coherence of 0 indicating an absence of a linear relationship between the signals, and a value of 1 signifying two identical signals. The coherence estimates can be interpreted as providing an estimate of the contribution of EEG to LFP activity and *vice versa*.

Coherence values were given an approximately normal distribution for statistical parametric analysis (see section 2.5.1) using the Fisher transformation of the modulus of the coherency (square root of the coherence).

The division of the cross spectrum by the respective autospectra to give coherence, however, means that artifacts common to the two signals, result in inflated values coherences. The artifacts can arise from volume conduction between electrodes or through cross-talk within leads or amplifiers (Grosse et al., 2002). However, these artifacts are usually restricted to low or high frequencies, such as oculographic and electromyographic artifacts, respectively (see section 2.2.5).

2.3.3 Partial coherence

First-order partial coherence functions were estimated in chapter 3, to assess the extent to which a third process (the 'predictor') accounted for the relationship between two other processes (Halliday et al. 1995; Rosenberg et al. 1989, 1998). In chapter 3, the partial coherence represents the fraction of coherence between, for example, Cz-Fz and STN-ME that is not shared with a third signal, say P3-Pz. In this case, if the signal between Cz-Fz, STN-ME and P3-Pz were to be 100% coherent, then partialization of the coherent activity between Cz-Fz and STN –ME, with P3-Pz as the predictor would lead to zero coherence. On the other hand, if the coherent activity between Cz-Fz and STN-ME were kept completely separate from P3-Pz, partialization with P3-Pz as the predictor, would have no effect on the coherence between Cz-Fz and STN-ME signals. However, in the case that the partial coherence does not prove to be different (lower) than the ordinary coherence, this can also be

due to non-linear interactions between the signals. These non-linear interactions, cannot be accounted for by the partial coherence function, since it is based on the assumption of linearity.

Examples of applications of first-order partial coherence functions are given in Spauschus et al. (1999), Halliday et al. (1999), Kocsis et al. (1999) and Mima et al. (2000a).

2.3.4 Phase

If the coherence between two signals is high enough at a certain frequency or frequency band, then the phase relation between the two activities can also be very useful in describing the temporal relationship between the signals.

In chapter 3, timing information between the EEG and LP signals was calculated from the phase spectrum, defined as the argument (arctangent) of the cross-spectrum: $\arg\{f_{AB}(\lambda)\}$. Phase was only analysed over those frequencies showing significant coherence between LFPs and cortex.

The constant time lag between two signals was calculated from the slope of the phase estimate (radians/Hz) which was divided by 2π, after a line had been fitted by linear regression (Gotman, 1983; Grosse et al., 2002). When the gradient of the slope is negative the input signal is leading the output signal and vice versa. The phase estimate from a single frequency is ambiguous (Grosse et al., 2002). Thus, the time lag was only calculated for the gradient from a minimum of 4 contiguous points of

significant coherence and where a linear relationship accounted for (r^2) $\geq$ 80% of the variance ($p < 0.05$).

However, there is still the possibility that a calculated phase estimate can constitute a mixture of phases, when there is an overlap of coherent activities in a particular frequency band.

Cross-talk of artifacts and volume conduction were mentioned as one disadvantage of coherence (section 2.3.2). Phase is therefore important in ruling out cross-talk and volume conduction as these would have zero lag between signals.

2.3.5 Polarity reversal

To demonstrate the focality of recorded LFP activity a waveform cross-correlation was performed (Spike2 v4.0) between the pass-band filtered signals of adjacent bipolar macroelectrode contact pairs (e.g. 01 with 12 and 12 with 23). Polarity reversal (see section 2.2.4), indicating a dipole at the site of the shared macroelectrode contact, was considered to occur when there was a peak around time 0 that was negative and maximal amongst other negative peaks in the waveform cross-correlogram. For localization of lower frequencies (7-32 Hz, chapter 3) the peak should be at 0 ± 10 milliseconds (ms), whereas for higher frequencies (65-85 Hz, chapter 4) it should be at 0 ± 3 ms. For example polarity reversal around contact 1 would be confirmed by a negative peak around time zero in the cross-correlation of the LFP recorded at contacts 01 and 12. Note that this technique cannot show polarity reversal at contact 0 or 3.

For contacts not showing polarity reversal the power gradient can be calculated, by expressing either the mean (un-logged) power of the relevant frequency range at each contact as a percent of the peak mean power in that band (see chapter 3); or the (un-logged) amplitude at each contact as a percent of the peak amplitude (see chapter 4). This too can provide support for a local dipole, if the power or amplitude gradient is steep.

2.3.6 Temporal correlations

Spectral power correlations provide a means to investigate the extent to which the amplitude of activities at different frequencies is correlated. This method has two main advantages. First, as opposed to coherence where the contribution of the amplitude versus the phase between two signals cannot be disassociated, power correlations only determine the relationship between the amplitude of two activities. Second, power correlations provide a means to investigate the relationship between activities at two different frequencies.

In chapter 4, the temporal correlation between spectral power at different frequencies $C(f_1, f_2)$ were computed. This was obtained by computing a log-transformed power spectrum $P_{xx}^{\ i}$ for each 4 second (s) epoch i and then the correlation coefficient of the two time series $P_{xx}^{\ i}(f_1)$ and $P_{xx}^{\ i}(f_2)$. By performing this computation for a two-dimensional grid in f_1, f_2 space, two-dimensional images of negative and positive spectral correlations were generated. The spectral power $P_{xx}^{\ i}(f)$ and the correlation $C(f_1, f_2)$ do not contain phase information.

The temporal correlation between spectral power at different frequencies has been previously used to analyse LFP (Sarnthein et al, 2003; Bekisz and Wróbel, 2003; Masimore et al., 2004) and magnetoencephalographic signals (Llinás et al., 1999).

2.3.7 Control charts

Significant power peaks in chapter 4 were confirmed by control charting using commercial software (Change-Point Analyser 2.0 shareware program; Taylor Enterprises, Illinois, IA, USA). Control charts are well suited for detecting changes in noisy data. They require multiple observations and are based on serial deviations from the mean of these values (power in this case). Control limits determine the maximum range that values are expected to vary (with a 99% probability in this case), if it is assumed that no change has occurred. Significant power peaks in chapter 4 were defined as changes with probabilities of more than 99%.

2.4 Clinical assessment

2.4.1 UPDRS

The Unified Parkinson's Disease Rating Scale (UPDRS) is the gold standard in the evaluation of parkinsonian symptoms (Fahn et al., 1987). It is a quantitative scale of 5 points, measuring the severity of parkinsonian symptoms, with 0 = absent, 1= slight, 2=mild-moderate, 3=marked, and 4=severe. The scale is divided into mental, history of signs and a motor examination. Each subsection can be used and summed separately. In this thesis, only the total score of the motor examination (UPDRS III) is quoted throughout. During the motor examination, a clinician scores the motor features of the patient, observed at a single point in time. These features include

speech, rest and action tremor, rigidity, bradykinesia/hypokinesia, mobility, gait and posture. For tremor, rigidity and bradykinesia, each hand and leg are evaluated separately. In addition, scores for tremor and rigidity of the head are given.

In chapter 4, in addition to the UPDRS III, dyskinesias were also scored. These were assessed during the recording using the levels of severity described in item 33 of the UPDRS, with a score of 0=non disabling, 1=mild, 2=moderate, 3=severe and 4=completely disabled.

The disadvantage of the UPDRS score is that it is rated subjectively so that scores may vary both within and between examiners.

2.4.2 BRAIN TEST

For a more objective assessment of bradykinesia, the Bradykinesia Akinesia Incoordination test (BRAIN TEST) was used. This is an objective and validated test evaluating bradykinesia in PD (Giovanni et al., 1999; Homann et al., 2000). The test is a simple computer software program run on a standard laptop. This test essentially consists of rapid movement of the index finger between two keys on a keyboard completed over 30 seconds and repeated for each arm. The target keys ("S" and ";") were 15 cm apart and were marked with red dots. The subjects were instructed to tap as fast and as accurately as possible (Giovanni et al., 1999; Homann et al., 2000). The mean kinesia time (KT) is the average time between consecutive taps in milliseconds, so that the longer the KT the worse the performance. This variable was used to evaluate bradykinesia in chapter 5.

2.5 Statistical analysis

SPSS 11.0 for Windows (SPSS Inc., Chicago, Illinois, USA) and Excel (Microsoft office 2000 SR-1 Professional) software were used for the statistical analysis in this thesis.

2.5.1 Normal distribution

Observations that are distributed symmetrically around the mean are referred to as normally distributed. Another characteristic of the distribution is that 68% and 95% of all values under the curve lie within one and two standard deviations of the mean, respectively.

The Kolmogorov Smirnov test is used to determine whether a set of data are normally distributed. It compares the observed data with the theoretical normal distribution. If $p > 0.05$ then the distribution is not significantly different to the theoretical normal distribution. If $p < 0.05$ then the data are considered non-parametric.

2.5.2 Z-score

The Z-score is a way of standardising the raw score by expressing it in terms of its location away from the mean of the distribution, in standard deviation units. The Z-score is calculated by subtracting the mean of the distribution from the raw score and dividing by the standard deviation (Norman and Streiner, 2000a). Thus, distributions are transformed to the same scale and this is important when comparing scores from different measures or tests.

2.5.3 Standard error and confidence intervals

Throughout the text, mean values are given with the standard error of mean (SEM), which is the standard deviation divided by the square root of the sample size.

95% confidence limits are calculated using the following equation:

$$CI = \bar{x} \pm z_{\alpha/2}(s/\sqrt{n})$$

where CI is the confidence limit, $\bar{x}$ the mean, s the standard deviation, Z the Z-score, $\alpha = 0.05$, and n the sample size.

For $\alpha = 0.05$, the upper and lower limits indicate the interval above and below the mean where 95% of the distribution lies, so that there is a 2.5% chance that the mean is above or below the upper and lower limit, respectively.

2.5.4 T-tests

T-tests are used to compare the means of two groups. The t-test is based on the ratio of the difference between the two groups and the standard error of the difference (Norman and Streiner, 2000b).

T-tests can be either one-tailed, when the direction of the difference is specified in advance, or two-tailed, where the difference regardless of direction is tested (Norman and Streiner, 2000c). In this thesis, two-tailed t-tests were used, unless specified otherwise.

There are two main categories of t-tests:

The first is the paired Student's t-test, which compares the distribution of two variables in one group. The difference between the values of the two variables is

computed. The t-test determines whether the average of this difference is different from zero.

The second is an independent t-test, which compares the means of two independent groups of cases on one variable.

The non-parametric equivalent of the paired and independent t-tests that are used in this thesis are the Wilcoxon and Mann-Whitney tests, respectively. These are used when there are no a priori assumptions about the distribution of the values, when these are not normally distributed, or when the variable is ordinal.

2.5.5 ANOVA and Friedman's test

Repeated measures general linear models of analysis of variance (ANOVA) is used to compare two or more related variables in each subject. Several factors with a number of levels are investigated. The ANOVA provides information about the main effects for each factor in addition to the interactions between factors.

The ANOVA relies on an assumption of sphericity for the dependent variables. This means that the variables have equal variances across time (Norman and Streiner, 2000d). However, most data do not meet this criterion. Sphericity can be tested using the Mauchly sphericity test. If the test is significant ($p<0.05$), then the assumption of sphericity has been violated. In these cases, a Huynh-Feldt correction for non-sphericity should be incorporated. The Huynh-Feldt correction was incorporated throughout the thesis, unless stated otherwise.

The F-ratio, which is the "signal-to-noise ratio of the differences between groups to the variation within groups" (Norman and Streiner, 2000e, p.70), is also calculated.

After a significant effect has been found, post hoc multiple comparison tests are then used to determine which variables differ. In this thesis, the Bonferroni test is used to adjust for the multiple comparisons made. The significance level is adjusted so that for n comparisons, the test is considered to be significant at the 0.05/n level.

The multivariate test is another way of testing for the main effect and is valid whether or not sphericity is satisfied. Here the difference between the groups is tested based on all the dependent variables at once.

For non-parametric values, the Friedman's test is used to compare the distributions of two or more variables.

2.5.6 Fisher's exact test

The Fisher's exact test is used to determine if there are associations between two categories of variables. The test is based on a 2*2 table, with the frequency of an event in each cell. The test determines whether the ratios of the variables are significantly different.

2.5.7 Correlations

Correlations measure the linear relationship between two variables. The correlation coefficient, r, is calculated using the following equation:

$$r = \frac{\sum (x - \bar{x})(y - \bar{y})}{\sqrt{\sum (x - \bar{x})^2 \sum (y - \bar{y})^2}}$$

where $\bar{x}$ and $\bar{y}$ are the means of the variables x and y, respectively.

Correlation coefficients of –1 and + 1 are an indication of a perfect negative and positive linear relationship, respectively: while a correlation coefficient of 0 is an indication that there is no linear relationship between the two variables.

Pearson's correlation coefficient is used for normal distributed values, while the Spearman's correlation is used for non-parametric distributions or rank orders.

The significance test of correlation is given by the following equation:

$$t = r\sqrt{\frac{n-2}{1-r^2}}$$

where r is the correlation coefficient and n is the sample size.

CHAPTER 3: Different functional loops between cerebral cortex and the subthalmic area in Parkinson's disease

3.1 Introduction

As discussed in the introduction there are several types of synchronisation that have been identified in the untreated parkinsonian state and their relative importance in the pathophysiology of Parkinson's disease remains unclear (Brown, 2003). There is excessive synchronisation in the frequency range of the rest and action tremor, as well as increased synchronisation in the beta band, in the parkinsonian basal ganglia (see section 1.5.2). However, whether activity throughout the beta band is of similar significance is unclear, and there have been some suggestions that the lower and upper beta bands may be functionally distinct (Priori et al., 2002; Williams et al., 2002; Vorobyov et al., 2003). Similarly, previous studies have failed to distinguish between STN-EEG coherence in the theta band, covering the frequency range of parkinsonian rest tremor, and that in the alpha band (Williams et al., 2002). Further, no one study has determined which activities predominate in STN-cortical circuits in untreated PD, nor whether the oscillatory activities in this state are independently generated or harmonically related. Finally, although there is some evidence to suggest that the beta activity is driven from the cortex (Marsden et al., 2001; Brown et al., 2001; Williams et al., 2002), it remains unclear whether this drive is identical throughout the beta band and whether synchronisation in the theta and alpha bands is driven by cortex or drives motor cortex.

In this study it was postulated that the more functionally significant forms of synchronisation within the basal ganglia of untreated PD will involve simultaneous

activity in large populations of local neurons, and thereby oscillations in local field potentials (Goldberg et al., 2004; Magill et al., 2004a,b; Kühn et al., 2005), and will be coupled to a similar activity in motor areas of the cerebral cortex and hence coherent with EEG.

Accordingly, scalp EEG and local field potentials (LFPs) from macroelectrodes (MEs) inserted in the area of the subthalamic nucleus (SA) were simultaneously recorded in awake PD patients in the few days following functional neurosurgery. Data were collected following overnight withdrawal of dopaminergic treatment, so as to promote oscillation at tremor and beta frequency (Brown et al., 2001; Williams et al., 2002).

The aims of this study were first to determine the predominant frequencies in the coupling between cortical and subthalamic activities and second to determine the extent to which coupling in different frequency bands may be differentiated with respect to cortical topography and direction of drive. The study has been published (Fogelson et al., 2005c).

3.2 Methods

3.2.1 Patients and surgery

Nine patients were studied (mean age of 59.7, range 54 to 66 years, 3 Female) with PD (mean duration of disease 16.1, range 8 to 36 years). Their clinical details are summarised in Table 3.1.

Case	Sex	Age (years)	Disease duration (yrs)	Pre-operation Medication (daily dose in mg)	Post- operation medication (daily dose in mg)	Predominant symptoms	Side studied	Clinically effective contact - monopolar
1	M	57	8	1200 L-dopa 1.25 Pergolide	750 L-dopa 2 Pramipexole	bradykinesia, rigidity	RT LT	1 3
2	F	65	25	200 L-dopa 300 Amantadine 1.8 Lisuride 5 Selegeline	125 L-dopa 300 Amantadine 0.8 Lisuride	bradykinesia	RT LT	1 2
3	M	54	15	600 L-dopa 8 Pergolide	500 L-dopa 5 Pergolide	bradykinesia, tremor	RT LT	12 1
4	F	56	13	600 L-dopa 10 Selegeline 300 Amantadine 300 Entacapone	300 L-dopa 5 Selegiline 100 Amantadine 0.8 Pramipexol	dyskinesias	RT LT	12(bipolar) 1
5	M	54	11	500 L-dopa 4 Benzhexol	200 L-dopa 2 Benzhexol	tremor, dyskinesias	RT LT	02 12
6	M	63	16	750 L-dopa 1200 Entacapone 300 Amantadine 4 Pergolide	600 L-dopa 1200 Entacapone 200 Amantadine 4 Pergolide	tremor, dyskinesias	RT LT	0 01
7	M	56	11	1900 L-dopa 3 Pergolide 200 Amantadine 800 Entacapone	700 L-dopa 3 Pergolide 200 Amantadine 30 Domperidone	bradykinesia tremor, rigidity	RT LT	0 1
8	F	66	36	450 L-dopa 5 Selegiline 5 Ropinirole	400 L-dopa 11 Roprinirol	tremor, rigidity, bradykinesia	RT LT	13 (bipolar) 1
9	M	66	10	800 L-dopa	300 L-dopa 4 trihexyphenidyl	tremor, bradykinesia, rigidity.	RT LT	1 1

Table 3.1 Clinical details. RT = Right; LT= Left; L-dopa was combined with a decarboxylase inhibitor.

Simultaneous implantation of bilateral MEs was performed in all cases. The intended coordinates at contact 1 were 11-13 mm from the midline, 0-3 mm behind the midcommissural point and 4-6 mm below the AC-PC line. Intraoperative electrode localization was tested by macro-stimulation in all patients. No microelectrode recordings were made.

The patients derived a mean 51 $\pm$(SEM) 6 % and 40 $\pm$ 8 % reduction in OFF treatment motor UPDRS scores with levodopa and therapeutic deep brain stimulation, respectively. Pre-operative assessment of the clinical efficacy of levodopa was determined less than four months prior to surgery. Post-operative scores were collected 6 months after the operation. There was a significant difference between pre and 6 months post-operative equivalent total daily levodopa dose (Wilcoxon, p=0.011). Post-operative equivalent total daily levodopa dose was reduced to 66 $\pm$ 8% of the pre-operative dose. No post-operative imaging was performed in the patients.

3.2.2 Recordings

Subjects were supine or seated and recorded while at rest after the patient had been off medication overnight (OFF).

Deep brain activity was recorded from the adjacent 4 contacts of each macroelectrode in the subthalamic area (SA-ME) giving three bipolar recordings; 0-1, 1-2 and 2-3.

EEG was picked up from Ag-AgCl electrodes using the 10/20 system. The positions of electrodes C3 and C4 had to be adjusted according to the position of the burr holes

to a maximum of 1 cm anterior to their accurate 10/20 positions. Burr holes were sited posterior to C3/C4.

LFPs and EEG signals were filtered at 1-300 Hz, amplified 20,000 times and were sampled at either 500 or 1000 Hz and recorded and monitored on line. Electrode impedance was less than 5 kΩ.

3.2.3 Analysis

Recorded activity was analysed in Spike2 v4.0 (Cambridge Electronic Design, Cambridge, UK).

For the estimation of coherence, 400 seconds of artifact-free data were selected for each subject OFF medication (359, 380, and 398 seconds from three recordings).

LFP and EEG signals were originally recorded referenced to linked ears but later the following bipolar electrodes were derived and analysed off-line: left (L) and right (R) SA-ME 0-1, 1-2, 2-3 and Cz-Fz, Pz-Cz, C3-F3, P3-C3, C4-F4, P4-C4.

The four frequency bands of interest were defined as follows: theta (3-7 Hz), alpha (8-13 Hz), lower beta (14-20 Hz) and upper beta (21-32 Hz).

3.2.3.1 Coherence

Coherence was evaluated and normalised using methods described in section 2.3.2. The following analyses were then performed:

1) Averaged coherence spectra between the three SA-ME bipolar contacts on each of the 18 sides and the six EEG electrode pairs (Cz-Fz, Pz-Cz, C3-F3, P3-C3, C4-F4, P4-C4) were calculated.
2) The bipolar SA-ME contact on each side in each subject that had the greatest coherence with Cz-Fz, in each of the four frequency bands, was determined.
3) Friedman's test (section 2.5.5) was used to determine the statistical differences of the distribution of contacts with maximal coherences within the four frequency bands.
4) Correlation between contact position and the occurrence of maximal coherence with EEG in the four frequency bands was determined using Spearman's rho (section 2.5.7).
5) Coherences between the bipolar SA-ME contact determined in point (2) and the six EEG electrode pairs were evaluated.
6) The average coherence in each of the four frequency bands for three cortical areas of interest was calculated. The areas were defined as follows: **midline** – average of CzFz to L-SA-ME, PzCz to L-SA-ME, CzFz to R-SA-ME, PzCz to R-SA-ME; **ipsilateral to the ME** - average of C3F3 to L-SA-ME, P3C3 to L-SA-ME and C4F4 to R-SA-ME, P4C4 to R-SA-ME; **contralateral to the ME** - average of C3F3 to R-SA-ME, P3C3 to R-SA-ME and C4F4 to L-SA-ME, P4C4 to L-SA-ME coherence.
7) Two-way ANOVA (section 2.5.7) was utilised for the comparison of the cortical topography of the four frequencies across the subjects. Frequency band (3-7 Hz, 8-13 Hz, 14-20 Hz and 21-32 Hz), and area (midline, ipsilateral and contralateral to the SA-ME) were used as factors.

8) Relevant post-hoc 2-tailed paired t-tests (section 2.5.4) were performed.
9) To determine the differences in relative topography between frequency bands, for each subject the coherence was normalised to that which was greatest out of the three cortical areas. This was performed for each of the four frequency bands, giving the relative coherence over ipsilateral, midline and contralateral cortex.
10) Three separate Friedman's tests for each of the three areas across the four frequency bands were then performed.
11) Relevant post-hoc Wilcoxon tests (section 2.5.4) were performed.

3.2.3.2 Partial coherence

Partial coherence analysis was evaluated and normalised according to methods described in section 2.3.3 and was used to confirm that the results were related to independent loops of coherent activity between the SA-ME and lateral and mesial cortical areas. In particular, partial coherence was used to address two possible confounds.

First, the prominent alpha peak in SA-ME to EEG coherence might not specifically relate to coupling in the alpha band between SA and frontal cortex, but rather to volume conduction from more posterior cortical areas where alpha activity can be more prominent. To this end, partialization of C3F3 to L-SA-ME and C4F4 to R-SA-ME coherence with P3Pz and P4Pz signals as respective predictors was used. The bipolar SA-ME contact on each side in each subject that had the greatest coherence with CzFz, in the alpha band, was used in the analysis. A paired t-test comparing the 9

pairs (n=18) of partialized coherences with the corresponding un-partialized coherences (C3F3 to L-SA-ME and C4F4 to R-SA-ME) was performed.

The second possible confound was that much of the cortical activity recorded over lateral and mesial cortical areas was the same given the use of bipolar EEG electrodes. Accordingly, partialization of C3F3 to L-SA-ME and C4F4 to R-SA-ME coherence with the CzFz signal as predictor (ipsilateral partial coherence) and partialization of CzFz to L-SA-ME and CzFz to R- L-SA-ME coherence with C3F3 and C4F4 signals as predictors (midline partial coherence), respectively, were used. The bipolar SA-ME contact on each side in each subject that had the greatest coherence with CzFz, in each of the four frequency bands, was used in the analysis.

A two-way ANOVA was utilised for the comparison of the topography of the partialized coherences in the four frequencies across the 18 SA-MEs. Frequency band (3-7 Hz, 8-13 Hz, 14-20 Hz and 21-32 Hz), and area (midline and ipsilateral to the SA-ME) were used as factors. Relevant post-hoc 2-tailed paired t-tests were then performed

To determine the differences in relative topography between frequency bands, for each subject the partial coherence was normalised to that which was greatest out of the two cortical areas (ipsilateral and midline). This was performed for each of the four frequency bands, giving the relative coherence over ipsilateral and midline cortex. Two separate Friedman's tests were performed for each of the two areas across the four frequency bands. Relevant post hoc Wilcoxon tests were then performed.

3.2.3.3 Phase

Phase was evaluated according to methods described in section 2.3.4. Phase was calculated for the SA-ME contacts with the highest coherences with EEG electrodes CzFz, C3F3 and C4F4.

Mann-Whitney tests were used to evaluate the statistical difference in phase between the four frequency bands.

3.2.3.4 Polarity reversal

To demonstrate the focality of recorded LFP activity, a waveform cross-correlation was performed between the pass-band filtered (7-32 Hz) signals of adjacent bipolar SA-ME contact pairs (see section 2.3.5). Polarity reversal, was considered to occur when there was a peak at time 0 ± 10 ms that was negative and maximal amongst other negative peaks in the waveform cross-correlogram. The number of polarity reversals detected ($n = 9$) precluded any statistical comparison of the number of contacts showing both polarity reversal and being used for clinical stimulation versus the number of such associations arising by chance.

3.3 Results

3.3.1 Spectral analysis

All patients were studied after an overnight withdrawal of antiparkinsonian medication. Three of the patients (cases 2, 4 and 9) showed clinical evidence of temporary microlesional/edema effects from surgery in so far as tremor and off-period

severity were reduced during the first few days after surgery (depth LFP recordings were made during this period in these three subjects).

Figure 3.1A shows an example of raw SA-ME LFPs and EEG recorded in case 8. Note that EEG is generally of higher amplitude than the bipolar SA-ME LFP. Oscillatory activity at around 20 Hz is evident in the latter. Average coherence spectra between the three SA-ME bipolar contacts on each side and the six EEG electrode pairs (Cz-Fz, Pz-Cz, C3-F3, P3-C3, C4-F4, P4-C4) showed a broad band of elevated coherence from 3-32 Hz with peaks in the alpha and upper beta frequency range (Figure 3.1B). There was no clear evidence of discrete peaks in the theta and lower beta bands in the averaged data, although in cases 4, 5 and 8 coherence in the theta band exceeded that in the alpha band and in cases 2 and 3 coherence in the lower beta band was greater than that in the upper beta band. In addition, there were subjects in whom theta and alpha (cases 3 and 9) and lower and upper beta (cases 3, 5 and 9) had peaks of similar size.

No peaks in coherence were seen from 35-250 Hz.

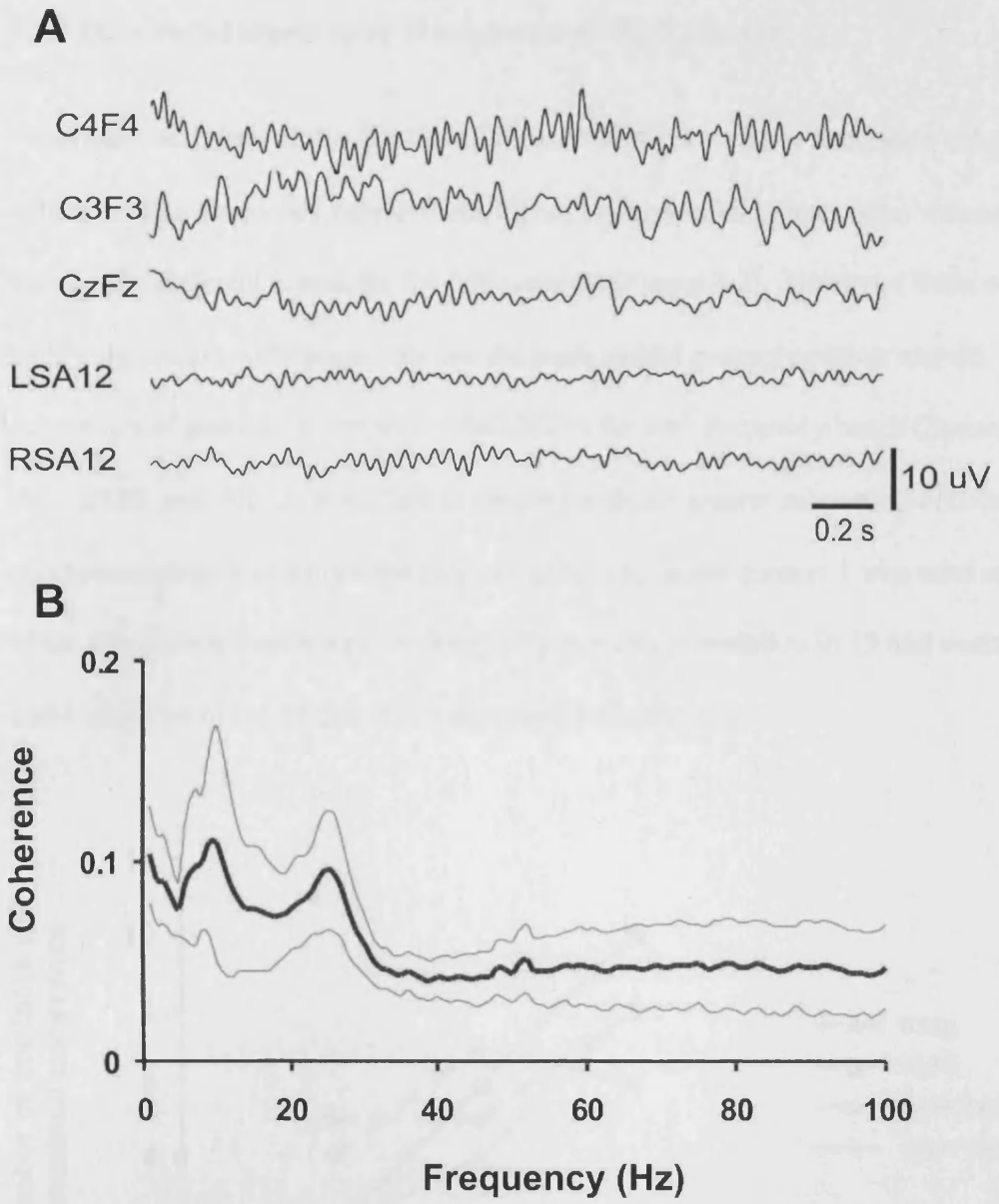

Figure 3.1 Raw signals and coherence peaks. (A) LFP from the right (R) and left (L) SA-ME contact pair with the strongest coherence with EEG and simultaneously recorded EEG in case 8. Note the beta frequency band activity in the SA-LFP (signals low pass filtered at 40 Hz to facilitate visualisation of oscillations in the beta band). (B) Spectra of transformed coherence from the six SA-ME bipolar contacts with the six EEG electrode pairs (CzFz, PzCz, C3F3, P3C3, C4F4, P4C4), averaged in each patient and averaged across the 9 subjects. The predominant peaks are in the alpha and upper beta frequency range. Thin lines are the 95% confidence limits.

3.3.2 Differential topography of coherence in the STN area

Friedman's test showed that the distribution of contacts with the maximum coherence within the four frequency bands (theta, alpha, lower beta and upper beta) was not statistically different across the SA-ME contacts (Figure 3.2). However, there was a highly significant correlation between the more caudal contact position and the occurrence of maximal coherence with EEG in the four frequency bands (Spearman's rho =0.850, $p<0.0001$). Note that, in keeping with the greater subcortico-cortical coherence caudally and intended surgical targeting, caudal contact 1 was used as part of the stimulation parameters for chronic therapeutic stimulation in 13 and contacts 0 and 1 in 16 out of the 18 SA-MEs, respectively (Table 3.1).

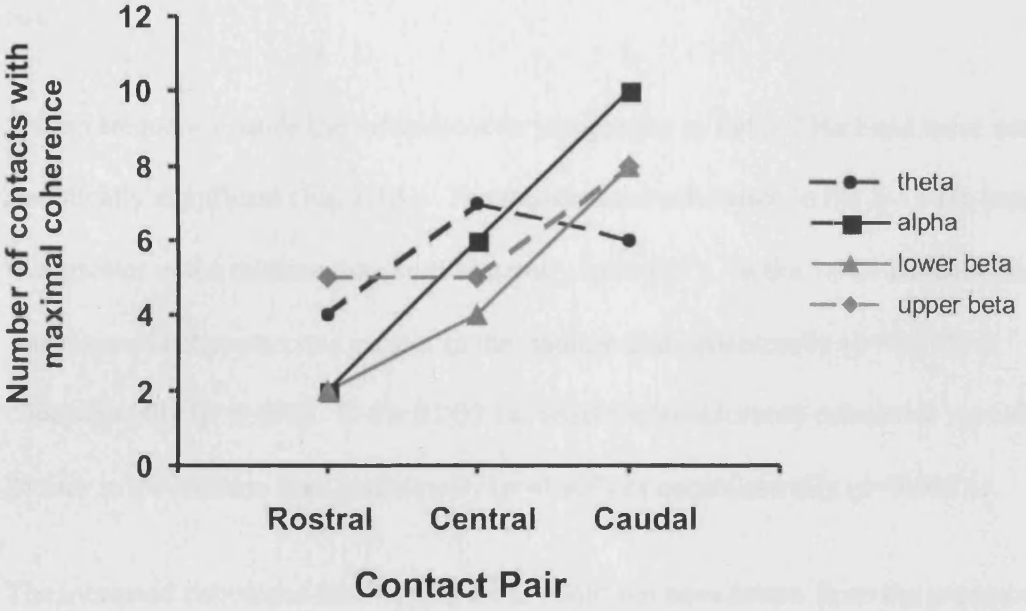

Figure 3.2 Distribution of maximal coherence. The number of contacts with maximal coherence (with Cz-Fz) at the rostral (23), central (12) and caudal (01) bipolar contacts in each of the four frequency bands. The coherence was greatest at the caudal contacts.

3.3.3 Differential topography of coherence at the cortex

Frequency band (3-7 Hz, 8-13 Hz, 14-20 Hz and 21-32 Hz), and area (midline, ipsilateral and contralateral to the SA-ME) were used as factors, in a two-way ANOVA.

There was no main effect for frequency band, but there was a significant main effect for area ($F_{[2,16]} = 21.441$, $p<0.0001$) and an interaction between area and frequency band ($F_{[4,29]} = 4.509$, $p=0.007$).

Mean transformed subcortico-cortical coherence averaged across all four frequency bands was greater in the midline (0.119 ± 0.02) than over lateral areas ipsilateral (0.089 ± 0.02, $p = 0.002$) and contralateral (0.082 ± 0.01, $p < 0.0001$) to the sampled SA.

Within frequency bands the differences in topography in the 3-7 Hz band were not statistically significant (Fig 3.3A). The transformed coherence in the 8-13 Hz band was greater in the midline than contralaterally ($p=0.007$). In the 14-20 Hz band the transformed coherence was greater in the midline than ipsilaterally ($p=0.013$) or contralaterally ($p=0.003$). In the 21-32 Hz band the transformed coherence was also greater in the midline than ipsilaterally ($p=0.007$) or contralaterally ($p=0.005$).

The increased coherence with mesial areas could not have arisen from the presence of burr holes as this would have had the converse effect, leading to elevated coherence in lateral cortical areas close to the burr holes.

Three separate Friedman's tests for each of the three areas across the four frequency bands were used to determine the differences in relative topography between

frequency bands. There were differences between the four frequency bands ipsilaterally ($p=0.004$) and contralaterally ($p=0.013$), but not in the midline (Fig 3.3B).

Post hoc Wilcoxon tests showed that ipsilaterally the relative coherence in the theta ($p=0.028$) and alpha ($p=0.008$) bands was greater than that in the upper beta range. There was also a trend for lower beta to be greater than upper beta ($p=0.051$). Contralaterally, the relative coherence in the theta band exceeded that in the upper beta range ($p=0.038$).

Figure 3.3 illustrates both the absolute and relative mean coherences for the four frequency bands and confirms that the topographical distribution of coherence was different across the frequency bands. Figure 3.3A demonstrates that the topographical distribution of the absolute coherence of lower beta and upper beta is similar with prominence over the midline. Alpha coherence was more evenly distributed over midline and ipsilateral cortex, while coherence in the theta band was fairly evenly distributed over all areas. Figure 3.3B demonstrates that the mean relative coherence of theta and alpha is greater ipsilaterally. There is also a suggestion that the lower beta coherence may be more evenly distributed over midline and ipsilateral cortex, than the upper beta activity.

Figure 3.3 Topography of coherence. Absolute (A) and relative (B) mean transformed coherence at the midline (blue in C), ipsilateral (yellow in C) and contralateral (green in C) to the SA-ME for the four frequency bands; theta, alpha, lower beta and upper beta (9 subjects). Bars = standard errors of mean. Topographic maps (C) illustrating the cortical topography of the coherence in the four frequency bands. Red lines = bipolar electrodes.

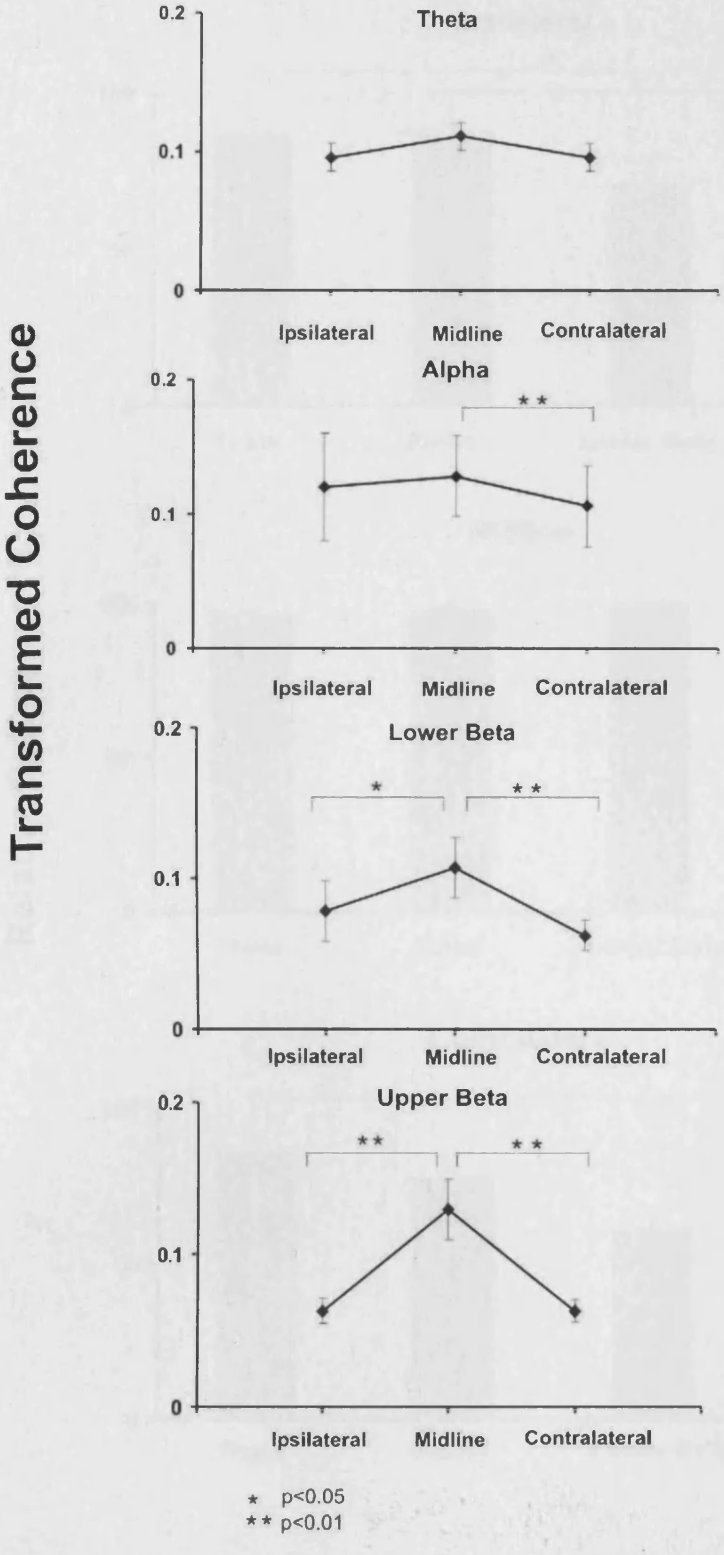
Transformed Coherence
Theta
Alpha
Lower Beta
Upper Beta
0.2
0.1
0
Ipsilateral
Midline
Contralateral
* p<0.05
** p<0.01

Figure 3.3 A

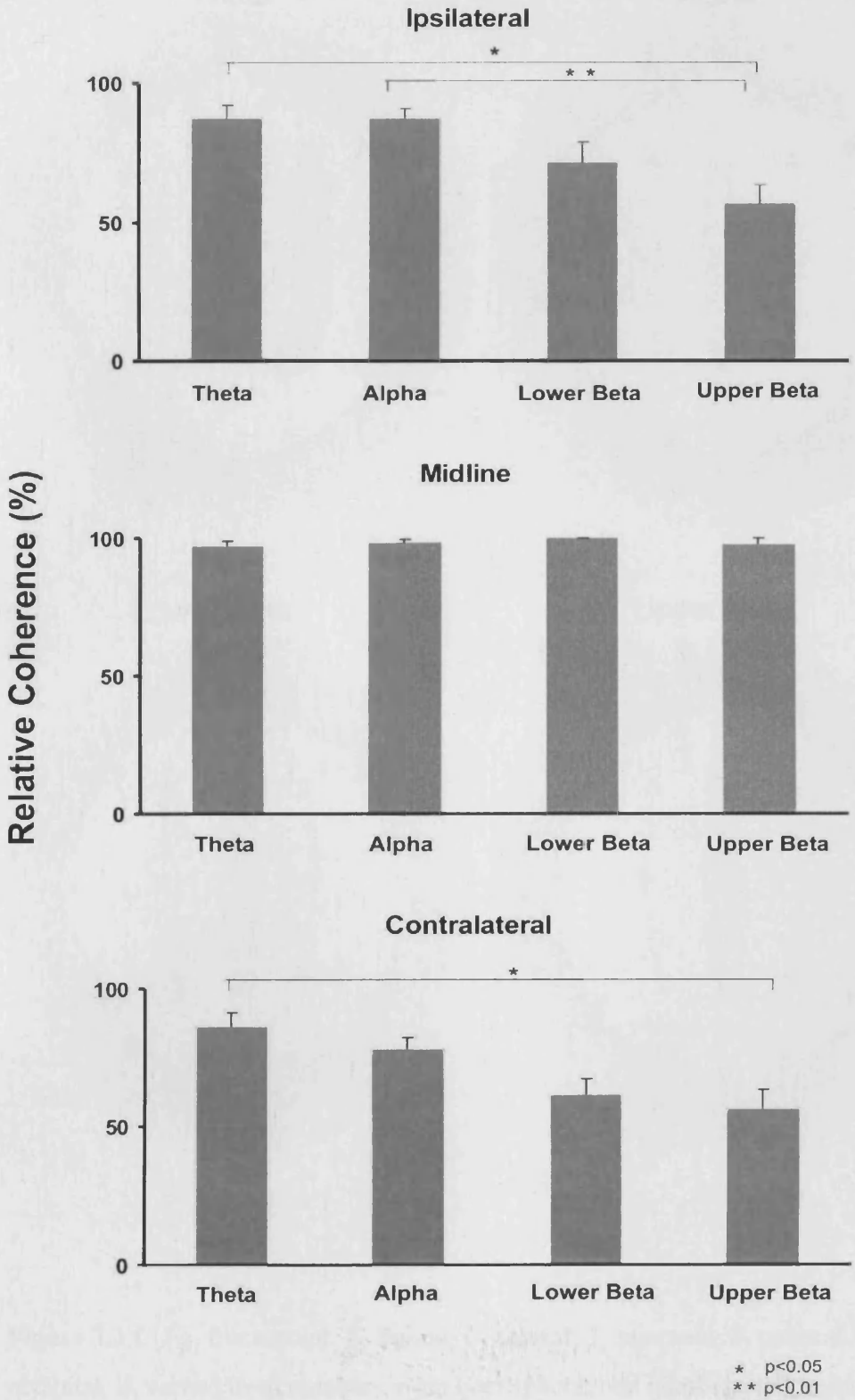
Ipsilateral
*
* *
100
50
0
Theta
Alpha
Lower Beta
Upper Beta
Midline
Relative Coherence (%)
100
50
0
Theta
Alpha
Lower Beta
Upper Beta
Contralateral
*
100
50
0
Theta
Alpha
Lower Beta
Upper Beta
* p<0.05
* * p<0.01

Figure 3.3 B

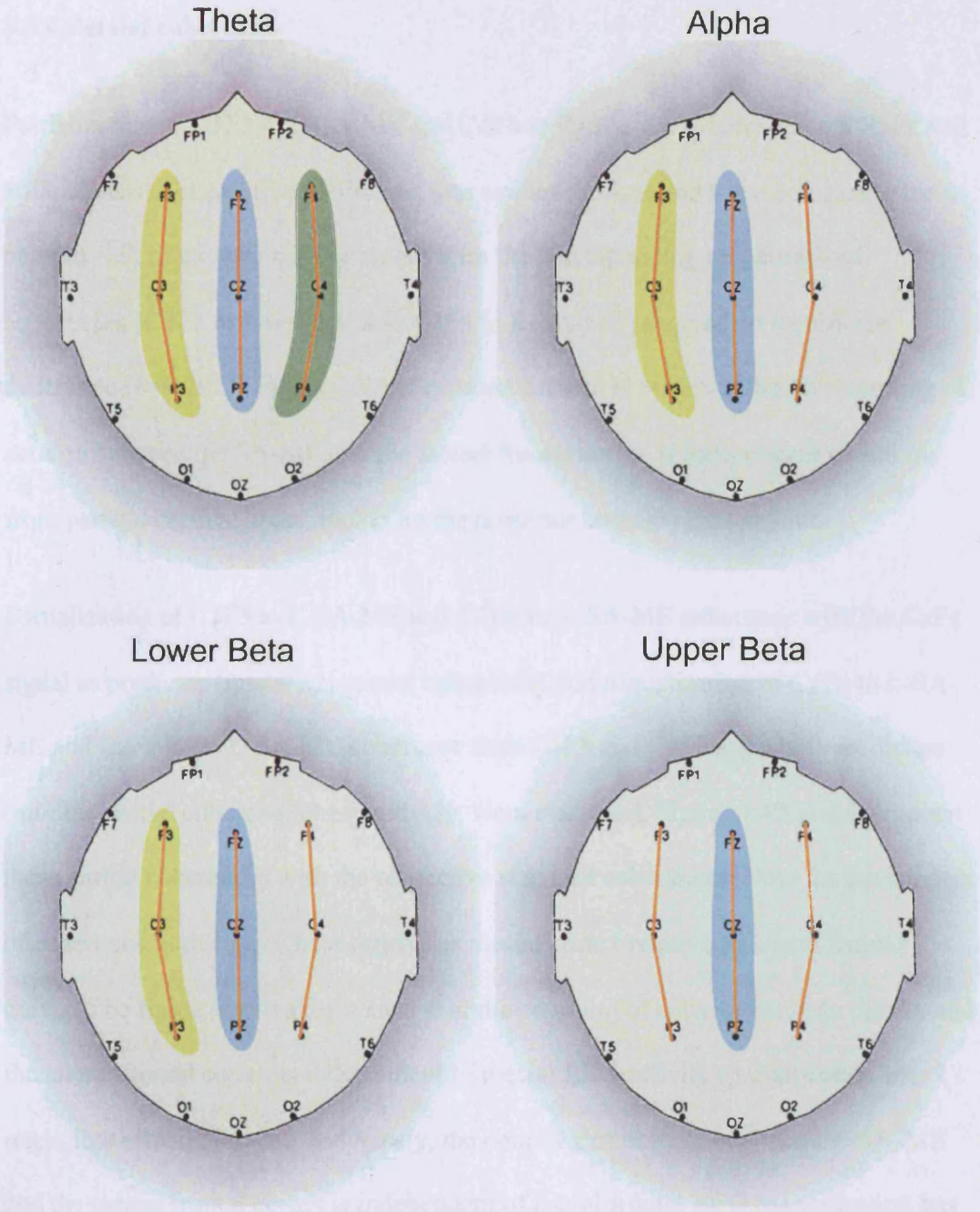

Figure 3.3 C Fp, frontopolar; F, frontal; C, central; T, temporal; P, parietal, O, occipital; Z, vertex; even numbers, right hemisphere; odd numbers, left hemisphere.

3.3.4 Partial coherence

Partialization of C3F3 to L-SA-ME and C4F4 to R-SA-ME coherence with P3Pz and P4Pz signals as respective predictors, was evaluated. A paired t-test comparing the 9 pairs (n=18) of partialized coherences with the corresponding un-partialized coherences (C3F3 to L-SA-ME and C4F4 to R-SA-ME) showed no significant difference (p=0.291). Figure 3.4A illustrates this and is evidence that the coupling of activity between the SA-ME and the lateral frontal cortex is independent of activity from parietal cortical areas, including the posterior cortical alpha rhythm.

Partialization of C3F3 to L-SA-ME and C4F4 to R-SA-ME coherence with the CzFz signal as predictor (ipsilateral partial coherence) and partialization of CzFz to L-SA-ME and CzFz to R- L-SA-ME coherence with C3F3 and C4F4 signals as predictors (midline partial coherence), respectively, were evaluated. Figure 3.4B and C contrast these partial coherences with the respective standard coherences. Note the prominence of coherence in the upper beta band over mesial cortex relative to lateral frontal cortex. The figure also makes it clear that the coupling of activity between the SA and the lateral frontal cortex is independent of mesial EEG activity (partialisation has negligible effect) and that, conversely, the coupling of activity between the SA-ME and the mesial frontal cortex is independent of lateral frontal EEG (partialisation has negligible effect).

Frequency band (3-7 Hz, 8-13 Hz, 14-20 Hz and 21-32 Hz), and area (midline and ipsilateral to the SA-ME) were used as factors, in a two-way ANOVA for the comparison of the topography of the partialized coherences in the four frequencies across the 18 SA-MEs. There was no main effect for frequency band, but there was a significant main effect for area ($F_{[1,17]} = 6.886$, p=0.018) and an interaction between

area and frequency band ($F_{[2,34]} = 6.526$, p=0.004). Mean transformed partial coherence averaged across all four frequency bands was greater in the midline (0.106 $\pm$ 0.01) than over lateral frontal areas (0.079 $\pm$ 0.01, p=0.018). The differences in topography in theta, alpha and lower beta bands between the ipsilateral and midline partial coherence with the SA-ME were not significant (Fig 3.5A). However, the partial coherence of CzFz to SA-ME was greater than that of C3F3/C4F4 to SA-ME in the upper beta band (p<0.0001). The fact that the topographic difference in the upper beta band persisted when lateral and midline partial coherences were studied further indicates that the upper beta's midline prominence was not due to the superimposition of the effects of bilateral burr holes in this area: removal of the effects of EEG recorded near either burr hole (use of C3F3 or C4F4 as predictors) still left mesial coherence that exceeded lateral frontal coherence in this frequency band.

Two separate Friedman's tests for each of the two areas across the four frequency bands were used to determine the differences in relative topography between frequency bands. There were differences between the four frequency bands ipsilaterally (p=0.018) and but not in the midline (Figure 3.5B-C). Post hoc Wilcoxon tests showed that ipsilaterally the relative partial coherence in the theta (p=0.013), alpha (p=0.025) and lower beta (p=0.011) bands was greater than that in the upper beta range (Figure 3.5B), in keeping with the results of standard coherence analysis.

Figure 3.4 Comparison of partial and standard mean transformed coherences. Partial and standard mean transformed coherence (18 sides) of (A) C3F3 to L-SA-ME and C4F4 to R-SA-ME coherences with P3PZ and P4PZ signals as respective predictors, using those SA-ME contacts with highest alpha coherence; (B) C3F3 to L-SA-ME and C4F4 to R-SA-ME coherences with CzFz signal as predictor; and of (C) CzFz to L-SA-ME and CzFz to R-SA-ME coherences with C3F3 and C4F4 signals as respective predictors. For (B) and (C) SA-ME bipolar contacts with the highest coherence in the upper beta band were used. Note that partialization of C3F3 to L-SA-ME and C4F4 to R-SA-ME coherence with CzFz signal as predictor had a paradoxical effect in that coherence in the beta band was actually increased relative to the standard coherence spectrum. This may arise because removal of the CzFz effect by partialization is equivalent to eliminating a 'noise term' from the C3F3 to L-SA-ME and C4F4 to R-SA-ME coherence (Lopes da Silva et al., 1980). Removing this noise term leads to a relative increase of the frequency components shared by lateral frontal cortical areas and the SA-ME, and is further evidence of the independence of coupling of lateral and mesial frontal cortical areas with SA-ME recorded activity.

Figure 3.5 Topography of partial coherence. Absolute (A) and relative (B-C) mean transformed partial coherence of C3F3 to L-SA-ME and C4F4 to R-SA-ME coherences with CzFz signal as predictor; and of CzFz to L-SA-ME and CzFz to R-SA-ME coherences with C3F3 and C4F4 signals as respective predictors for the four frequency bands (18 sides). Bars = standard errors of mean.

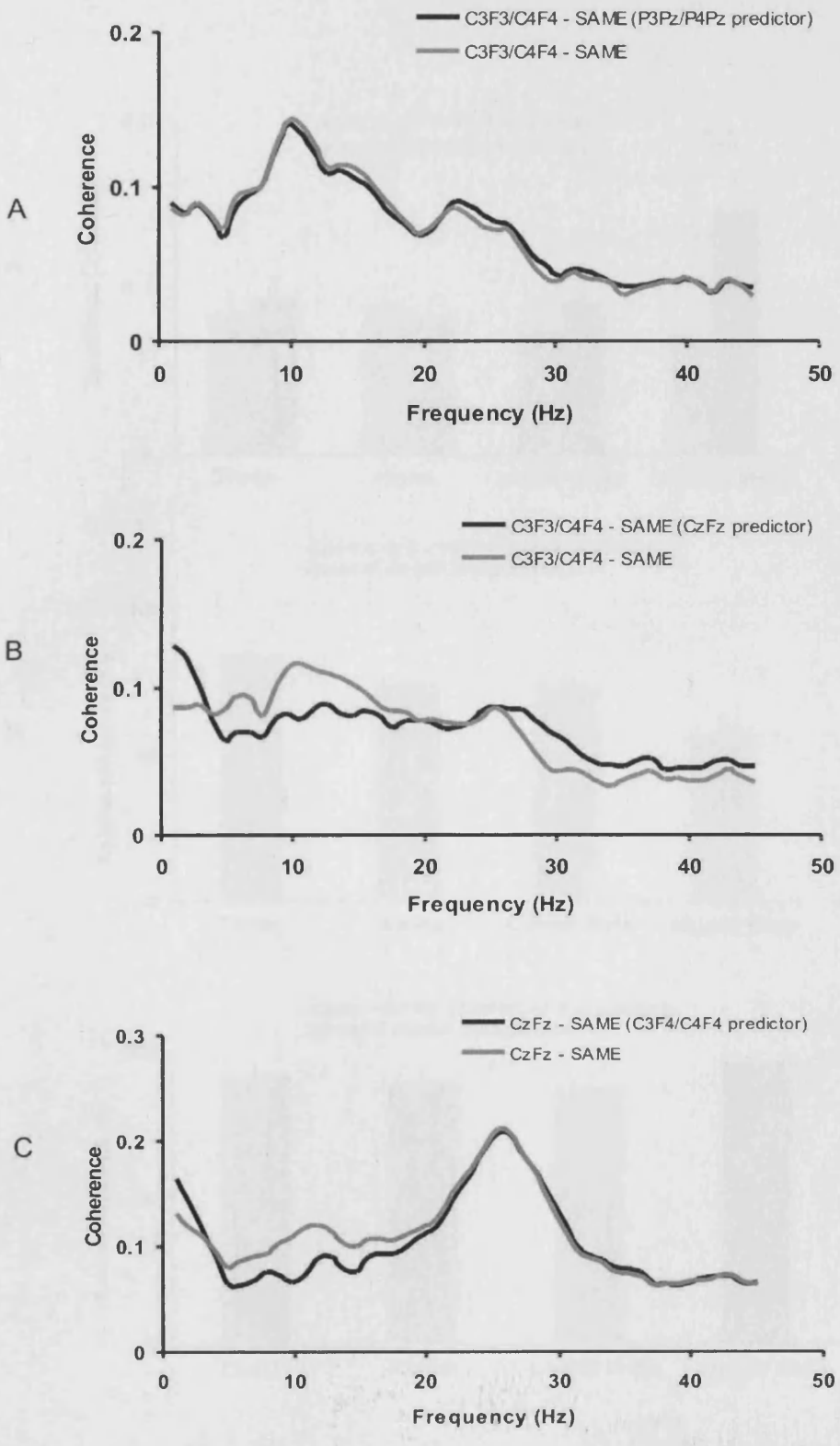
A
C3F3/C4F4 - SAME (P3Pz/P4Pz predictor)
C3F3/C4F4 - SAME
Coherence
0.2
0.1
0
0
10
20
30
40
50
Frequency (Hz)
B
C3F3/C4F4 - SAME (CzFz predictor)
C3F3/C4F4 - SAME
Coherence
0.2
0.1
0
0
10
20
30
40
50
Frequency (Hz)
C
CzFz - SAME (C3F4/C4F4 predictor)
CzFz - SAME
Coherence
0.3
0.2
0.1
0
0
10
20
30
40
50
Frequency (Hz)

Figure 3.4

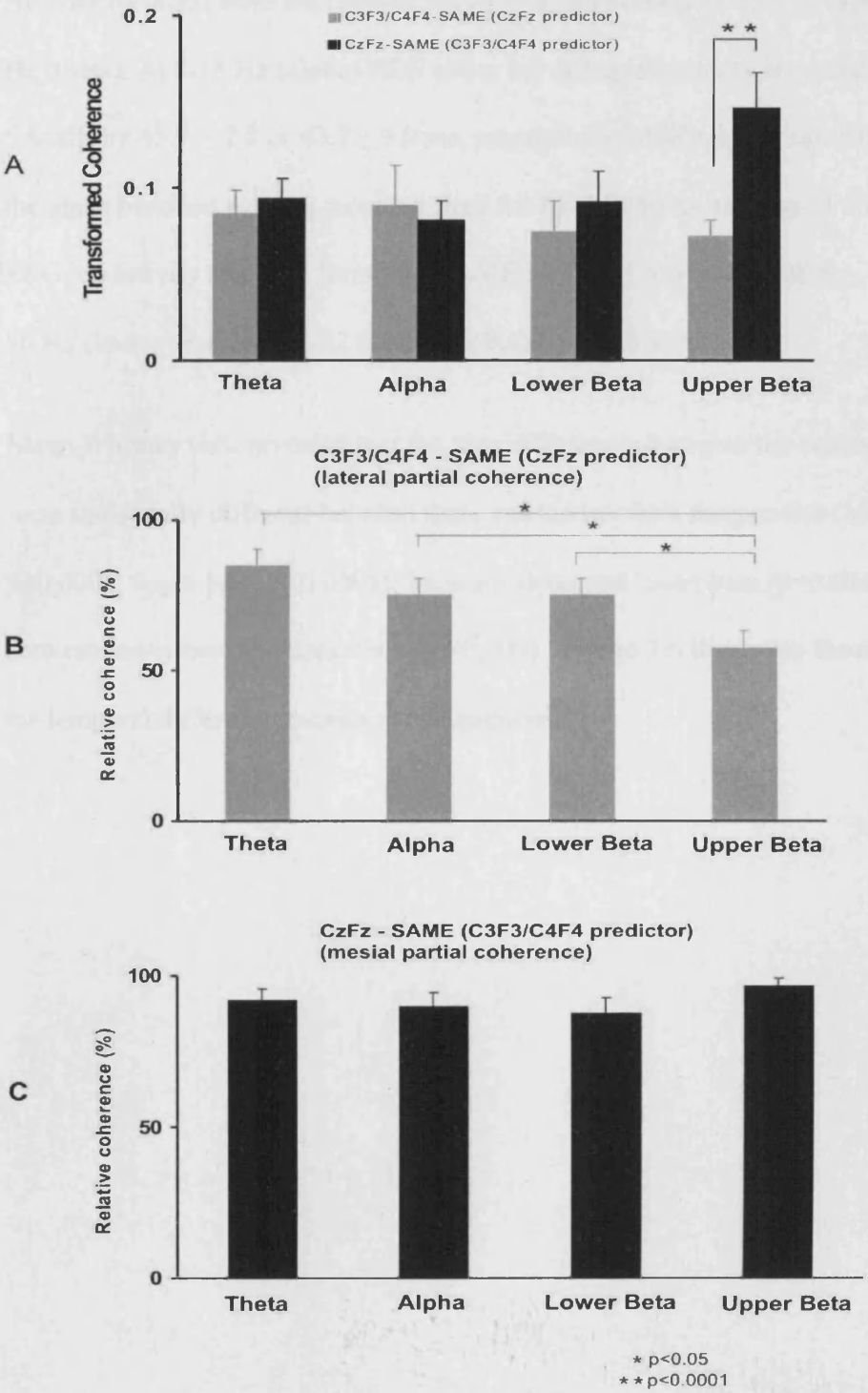
A
0.2
0.1
0
Transformed Coherence
C3F3/C4F4-SAME (CzFz predictor)
CzFz-SAME (C3F3/C4F4 predictor)
* *
Theta
Alpha
Lower Beta
Upper Beta
B
C3F3/C4F4 - SAME (CzFz predictor)
(lateral partial coherence)
100
50
0
Relative coherence (%)
*
*
*
Theta
Alpha
Lower Beta
Upper Beta
C
CzFz - SAME (C3F3/C4F4 predictor)
(mesial partial coherence)
100
50
0
Relative coherence (%)
Theta
Alpha
Lower Beta
Upper Beta
* p<0.05
* * p<0.0001

Figure 3.5

3.3.5 Phase

Activity recorded from the SA-ME led EEG by an average of 35.1 $\pm$ 13.8 ms at 3-7 Hz (theta). At 8-13 Hz (alpha) EEG either led or lagged activity recorded from the SA-ME by 45.9 $\pm$ 7.5 or 43.7 $\pm$ 9.0 ms, respectively, although, overall EEG activity in the alpha band led activity recorded from the SA-ME by an average of 5.6 $\pm$ 11.7 ms. EEG led activity recorded from the SA-ME by 42.0 $\pm$ 5.0 ms and 28.8 $\pm$ 1.5 ms at 14-20 Hz (lower beta) and 21-32 Hz (upper beta), respectively.

Mann-Whitney tests revealed that the time differences between the cortex and the SA were statistically different between theta and the two beta frequencies (lower beta, $p<0.0001$; upper beta, $p<0.0001$); between alpha and lower beta ($p=0.024$) and also between lower beta and upper beta ($p=0.009$). Figure 3.6 illustrates the distribution of the temporal differences across the frequencies.

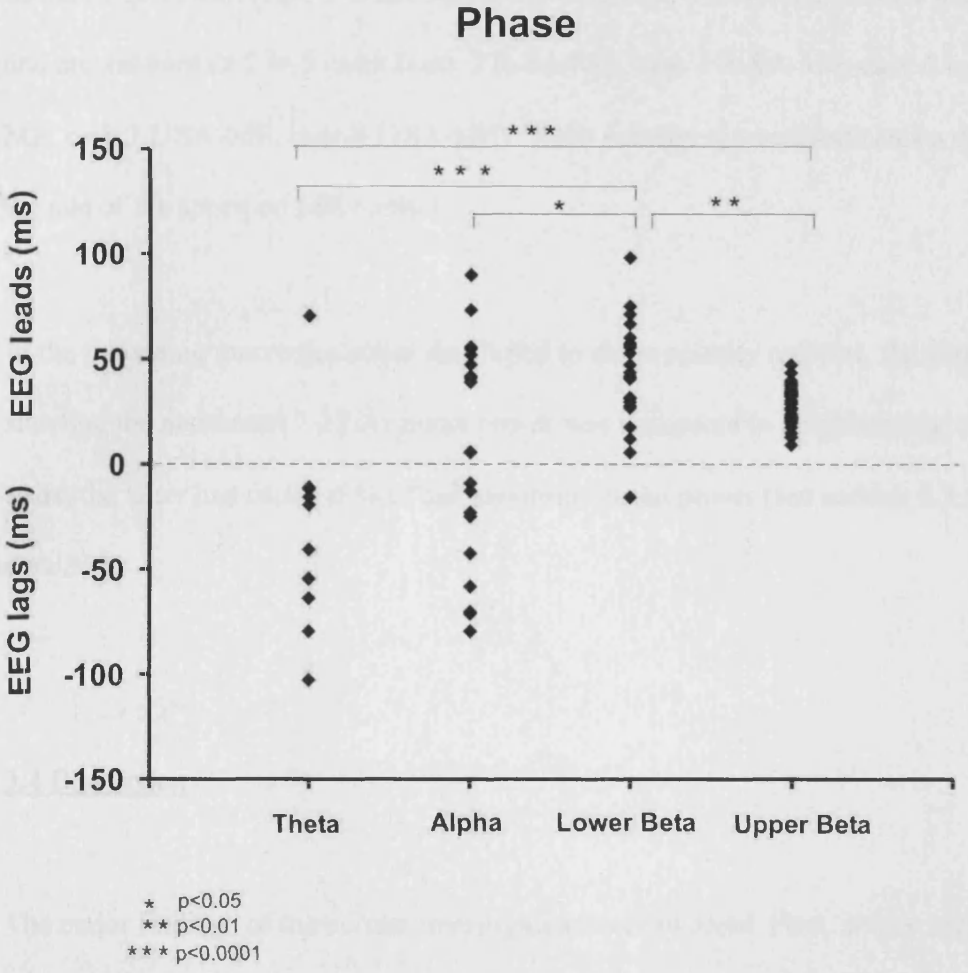

Figure 3.6 The distribution of phase across the four frequencies. SA-ME LFPs led EEG by a mean of 35.1 ± (SEM) 13.8 ms in the theta band, while EEG led the depth LFP by 42.0 ± 5.0 and 28.8 ± 1.5 ms in the lower and upper beta bands, respectively. EEG could lead or lag LFPs by 40 ms in the alpha band.

3.3.6 Polarity reversal

Polarity reversal was observed in 9/18 SA-MEs. Polarity reversal was seen around contact 1 in 4 cases (case 1 L-SA-ME/R-SA-ME, case 4 L-SA-ME, case 9 R-SA-ME) and around contact 2 in 5 cases (case 2 R-SA-ME, case 3 R-SA-ME, case 6 L-SA-ME, case 7 L-SA-ME, case 8 L-SA-ME). Such polarity reversal indicates a dipole at the site of the specified ME contact.

In the remaining macroelectrodes that failed to show polarity reversal, the contact pair showing the maximum 7-32 Hz mean power was compared to neighbouring contact pairs, the latter had 68.9 ± 6 % of the maximum mean power (see section 2.3.5 for details).

3.4 Discussion

The major findings of the current investigation were twofold. First, it was found that there is a strong coupling between LFP activities recorded with MEs in the STN area (SA) and cortical EEG over a wide range of frequencies in the untreated parkinsonian patient. This coupling was greatest in the alpha and upper beta bands, and not at rest tremor frequencies. Second, it was demonstrated that oscillatory activities within different frequency bands in the SA-cortical loop are partially functionally segregated into circuits that may have their own pathophysiological relevance.

The study of partial coherences demonstrated that the coupling of activity between the SA and the lateral frontal cortex was independent of mesial EEG activity and that,

conversely, the coupling of activity between the SA and the mesial frontal cortex was independent of lateral frontal EEG. In addition, the use of partial coherence showed that coupling between lateral frontal cortex and the SA was independent of posterior cortical activity, especially the posterior alpha rhythm. Coherent subcortico-cortical loops of different frequency were not only topographically organised at the cortex, but also characterised by differences in phase relationships between EEG and SA. These results extend the findings of Williams et al. (2002) that suggested differences in the cortical topography of STN-cortical coupling when coherence was divided into activities below and above 10 Hz in four subjects.

3.4.1 Experimental limitations

Before considering the findings of this study in greater detail some of the limitations of the experimental approach should be stressed.

First, as discussed in section 2.1.3, without histological verification of electrode site or support from post-operative imaging, placement in STN should be considered presumptive, even though the surgical coordinates were those of STN. The conclusion that the macroelectrodes were in the SA is supported by the effectiveness of intra-operative and chronic post-operative stimulation and the ability to significantly reduce antiparkinsonian medication post-operatively. The significant increase in coherence between EEG and LFPs from rostral to caudal contacts of the SA-MEs and the predominant use of caudal contacts for clinical stimulation also suggests that the surgery was consistent in achieving similar placement across patients, with contact 1 intended to be in STN.

Second, with regards to the question of volume conduction of synchronous activity from sources such as the cerebral cortex, as discussed in section 2.2.5 bipolar recordings were were used to try and avoid this problem. In addition, as mentioned above, recordings from adjacent macroelectrode contact pairs showed a clearly increasing rostral to caudal gradient inconsistent with volume conduction of cortical activity. Furthermore, there were significant temporal differences between the cortical and depth signals that were incompatible with volume conduction. Finally, the polarity reversal evident in 50% of the recorded sides is a good indication that the 7-32 Hz activity is locally generated at the site of the polarity reversal.

Third, the possibility should be considered that some or all of the coherent activities shown in this study are harmonically related, in which case they might represent non-sinusoidal components in the same basic pattern of oscillation, rather than independently generated biological rhythms. Very much against this possibility, however, is the fact that activities in the various pass-bands differed both in their cortical topography and in their phase relationships.

Finally, the contribution of the burr holes to the cortical topography of the coherence should be considered. C3 and C4 were only just anterior to the burr holes required for surgical implantation, and the local skull breech would have reduced the local filtering effects of the skull and other interposing tissues, leading to higher EEG voltages over local scalp areas. Nevertheless, this would have been expected to affect all EEG frequencies equally, if not disproportionately favour higher frequency activities, such as those in the upper beta band (Spehlman, 1981c). Skull breech effects cannot therefore account for the fact that relative SA LFP to EEG coherence was less in the high beta band than in the remaining bands over lateral frontal areas.

Neither can skull breech effects explain why overall, and in the low and high beta frequency bands in particular, SA LFP to EEG coherence was greater over mesial than lateral frontal cortex, given that electrodes in the former region were further from the burr holes.

3.4.2 Is coherence between the subthalamic LFP and EEG in PD pathological or physiological?

A strong coherence was found between the SA LFP and EEG. There is no way of presently establishing whether this coupling is physiological or related to the pathophysiology of Parkinson's disease. However, the results of non-human primate studies and of pharmacological studies in patients suggests that the coherence between the SA LFP and EEG represented, at the very least, a pathological exaggeration of physiological activity. Thus treatment with levodopa or apomorphine suppresses oscillatory beta activity in STN and STN-EEG coherence in PD (Levy et al., 2000; Cassidy et al., 2002; Williams et al., 2002), while recordings in healthy primates demonstrate relatively little synchronisation of neuronal activity within STN (Wichmann et al., 1994 a,b). On the other hand, cortical synchronisation does occur within the bands considered (Steriade et al., 1990), and there is evidence for physiologically reactive beta synchronisation in the basal ganglia (albeit not STN) in monkeys and humans (Courtemanche et al., 2003; Sochurkova and Rektor, 2003). It is concluded that the coherence between the SA LFP and EEG in the untreated PD patients in this study was, at least in part, likely to be due to a pathological exaggeration of physiological activity.

One of the major findings in the current study was the demonstration of a partial functional segregation of oscillatory activities within different frequency bands in

loops linking the SA with cerebral cortex. The question arises as to whether this pattern of organisation was primarily physiological or related to the pathophysiology of Parkinson's disease. It is difficult to say, however, several studies have shown evidence of a loss of functional segregation in PD, and have suggested that even more segregation might be evident in the healthy human (Filion et al., 1994; Nini et al., 1995; Bergman et al., 1998; Levy et al., 2000).

3.4.3 Quantitive differences between subcortico-cortical coupling over different frequency ranges

The coupling between LFP activities recorded with SA MEs and cortical EEG did not decay monotonically with frequency, but demonstrated clear peaks in the alpha and upper beta bands. Activities in the theta band, similar in frequency to parkinsonian rest tremor, and in the lower beta range were far less prominent in the cohort of patients in this study. The modest coupling between the SA LFP and EEG in the theta band contrasts with the prominence of tremor related neuronal activity upon microelectrode recordings in STN (Bergman et al., 1994; Levy et al., 2002b). However, although tremor related STN activity may occur in the theta band, this may not be coupled to activity in the cortex. This would be of importance, as it would undermine theories that seek to explain bradykinesia through the effect of propagated synchronisation at rest tremor frequencies on the cortex (Brown and Marsden, 1998). Indeed the extent of synchronisation of STN activity at rest tremor frequencies is uncertain. Thus, unlike activity in the beta band, the phase between pairs of STN units varies in the rest tremor range, indicating imperfect synchronisation (Levy et al., 2000). Furthermore, at least in GPi, neuronal activity at rest tremor frequencies is only

transiently locked to rest tremor, suggesting that there may be multiple, independent tremor generators, rather than global synchronisation at rest tremor frequencies (Hurtado et al., 1999). Consistent with this, PD tremor is largely asynchronous between limbs and sides of the body (Hurtado et al., 2000).

On the other hand it could be posited that the major effect of tremor related neuronal activity on the cortex is exercised through oscillatory activity at harmonically related frequencies in the alpha band. This would be consistent with reports of rest tremor locking with cortical activity at harmonically related frequencies (Hellwig et al., 2000; Salenius et al., 2002; Timmermann et al., 2003). It is noteworthy that the phase relationships between oscillations in the alpha band suggests that this oscillation in the SA consisted of two activities, one that is driven by cortex and was likely to be independent of the activity in the theta band, and another which, like theta, tended to drive cortex. The latter cortical driving alpha activity may possibly reflect a harmonic of rest tremor activity.

Another feature of interest was the dominance of subcortico-cortical coupling in the upper beta band over that in the lower beta band. This is in accordance with the results of Priori and colleagues (2002) who demonstrated a preponderance of LFP activity in the upper beta range in STN recordings, but of low beta activity in the GPi. This led these authors to suggest that oscillatory activity in the upper beta range is particularly characteristic of the indirect pathway. Nevertheless, it should be stressed that two patients in the present study had greater coherence with cortex in the lower beta band, so any preferential tuning of rhythmic activity in the SA to the upper beta range is not universal.

3.4.4 Topography of subcortico-cortical coupling

The coherence between SA LFPs and cortical EEG over different bands tended to involve different cortical regions. Coherence in the theta band was widespread, involving mesial and both lateral areas, and similar to the cortical distribution of modulatory STN activity in 6-OHDA rats (see section 1.5.2.1) as reported by Steiner and Kitai (2001). In contrast, coherence in the alpha band preferentially occurred between SA LFPs in both the mesial and ipsilateral cortex, while that in the upper beta band principally involved mesial motor areas, including the supplementary motor area. There is also a suggestion that coherence in the lower beta range involved ipsilateral areas more than that in the upper beta band. These findings are mirrored in the distribution of cortical beta activity. In particular, there is recent evidence that the beta activity recorded in the EEG of healthy individuals consists of a lower beta activity (around 15 Hz) that is most evident over the sensorimotor corticies and upper beta activity (centred around 25 Hz) that predominates over the mesial cortical regions, including the supplementary motor area (Pfurtscheller et al., 1997; 2003). It is noteworthy that mesial motor cortical areas are believed to be more involved in internally than externally generated movements (Jenkins et al., 2000) and it is internally generated movement that is most impaired in PD. In line with this, positron emission tomography studies in PD patients show underactivity of SMA and anterior cingulate cortex in internally cued movement tasks (Samuel et al., 1997). It may therefore be relevant that the major SA LFP activity in the beta band occupied the upper range and was coupled with mesial rather than lateral cortical areas.

3.4.5 Phase relationships between SA LFPs and cortical EEG

The coherence between SA LFPs and cortical EEG over different bands was accompanied by frequency selective phase relationships between cortex and the SA; further evidence that coupling at different frequencies reflected functionally segregated activities. SA LFP activity led EEG in the theta band, consistent with the driving of GPi by STN at tremor frequency (Brown et al., 2001) and with the observation that activity in GPi's thalamic projection site, the ventralis anterior thalami, precedes cortical activity (Volkmann et al., 1996). Together these studies suggest the net driving of motor cortical areas at tremor frequencies through the STN-GPi-thalamo-cortical pathway. As discussed in section 3.4.3, the situation is less clear in the alpha band as the phase seems to be determined by two activities, one with cortex and the other with the SA leading.

In contrast, EEG led SA LFPs in the lower beta and upper beta bands, in keeping with previous reports (Marsden et al., 2001; Williams et al., 2002). In the upper beta band EEG led by about 20 ms. This is likely to be longer than the conduction time in 'hyperdirect' cortico-subthalamic projections. Stimuli applied within the motor cortex of the monkey facilitate STN neurones with a mean latency of 5.8 ms (Nambu et al., 2000) and frontal cortical potentials may be elicited with a latency of 5-8 ms after probable antidromic activation of the direct cortico-subthalamic pathways in humans (Ashby et al., 2001). Thus the cortical lead of 20 ms or so suggests involvement of the indirect corticostriatal-GPe-STN pathway (Alexander and Crutcher, 1990; Parent and Hazrati, 1995). Consistent with the above, synchronisation has been noted within the beta band in the striatum of healthy primates (Courtemanche et al., 2003) and animals treated with MPTP or dopaminergic antagonists, as determined by

microelectrode and LFP recordings (Yurek and Randall, 1991; Dimpfel et al., 1992; Raz et al., 2001). Note that the cortical lead was longer in the lower beta than the upper beta band, further evidence of the functional heterogeneity of coupling in the two beta bands and suggesting lower beta cortical drive has longer nuclear delays or more indirect transmission that the upper beta drive.

3.4.6 Multiple functionally distinct oscillatory subcortico-cortical loops

The major significance of the present findings is that they suggest the presence of multiple oscillatory circuits between the SA and cerebral cortical motor areas, distinguished by their frequency, cortical topography and temporal relationships even in the same pharmacological state of PD patients withdrawn from antiparkinsonian medication. Previously, Williams et al. (2002) have also drawn attention to the functional differences between oscillatory activities in the STN-cortical circuit in PD patients off and on medication. Thus the 'motor circuit' promoted in the Albin-DeLong model (Albin et al., 1989; DeLong, 1990) may, in functional terms, consist of several, largely segregated sub-loops coupling basal ganglia and cortical activities. Coherent activity in these sub-loops preferentially occurs in distinct frequency bands, perhaps reflecting the different resonance properties of the networks concerned. It is possible that the frequency of synchronisation may be exploited as a means of marking and segregating processing in the different functional sub-loops, over and above any anatomical segregation of processing streams. A prediction of the latter that remains to be tested is that synchronisation within different frequency bands may be associated with different functional deficits in PD. In addition, the strong coherence within the different bands in patients off medication suggests that large

neuronal populations are synchronised within these functional sub-loops. Dopaminergic stimulation reduces STN-cortical coupling at frequencies under 30 Hz (Cassidy et al., 2002; Williams et al., 2002), presumably by reducing the synchronisation between neurons within the functional sub-loops dominating in the off-state. Thus, the significant coupling of SA LFPs with cortical activities in untreated PD patients may be considered further evidence of an impairment of functional segregation in PD (Filion et al., 1994; Nini et al., 1995; Bergman et al., 1998; Levy et al., 2000), while also demonstrating that the subcortico-cortical loops involving the SA have the capacity to preserve information about the timing of activity in groups of neurons across multiple intervening levels (Kimpo et al., 2003).

3.5 Summary of key points

- Coherence between EEG and SA LFPs was apparent in the theta (3-7 Hz), alpha (8-13 Hz), lower beta (14-20 Hz) and upper beta (21-32 Hz) bands, although activity in the alpha and upper beta bands dominated.
- Theta coherence predominantly involved mesial and lateral areas, alpha and lower beta coherence the mesial and ipsilateral motor areas, and upper beta coherence the midline cortex.
- SA LFPs led EEG in the theta band. In contrast, EEG led the depth LFP in the lower and upper beta bands. SA LFP activity in the alpha band could either lead or lag EEG.
- There are several functional sub-loops between the subthalamic area and cerebral cortical motor regions, distinguished by their frequency, cortical topography and temporal relationships.
- Tuning to distinct frequencies may provide a means of marking and segregating related processing, over and above any anatomical segregation of processing streams.

CHAPTER 4: Reciprocal interactions between oscillatory activities of different frequencies in the subthalamic region of patients with Parkinson's disease

4.1 Introduction

This study investigated whether there is an inverse relationship between local synchronisation at high gamma frequencies (65-85 Hz) and that at the lower frequencies implicated in bradykinesia. In the beta band, at least, there is some evidence to support this, as beta and gamma LFP activities behave in a reciprocal pattern during movement and when untreated and treated conditions are compared (Levy et al., 2002a; Cassidy et al., 2002; Williams et al., 2003; section 1.5.2.2). However, both instances involve the comparison between two very different states, so that differences in LFPs might be epiphenomenal. Any reciprocal relationship between gamma activity and tremor related oscillations is less clear as the evidence points to a net increase in LFP power following levodopa treatment (Silberstein et al., 2003; Priori et al., 2004). More significant evidence for the reciprocal nature of population synchrony at high and low frequencies would come from the demonstration of a spontaneous negative correlation between activities at low frequency and those at 65-85 Hz across short time epochs at rest, *i.e.* in the absence of gross state changes.

In this study the functional relationship between LFP activity in the 5-32 Hz and the 65-85 Hz bands was investigated by determining whether spontaneous fluctuations in their strength are correlated across time. To this end, recordings of LFPs from

macroelectrodes inserted in the subthalamic area of PD patients, after the administration of levodopa, were analysed. Part of the study has been published (Fogelson et al., 2005b).

4.2 Methods

4.2.1 Patients and surgery

Sixteen patients were studied (mean age, 54.9, range 37 to 72 years, 5 female, mean PD duration, 13.8, range 6 to 27 years) in whom the presence or absence of concurrent dyskinesias were documented and in whom a peak over 65-85 Hz in the power spectra of the LFPs from one or both subthalamic macroelectrodes was demonstrated. The clinical details of the patients are summarised in Table 4.1. Each patient had bilateral implantation of STN for treatment of their parkinsonism (section 2.1.2). Intraoperative electrode localization was tested by macro-stimulation in all patients. Microelectrode recordings were performed with a single microelectrode in cases 2, 3, 6, 7, 10, 11, and 16. All patients had post-operative MRI (except cases 1, 12 and 13 who were not imaged post-operatively, and case 6 who had a post-operative CT head). Post-operative imaging was consistent with the placement of at least one macroelectrode contact in the STN, where available, and was independently evaluated (blind to the electrophysiological data) by a neurosurgeon. The mean improvement in UPDRS motor score on and off bilateral stimulation was 50.4 ± (SEM) 5.1 % for the 16 patients (using pre-operative off scores in cases 1,7,12 and 13 in whom post-operative off scores were not recorded, see Table 4.1, or 51.3 ± 6 % for the 12 patients in whom postoperative off scores were available). Clinical post-operative scores and assessments of stimulation parameters were performed blind to the electrophysiological results.

Table 4.1 Clinical details. RT = Right; LT= Left; L-dopa was combined with a decarboxylase inhibitor.

Case	Sex/ Age (yrs)	Duration of PD (yrs)	Surgical centre	Pre-operative medication (daily dose in mg)	Pre-op Off/On drugs, UPDRS III	Post-op Off/On DBS, Off drugs, UPDRS III	Side (s)	Time of maximum negative correlation post levodopa (mins)	Dyskinesia in limbs contralateral to LFPs during recording*	Tremor in limbs contralateral to LFPs during recording	Frequency of maximum negative correlation (Hz) , and the corresponding r-value	Frequency of maximum gamma power (Hz)
1	M/56	11	Amsterdam	Levodopa 1900, pergolide 3, amantadine 200, entacapone 800	44/12	-/31	RT LT	47	RT Mild (1/4) LT Mild (1/4)	None None	75-22 (r=-0.30,p=0.0005) 74-22 (r=-0.30,p=0.0006)	74 72
2	F/56	9	Rome	Levodopa 1150, amantadine 100	61/47	74/20	RT	120	None	None	72-9 (r=-0.56,p=0.008)	71
3	F/69	15	Messina	Levodopa 1000, pramipexole 3	69/10	60/7	LT RT	90	Mild (1/4) Mild (1/4)	None None	79-28 (r=-0.23,p=0.004) None	81 79
4	M/37	10	Rome	Levodopa 150, ropinirole 4	65/7	66/48	RT	25	Mild (1/4)	None	69-23 (r=-0.34,p=0.004)	68
5	F/42	6	London	Levodopa 500, Cabergoline 6, Amantadine 400	61/13	61/14	RT	40	None	None	75-6 (r=-0.42,p=0.002)	73
6	F/49	17	Rome	Levodopa 1500, pergolide 1.5	80/12	62/39	LT	45	Severe (3/4)	None	70-30 (r=-0.46,p=0.002)	68
7	M/54	13	London	Levodopa 450, cabergoline 10, apomorphine 50, amantadine 100	70/28	-/50	LT RT	60	Mild (1/4) Mild (1/4)	Slight (1/4) None	80-18/19 (r=-0.25,p=0.048) None	79 80

Case	Sex/ Age (yrs)	Duration of PD (yrs)	Surgical centre	Pre-operative medication (daily dose in mg)	Pre-op Off/On drugs, UPDRS III	Post-op Off/On DBS, Off drugs, UPDRS III	Side (s)	Time of maximum negative correlation post levodopa (mins)	Dyskinesia in limbs contralateral to LFPs during recording*	Tremor in limbs contralateral to LFPs during recording	Frequency of maximum negative correlation (Hz), and the corresponding r-value	Frequency of maximum gamma power (Hz)
8	M/72	19	Berlin	Levodopa 1300, cabergoline 2.5, clozapine 50	51/27	60/25	LT RT	60	Severe (3/4) Severe (3/4)	None None	79-21 (r=-0.21,p=0.02) None	77 78
9	M/46	13	London	Levodopa 1000, apomorphine 3-6, pergolide 4, entacapone 600, amantadine 200	63/8	61/21	RT LT	60	Moderate (2/4) Mild (1/4)	None None	72-19 (r=-0.43,p=0.0007) 72-5 (r=-0.43,p=0.0008)	74 73
10	M/62	16	London	Levodopa 900, Entacapone 900, Benxhexol 9	39/21	35/20	LT	40	Moderate (2/4)	None	74-28 (r=-0.35,p=0.02)	75
11	M/62	13	London	Levodopa 300, entacapone 200, cabergoline 4	58/28	63/44	RT	38	Severe (3/4)	None	79-16 (r=-0.29,p=0.02)	78
12	F/56	13	Amsterdam	Levodopa 600, Selegeline 10, Amantadine 300, Entacapone 300	28/6	-/8	RT	42	None	None	74-24 (r=-0.25, p=0.004)	77
13	M/54	11	Amsterdam	Levodopa 500, Benzhexol 4	31/21	-/12	RT	65	None	None	76-31 (r=-0.17, p=0.02)	77

Case	Sex/ Age (yrs)	Duration of PD (yrs)	Surgical centre	Pre-operative medication (daily dose in mg)	Pre-op Off/On drugs, UPDRS III	Post-op Off/On DBS, Off drugs, UPDRS III	Side (s)	Time of maximum negative correlation post levodopa (mins)	Dyskinesia in limbs contralateral to LFPs during recording*	Tremor in limbs contralateral to LFPs during recording	Frequency of maximum negative correlation (Hz), and the corresponding r-value	Frequency of maximum gamma power (Hz)
14	M/37	10	Rome	Levodopa 1300, ropinirole 4	80/15	88/56	RT	None	None	None	None	78
15	M/61	27	Berlin	Levodopa 700, entacapone 600, amantadine 300	52/18	53/26	LT	None	Moderate (2/4)	None	None	81
16	M/65	17	London	Levodopa 750	57/32	56/40	RT	None	Moderate (2/4)	None	None	76

*Dyskinesia rated using the levels of severity described in item 33 of UPDRS simultaneously with LFP recording and only with respect to contralateral limbs.
Case 13 had tremor in the limbs ipsilateral to the LFPs.

4.2.2 Recordings

Subjects were studied a mean of 3.7 days (range 1 to 8 days) after electrode implantation, in the interval between this and subsequent connection to the subcutaneous stimulator. They were recorded while at rest (with the exception of any involuntary dyskinesias) and supine or seated following administration of levodopa (200 mg in a soluble preparation with decarboxylase inhibitor) after an over-night withdrawal of antiparkinsonian medication.

Most patients had only one rest recording performed but serial recordings were available in patients 1, 3, 6 and 11.

Dyskinesias were concurrently assessed with hemibody scores rated during the recording using the levels of severity described in item 33 of the United Parkinsons Disease Rating Scale (UPDRS).

Deep brain activity was recorded from the adjacent four contacts of each macroelectrode in the subthalamic area giving three bipolar recordings; 0-1, 1-2 and 2-3. An electrode on the forehead was used as ground. LFPs were filtered at 1-300 Hz, amplified and sampled at 500 - 2500 Hz and recorded and monitored on line.

4.2.3 Analysis

Records were visually inspected and those contaminated by movement artefact were rejected (4 subjects, 5 sides; details not included in Table 4.1).

Significant peaks in the gamma frequency band were defined as six or more contiguous data points, at 1 Hz resolution, whose average power over 65-85 Hz exceeded that of the bordering 6 data points to the left and right of the spectrum. These were confirmed by control charting (see section 2.3.7 for details). Only changes with probabilities of > 99% were considered. Records from 21 sides in the 16 subjects had significant peaks in the 65-85 Hz band and were analysed.

Data from these 21 recordings were filtered at 2-100 Hz and re-sampled to a common rate of 200 Hz using Spike2 4v.0 interpolation. Mean duration of records was 287 $\pm$ 39 (SEM) seconds (range: 74-575 seconds). Figure 4.1 summarises the stages involved in the core data analysis. Bipolar LFPs picked up by the macroelectrodes from the SA, were decomposed into their spectral components (through Fourier analysis rather than the band pass filtering shown for schematic purposes in Figure 4.1A), and the log transformed power of these components estimated every 4 seconds and correlated across the record (Figure 4.1B). Multiple correlation coefficients were plotted as a matrix (Figure 4.1C).

Spectra were estimated by dividing the data epochs into a number of non-overlapping sections of 1 second duration. Frequency resolution was 1 Hz. Data were Hanning-windowed to control spectral leakage. Spectral analysis was performed using the MATLAB function 'fft'. This function employs a high-speed radix-2 fast Fourier transform algorithm if the data length is a power of two, otherwise a slower mixed-radix algorithm if it is not.

Temporal correlations (see section 2.3.6 for details) were performed on the bipolar macroelectrode contacts with the maximum power in the 65-85 Hz range.

Individual matrices were represented after z-transformation of the correlation coefficients and thresholding of z scores at a level corresponding to the r-value at α=0.05 (Figure 4.1C). In this way, individual matrices contained information about both the significance of correlations between individual spectral components and the significance of these points across the whole distribution of the matrix. To average spectral correlations across patients, matrices were thresholded so that only correlations were shown that were significant at $\alpha = 0.05$ and n-2 degrees of freedom, where n was the number of blocks in the record. Insignificant and significant correlations were given scores of 0 and 1, respectively, and these correlation scores separately averaged for negative and positive correlations across patients (Figure 4.2). In this way, each patient with significant correlations contributed equally to the group average, so that the latter could not be dominated by high correlation coefficients in one or two subjects.

The relevance of negative and positive correlations in data from individual macroelectrodes, was determined. The reasoning here is that the most functionally relevant correlations would involve interactions with the specific frequency of the spectral peak in the 65 – 85 Hz band, which could vary between patients and sides (see Table 4.1). To this end, the number of macroelectrodes that afforded significant negative correlations between activities in the 5-32 Hz frequency range and spectral components at the frequency ($\pm$ 3 Hz) of the maximum value of the peak in the 65-85 Hz band in the respective LFP power spectrum, were assessed (compare Figure 4.1C

with D). Significant correlations received a score of 1 and these scores were then summed for interactions between activities at each frequency in the 5-32 Hz band and all other frequencies between 1 and 99 Hz. Significance was confirmed if the correlation scores at the frequency of the peak in the 65-85 Hz band (± 3 Hz) exceeded the upper 95% confidence limit determined from the correlation scores across all frequencies from 1-99 Hz. This procedure was repeated for positive correlations.

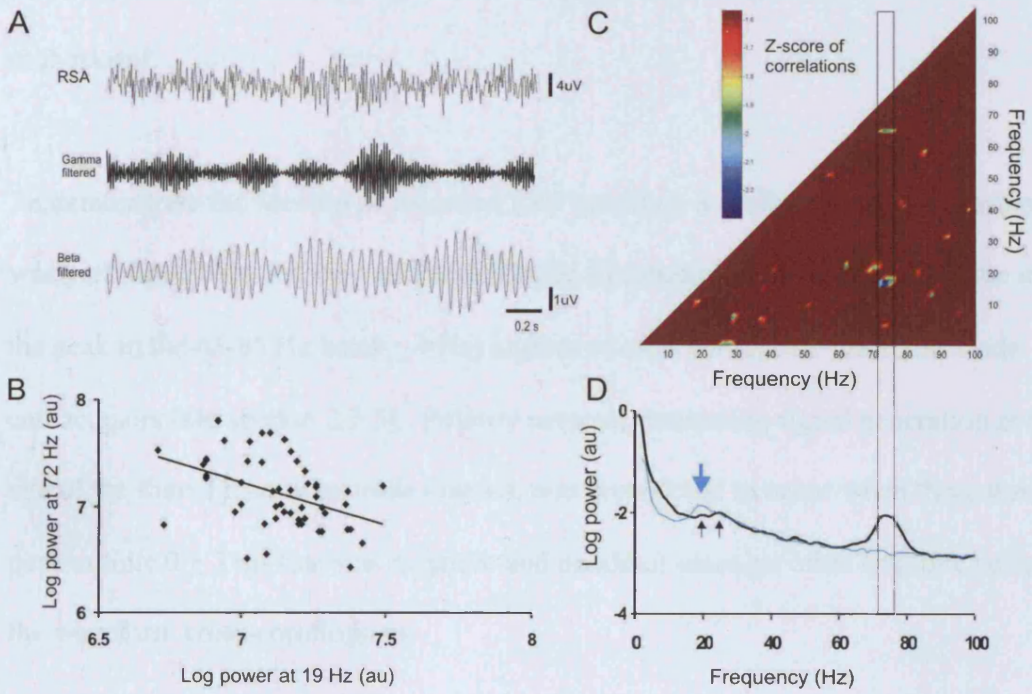

Figure 4.1 LFP recorded from the right subthalamic area (RSA) in case 9. (A) Raw LFP and pass-band filtered LFP in the gamma (72±4Hz) and beta (19±4Hz) frequencies. (B) Corresponding negative correlation for the frequencies of maximum negative correlation (72-19 Hz, r=-0.43, p=0.0007). (C) Matrix of negative correlations (values are z-transformed, and thresholded at a level corresponding to the r-value at α=0.05, *i.e.* in this case a z-score of 1.6) and (D) the corresponding power spectrum. The boxed area in (C) and (D) is the region ± 3Hz either side of the maximum value of the spectral peak in the 65-85 Hz band. Note that there are small peaks at 19 Hz and 21-25 Hz in the power spectrum (D). The activity at 19 Hz was more prominent in the off-medication condition (see thin blue line and blue arrow).

To establish the temporal evolution of negative correlations on a finer temporal scale, log-transformed power at the two frequencies showing maximum negative correlation was recomputed from consecutive 4 second periods and correlations estimated from 10 such points over overlapping 40 second epochs extending across the duration of each record.

To demonstrate the focality of recorded LFP activity a waveform cross-correlation was performed between the pass-band filtered (frequency of the maximum value in the peak in the 65-85 Hz band $\pm$ 4 Hz) signals of adjacent bipolar macroelectrode contact pairs (see section 2.3.5). Polarity reversal, indicating signal generation at the site of the shared macroelectrode contact, was considered to occur when there was a peak at time 0 $\pm$ 3 ms that was negative and maximal amongst other negative peaks in the waveform cross-correlogram.

4.3 Results

4.3.1 Average correlations

The average matrices of negative and positive correlation scores from the 21 sides are displayed in figure 4.2. The major feature in the matrix of scores for negative correlations is the occurrence of significant correlations between activities at 65-85 Hz and those over a band from 5-32 Hz (Figure 4.2A). This was confirmed by a comparison of the mean correlation score per 1 Hz^2 of 0.024 $\pm$ 0.006 for interactions between the 65-85 Hz band and 5-32 Hz activities with the mean correlation score per

1 Hz^2 of 0.012 ± 0.002 for interactions between the 65-85 Hz band and activities over the remaining 33-99 Hz band ($p=0.031$, Wilcoxon's test, $n = 21$).

The major feature in the average matrix of scores for positive correlations is the occurrence of significant correlations between frequencies to be along the diagonal, *i.e.* for activities of a given frequency to positively correlate with themselves or with activities of very similar frequency (Figure 4.2B). However, more importantly, there are no significant positive correlations between 65-85 Hz activities and those within the 5-32 Hz band.

Figure 4.2 Matrix of average negative (A) and positive (B) temporal correlation scores between spectral components of the LFP across 21 sides. Insignificant and significant correlations in individual matrices were scored as 0 and 1, prior to averaging. The matrix was spatially smoothed by averaging each bin across its adjacent bins. Note that significant negative correlations are essentially limited to those between spectral components in the 5-32 Hz and 65-85 Hz bands, compared to the rest of the spectrum. Significant positive correlations are absent at these frequencies, being essentially limited to the diagonal (reflecting autocorrelations). The horizontal and vertical yellow lines mark the 5-32 Hz and 65-85 Hz bands.

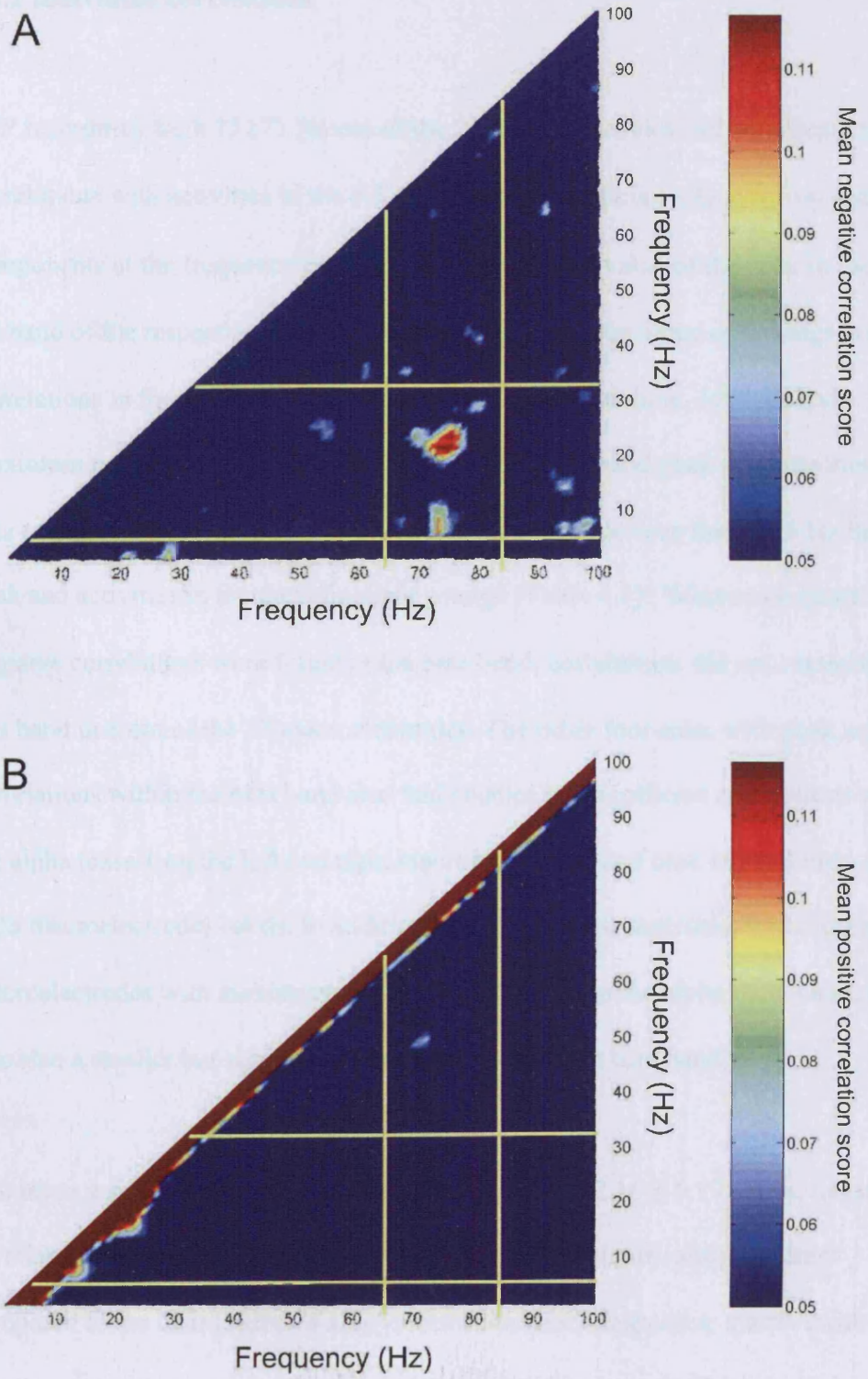
A
100
90
80
70
60
50
40
30
20
10
Frequency (Hz)
10 20 30 40 50 60 70 80 90 100
Frequency (Hz)
0.11
0.1
0.09
0.08
0.07
0.06
0.05
Mean negative correlation score
B
100
90
80
70
60
50
40
30
20
10
Frequency (Hz)
10 20 30 40 50 60 70 80 90 100
Frequency (Hz)
0.11
0.1
0.09
0.08
0.07
0.06
0.05
Mean positive correlation score

Figure 4.2

4.3.2 Individual correlations

LFP recordings from 15 (71 %) out of the 21 macroelectrodes had significant negative correlations with activities in the 5-32 Hz band that preferentially involved spectral components at the frequency (± 3 Hz) of the maximum value of the peak in the 65-85 Hz band of the respective LFP power spectrum. The mean value of the negative correlations in these 15 sides was –0.331 ± 0.028. Out of these, 12 sides had maximum negative correlations between the 65-85 Hz band peak and activities in the beta range, and 3 had maximum negative correlations between the 65-85 Hz band peak and activities in the theta frequency range (Table 4.1). Where maximum negative correlations were found in the beta band, correlations did not extend below this band in 8 out of the 12 macroelectrodes. The other four sides with peak negative correlations within the beta band also had smaller but significant correlations within the alpha (case 1 on the left and right macroelectrodes, and case 10) and theta (case 9 right macroelectrode) bands. In addition, in 1 (case 9 left macroelectrode) out of the 3 macroelectrodes with maximum negative correlations in the alpha-theta band, there was also a smaller but significant correlation within the beta band.

The mean z-score for the 15 negative correlations was 2.16 ± 0.17. Thus, negative correlations between 65-85 Hz and 5-32 Hz were also significantly different compared to the distribution of all r-values across each respective matrix (with a 1 in 65 chance that the mean z-score might have arisen by chance). This was also true when the negative correlations in the beta and theta-alpha band were considered separately (mean z-scores for the negative correlations were 2.10 ± 0.21 and 2.40 ± 0.18 for beta and theta-alpha, respectively).

None of the LFP recordings from the 21 macroelectrodes had significant positive correlations between activities in the 5-32 Hz band and spectral components at the frequency (± 3 Hz) of the maximum value of the peak in the 65-85 Hz band in the respective LFP power spectrum.

4.3.3 Timing of negative correlations and their phenomenological associations

The significant negative correlations from the 15 sides were recorded a mean of 56 minutes (range 25-120 minutes; Table 4.1) after administration of levodopa. Dyskinesias were observed in the limbs contralateral to LFPs *during* the recordings in 11 (73 %) out of 15 sides (Table 4.1). Of these 6 had slight (1/4), 2 moderate (2/4) and 3 prominent (3/4) dyskinesias. On the other-hand slight tremor (1/4) was observed in the limb contralateral to LFPs during the recording on only one side. Significant negative correlations were therefore associated with symptoms of dyskinesia (n=11), more often than tremor (n=1) (two tailed Fisher exact test, p = 0.0001). Note, however, that dyskinesias could occur in the absence of demonstrable negative correlations (*e.g.* case 3 right macroelectrode, case 7 right macroelectrode, case 8 right macroelectrode, cases 15 and 16).

Serial records at different times after the administration of levodopa in 4 of the patients (cases 1, 3, 6, and 11, giving 5 sides) were also available. Thus the strength of the negative correlations within the 65-85 Hz range over time could be investigated within these patients. The strongest negative correlations appeared at an average of 50 minutes (range of 30 to 90 minutes) after levodopa administration. Figure 4.3A and B illustrate the timing of peak dyskinesia with respect to the correlations in cases

1 (right macroelectrode) and 6. The negative correlations between 65-85 Hz and beta activity were strongest at 45-47 minutes, and dropped to insignificant levels 55-95 minutes after a test dose of levodopa, despite the patients remaining ON during this time.

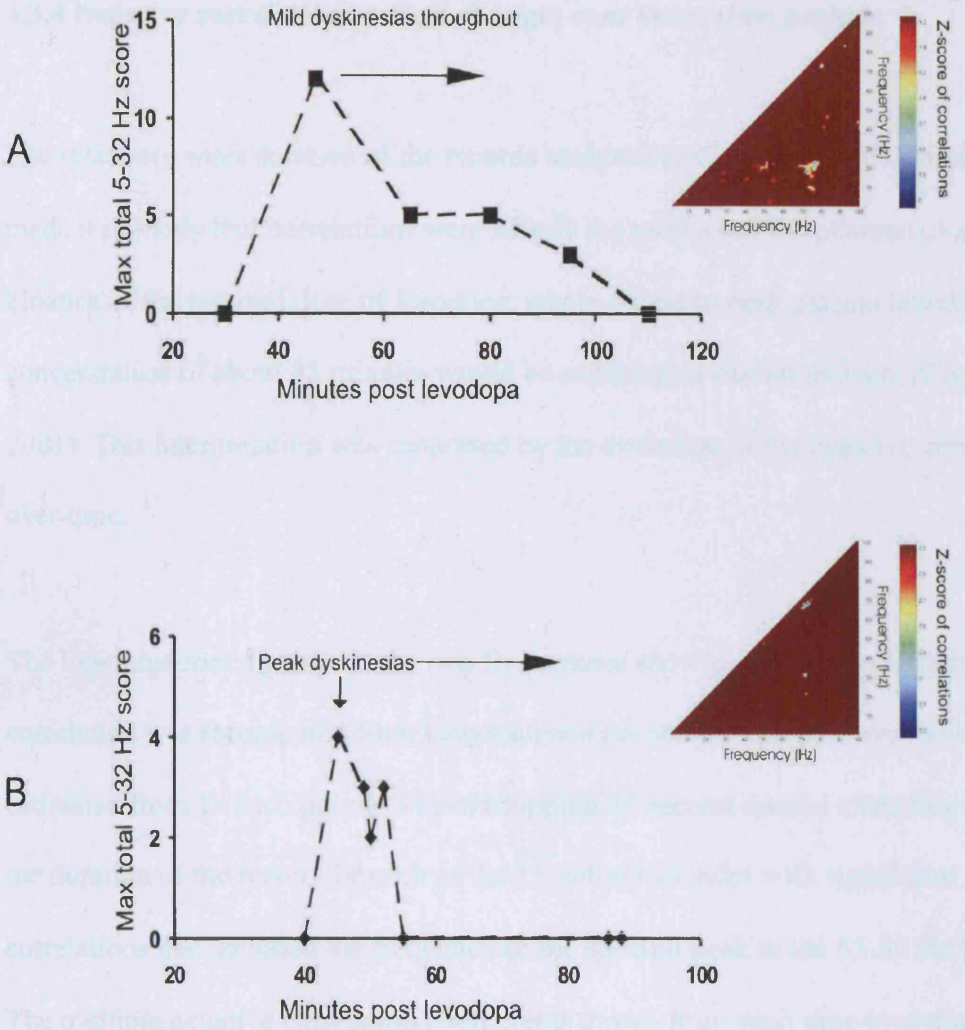

Figure 4.3 Timing of peak dyskinesias with respect to significant correlations. Maximum total scores in the 5-32 Hz frequency range for significant negative correlations with gamma activity at different time points after the administration of levodopa for case 1, right macroelectrode (A) and case 6, left macroelectrode (B). Matrices for recordings demonstrating the peak negative spectral correlations (Maximum correlations in A: 75-22 Hz, r = -0.30, p=0.0005, z=1.88; and in B: 70-30 Hz, r = -0.46, p=0.002, z=3.10) are illustrated on the right for each case (values Z-transformed, and thresholded to the significant r-value at α=0.05). Note in (B) there is also evidence of a strong negative correlation between different components within the 65-85 Hz range.

4.3.4 Negative correlations reflect changes over short-time periods

The relatively short duration of the records analysed (287 $\pm$ 39 seconds, 21 sides) made it unlikely that correlations were simply the product of the pharmacological kinetics of the test oral dose of levodopa, where a time to peak plasma levodopa concentration of about 45 minutes would be expected in similar patients (Contin et al., 2001). This interpretation was supported by the evolution of the negative correlation over time.

The log-transformed power at the two frequencies showing maximum negative correlation was recomputed from consecutive 4 second periods and correlations estimated from 10 such points over overlapping 40 second epochs extending across the duration of the record for each of the 15 individual sides with significant correlations that included the frequency of the spectral peak in the 65-85 Hz band. The multiple negative correlation coefficients drawn from such time-evolving data were significantly different from zero on each of the 15 sides ($p = 0.021$ in case 2, but $p < 0.0001$ in the remaining 14 sides). Figure 4.4 is an example from case 9 (right macroelectrode) and demonstrates that the peak negative correlations were generally negative throughout the recording.

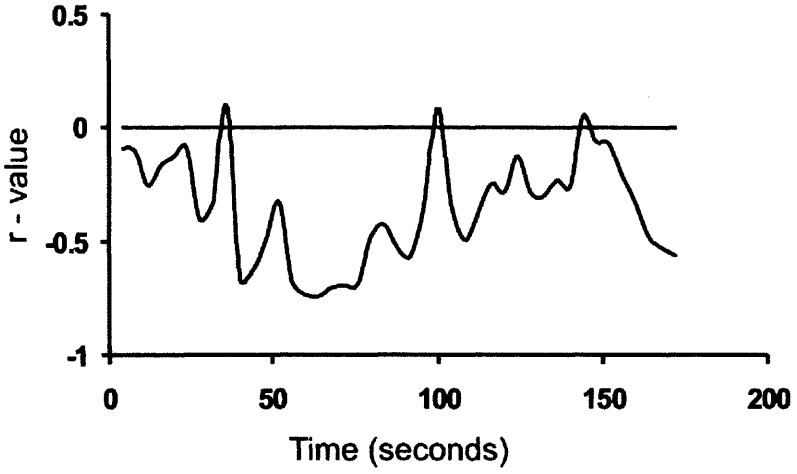

Figure 4.4 Temporal evolution of spectral correlations for the frequencies of maximum negative correlation. Correlations were calculated for overlapping 40 second epochs. Note that on average correlations are negative throughout the recording. LFP recorded from the right subthalamic area in case 9.

4.3.5 Focality of the 65-85 Hz spectral peak

Differential bipolar recordings, as used here, are greatly biased towards local signals. Moreover, polarity reversal was observed in 13/19 (68 %) of sides (right and left sides in case 3 were excluded as only one bipolar channel was recorded for each side). Polarity reversal was seen around contact 1 in five cases (case 9 on the right macroelectrode, case 11, 12, 13 and 14) and around contact 2 in eight cases (case 1 on the left macroelectrode and cases 2, 4, 6, 8 on the left and right macroelectrodes, 15 and 16). Such polarity reversal indicates a dipole at the site of the specified contact.

In the remaining macroelectrodes that failed to show polarity reversal, the contact pair showing the peak gamma power was compared to neighbouring contact pairs, the latter only had 46.1 $\pm$ 9.5 % of the peak gamma power (see section 2.3.5 for details).

Considering the 10 patients in whom post-operative MRI was available, all of the contact pairs (100%) exhibiting the highest ipsilateral gamma power included at least one contact that was independently judged to lie in STN. Conversely and equally importantly, none of the contact pairs with the highest gamma power per macroelectrode exclusively involved contacts outside of the STN. Six out of the eight sides (75 %) exhibiting polarity reversal with post-operative MRI demonstrated reversal at contacts judged to lie in STN.

The contact pair with the maximum power in the 65-85 Hz band included one or both contacts considered to be the most clinically effective upon stimulation in 74 % of macroelectrodes (14 out of 19 sides, 2 sides excluded as recordings were only available from one contact pair in case 3).

Furthermore, intra-operative microelectrode LFP recordings (see sections 2.1.2 and 2.2.2 for details), albeit in a different cohort of patients (not mentioned in table 4.1), showed gamma activity to be localized to the bordering cells and upper STN (figure 4.5). Eight out of twelve patients (9/15 sides) who displayed significant peaks (see 4.2.3) over 60-100 Hz in the power spectra of the LFP in at least one of the recorded depths, were studied (3 females, mean age 62.5 $\pm$ 2.1, duration of PD 13.8 $\pm$ 2.1).

Mean power over a 7 Hz band centreed on the gamma peak, 4-10 Hz and 13-30 Hz bands were calculated for a series of depth recordings in each side, and expressed as a percentage of the maximum power in each of the three frequency bands. Maximum power was evident at 1mm to 2 mm above STN, as defined by the microelectrode recordings, in the 4-10 Hz and the gamma frequency bands; and 1 mm below the STN border in the 13-30 Hz band (Figure 4.5B).

For further statistical analysis, three areas of depth recording were defined according to the microelectrode localization of the STN: 'above STN' - 2-6 mm above STN border; 'border/ upper STN' - 2 above to 1 mm below STN border; 'within STN' - 1 – 5 mm below STN border. Since 4 out of the 9 sides did not have depth recordings for the first area ('above the STN'), two separate ANOVAs were performed: one in which the two depths 'above STN' and 'border/upper STN' were compared in 5 sides, and another in which 'border/upper STN' and 'within STN' were compared in 9 sides. In both ANOVAs frequency (gamma, 4-10 Hz, 13-30 Hz) and depth (2 levels) were the main effects. A Kolmogorov Smirnov test showed the variables to be normally distributed.

In the first ANOVA there was no significant main effect for frequency, but there was a significant main effect for depth ($F_{[1,4]} = 65.365$, $p=0.001$). There was no significant interaction between frequency and depth. Mean percentage of maximal power was significantly greater in the 'border/upper STN' than 'above STN' in the gamma ($p=0.018$), 4-10 Hz ($p=0.016$) and 13-30 Hz ($p=0.006$) frequency bands (figure 4.5C).

In the second ANOVA there was no significant main effect for depth, but there was a significant main effect for frequency ($F_{[2,15]} = 5.667$, p=0.015). There was also a significant interaction between frequency and depth ($F_{[2,15]} = 4.370$, p=0.034). Within STN, mean percentage of maximal power was significantly greater in the 4-10 Hz (p=0.016) and 13-30 Hz (p=0.009) frequency bands than in the gamma frequency band. Mean percentage of maximal power was significantly greater in the 'border/upper STN' than 'within STN' in the gamma (p=0.004) frequency band. This is illustrated in figure 4.5D.

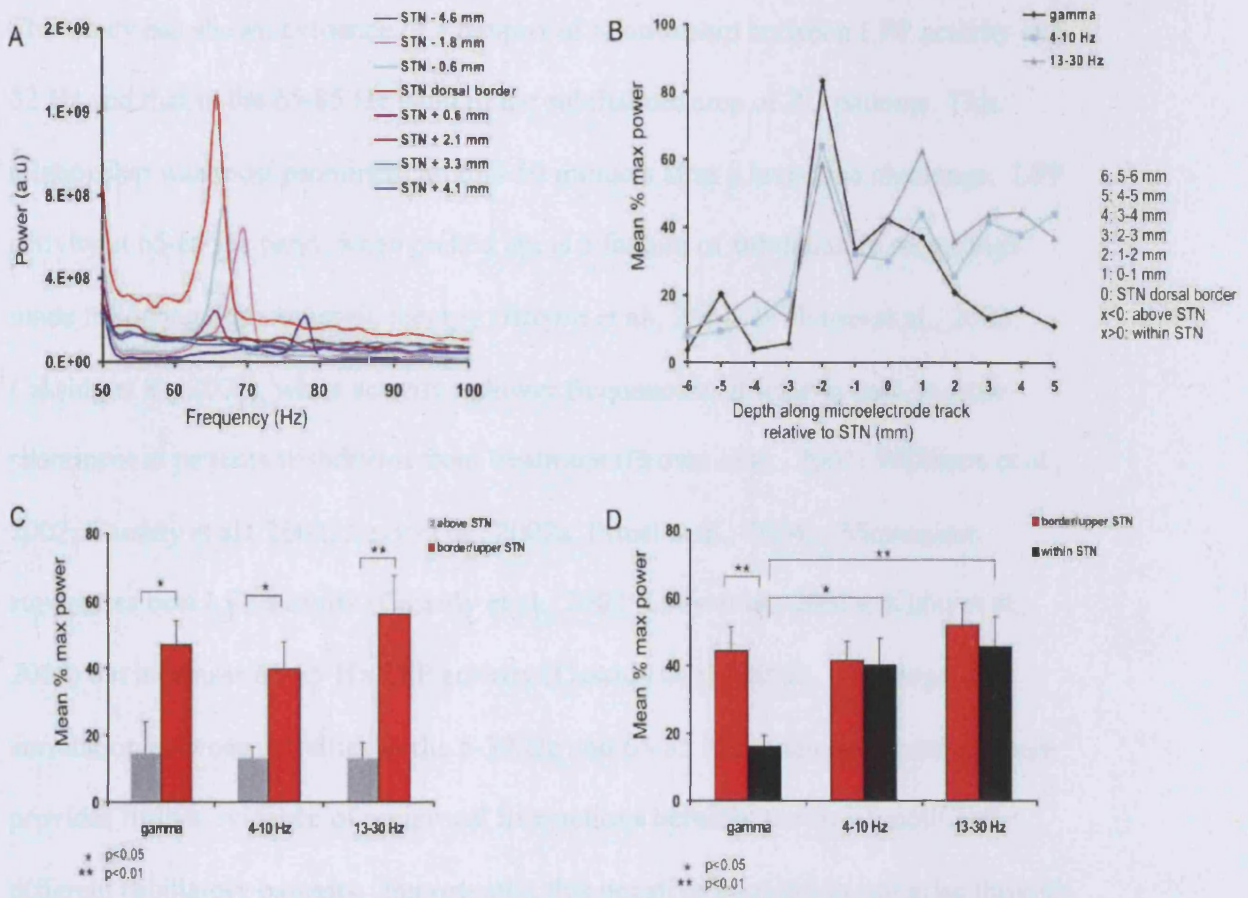

Figure 4.5 Microelectrode LFP gamma activity is localized to STN. (A) Power spectrum over the gamma frequency range in one side, for a series of depth recordings above (STN – x mm) and below (STN + x mm) the upper border of the STN as defined by microelectrode data. Distances are along the microelectrode track. (B) Mean percentage of maximum power in the three frequency bands (peak gamma ± 3 Hz, 4-10 Hz, 13-30 Hz), in nine sides. Note that the maximum LFP power is 2 mm along the microelectrode tack from the upper STN border, presumably in the area of ZI. (C,D) Comparison of the distribution of mean percentage of maximum power above and at the border of upper STN (C) and within and at the border of upper STN (D) for the three frequency bands. Bars = standard errors of mean.

4.4 Discussion

This study has shown evidence of a reciprocal relationship between LFP activity at 5-32 Hz and that in the 65-85 Hz band in the subthalmic area of PD patients. This relationship was most prominent around 50 minutes after a levodopa challenge. LFP activity at 65-85 Hz band, when picked up, is a feature of subthalamic recordings made following dopaminergic therapy (Brown et al., 2001; Williams et al., 2002; Cassidy et al., 2002), while activity at lower frequencies, at least in part, is more prominent in patients withdrawn from treatment (Brown et al., 2001; Williams et al., 2002; Cassidy et al., 2002; Levy et al., 2002a; Priori et al., 2004). Movement suppresses beta LFP activity (Cassidy et al., 2002; Levy et al., 2002a; Kühn et al., 2004) but increases 65-85 Hz LFP activity (Cassidy et al., 2002). The negative correlation between activities in the 5-32 Hz and 65-85 Hz bands demonstrated here provides further evidence of reciprocal interactions between the two functionally different oscillatory patterns. Importantly, this negative correlation can arise through spontaneous changes in subjects asked to rest quietly, *i.e.* in the absence of voluntary movement.

4.4.1 Experimental limitations

As discussed in section 2.1.3, without verification of electrode site, placement of the macroelectrodes should be considered presumptive. However, the contact pair with the highest gamma power always included at least one contact independently judged to lie in STN upon evaluation of post-operative MRI, where the latter was available. Moreover, all but two of the sites of polarity reversal were judged to lie in STN, when imaging was available. Furthermore, findings from microelectrode LFP recordings,

albeit in a different cohort of patients, suggest gamma activity generators to be localized to the bordering cells of the ZI and the upper STN.

The possibility that the correlations between 65-85 Hz and 5-32 Hz activity were spurious should be considered. Although artifacts with broad frequency characterisitics such as movement artifacts related to dyskinesias could lead to positive correlations across frequencies, they could not have caused negative correlations. If anything they would only serve to obscure negative correlations.

Possible contamination of LFP signals by dyskinetic EMG signals through volume conduction was discounted due to bipolar recordings (see section 2.2.4) and through evidence of polarity reversal in about 70 % of the recorded sides; strong support for a local generation of the 65-85 Hz activity at the site of polarity reversal. In the remaining macroelectrodes there was a clear gradient of LFP power across the bipolar contacts, consistent with a local source. In addition, spectral peaks in the 65-85 Hz band occurred in the absence of concurrent dyskinesias in four patients; a further argument against these peaks being due to contamination of LFP signals by dyskinetic EMG signals.

A peak at 65-85 Hz is common, but is not observed in all LFPs recordings from STN and GPi in treated PD patients. There may be several possible explanations for this. The first is that a distinct LFP spectral peak is dependent on a good clinical response to levodopa, not always realised in post-operative levodopa challenges. Second, high frequency activity tends to be more focal (Buzsáki and Draguhn, 2004). Thus, the recording of 65-85 Hz activity may be more critically dependent on accurate

localization of the electrodes than the recording of activities at lower frequencies. Third, synchronisation of activity at 65-85 Hz sufficient to be recorded with the macroelectrodes usually used to record LFPs in PD patients, may particularly occur in patients with prominent levodopa-induced dyskinesias (Brown and Marsden, 1998).

4.4.2 Relationship between dynamic oscillatory patterns and clinical state

A relationship between the presence of negative correlations and tremor seems unlikely as only one patient had tremor at the time of recording. On the other hand over 70% of the macroelectrodes showing negative correlations between 65-85 Hz and low frequency (5-32 Hz) LFP oscillations, were dyskinetic in the contralateral limb during the recording. As short-lived reciprocal effects on these oscillations are seen just before and during voluntary movement, this raises the possibility that the spontaneous fluctuations in the balance between these activities contributed to the dyskinesias. Indeed, involuntary movements might be predicted to be more likely when 'prokinetic' gamma activities are increased and when proportional decreases in 'antikinetic' low frequency activities are at their most pronounced (Brown, 2003). However, four sides had negative correlations without dyskinesias and five sides had dyskinesias without negative correlations, so if dynamic patterns of synchronisation are associated with dykinesias they are *not* sufficient in their own right to cause them, nor the exclusive cause.

4.4.3 Two reciprocal patterns of oscillatory synchronisation in the subthalamic area

At the systems level, the reciprocal interaction between frequencies may represent a tendency to flip between two functional states, one in which synchronisation at 65-85 Hz dominates, and one in which synchronisation over low frequencies dominates in the basal ganglia (Marsden et al., 2001; Williams et al., 2002; Brown, 2003). Thus, the basal ganglia, and perhaps the subthalamic nucleus in particular, may show a relative bistability, with the choice of state influenced by the level of the dopaminergic activity and other more dynamic factors. Such factors, can include processes related to planning and execution of movement or spontaneous endogenous fluctuations related to involuntary dyskinesias. The inverse relationship between low and high frequency oscillations may not be limited to the subthalamic area, as electrical stimulation in this region at 70 Hz also suppresses activity at 20 Hz in the pallidum (Brown et al., 2004).

The spontaneous tendency to shift between elevated 65-85 Hz power and low 5-32 Hz power and between low 65-85 Hz power and high 5-32 Hz power LFP states, preferentially occured around 50 minutes after oral levodopa, at a similar time to that of the peak plasma levodopa concentration (Contin et al., 2001). The relatively narrow time window over which spontaneous fluctuations may lead to correlations, may be one explanation for the absence of significant negative correlations in recordings from some patients, even when a gamma peak is detected. It seems that the negative correlations are a transient feature that preferentially occur around the time that dopaminergic deficit is reversed.

However, this does not necessarily mean that the negative correlations *per se* directly reflect the rising plasma levels of levodopa. Although rising levodopa levels would be anticipated to give a progressive suppression of beta activity and progressive increase in high frequency oscillations this would be expected to lead to negative correlations in data recorded over many minutes, through-out the 45 minute period of rising plasma levels (Contin et al., 2001). However, negative correlations were temporally restricted and consistently occurred over successive 40 second periods giving an upper limit to the time course of fluctuations between the low and high frequency LFP oscillations. In addition, at frequencies below the beta band, the evidence suggests that the power in the STN LFP is unchanged or increased by levodopa (Priori et al., 2004).

An alternative hypothesis is that the negative correlations arise from endogenous processes that lead to fluctuations in basal ganglia state with multi-second periodicities, which are increased by dopaminergic activity. It may therefore be relevant that similar fluctuations have been noted in neuronal discharge rate from many basal ganglia sites, including the STN, in the awake rodent, and that these are exacerbated by dopaminergic agonists, particularly in the setting of dopamine receptor supersensitivity (Ruskin et al., 1999; Allers et al., 2000; Ruskin et al., 2003). These slow fluctuations in discharge are highly correlated across units and basal ganglia nuclei (Ruskin et al., 2003), and offer a potential explanation for fluctuations in the amplitude of oscillatory processes over multisecond periods in the subthalamic area evident once plasma levodopa levels approach their peak. Interestingly, these multi-second periodicities have been associated with the appearance of apomorphine induced stereotypies in rats (Ruskin et al., 1999; Allers et al., 2000), while in the

parkinsonian patients in the present study, they largely occurred in tandem with dyskinesias.

4.5 Summary of key points

- The study has shown evidence of a reciprocal relationship between subthalamic LFP activity at 5-32 Hz and 65-85 Hz in parkinsonian patients, preferentially evident around the time that peak plasma levodopa levels would be expected and often concurrent with dyskinesias.
- The findings serve to highlight the inverse relationship between synchronisation at low frequencies and within the 65-85 Hz band in the subthalamic region in PD.
- Spontaneous fluctuations in these activities may be one possible mechanism for involuntary levodopa-induced dyskinesias.
- LFP activity in the gamma frequency band is focal to the STN and bordering ZI.

CHAPTER 5: Frequency dependent effects of stimulation in the region of the subthalamic nucleus in Parkinson's Disease.

5.1 Introduction

Excessive synchronisation at both tremor related and beta band frequencies have been considered as candidate pathophysiological mechanisms underlying the bradykinesia of PD, or are at least related to movement disruption (section 1.5.2). However, studies so far have only provided circumstantial or correlative evidence of a link between synchronisation in different frequency bands and motor function (Brown et al., 2001; Cassidy et al., 2002; Priori et al., 2002; Williams et al., 2002; Courtemanche et al., 2003; Kühn et al., 2004; Silberstein et al., 2003; Bergman et al., 1994; Nini et al., 1995; Hutchison et al., 1998; Magnin et al., 2000; Magarinos-Ascone et al., 2000; Goldberg et al., 2002).

A stronger support for a mechanistic role of such synchronisation in the genesis of bradykinesia would be the deleterious effect of direct stimulation of the basal ganglia at these frequencies.

So far, two studies have examined the effects of stimulation at low frequencies in chronically implanted PD patients, off their antiparkinsonian medication. Moro et al. (2002) found a significant decrement in hand tapping performance with 5 Hz stimulation of STN, and Timmermann et al. (2004) reported significant worsening of akinesia with STN stimulation at 10 Hz, with respect to no stimulation in the unmedicated state. Thus, there is preliminary evidence of a worsening of motor function during stimulation at 5 and 10 Hz, in the absence of L-dopa. However, the

effects of stimulation at 5 and 10 Hz (tremor related frequencies) have not been explicitly compared to one another or to the effects of stimulation over 15-30 Hz (beta band); nor have the effects of low frequency stimulation been evaluated, after dopaminergic therapy.

In addition, the excessive synchronisation at tremor and beta frequencies in the parkinsonian state imply first, that basal ganglia-cortical networks are preferentially tuned to oscillation at specific frequencies and second, that different types of oscillatory synchronisation may have distinct functional roles. However, it remains to be proven that the preferential tuning of synchronised activity to particular frequencies within the basal ganglia is of any functional consequence.

In this study, the effects of stimulation in the region of the STN, upon motor performance, at a variety of low frequencies over the 5-30 Hz range, including those in the beta band, are compared. These effects are also contrasted to the effects of clinically effective high frequency stimulation (section 1.4.3.2) and to performance without stimulation, within the same chronically implanted PD patients, both on and off their antiparkinsonian medication. Part of this work has been published (Fogelson et al., 2005a).

5.2 Methods

5.2.1 Patients and surgery

Seventeen patients were studied (mean age 60.8, range 47 to 72 years, 5 female, all right-handed) with PD (mean duration of PD 16.1, range 8 to 29 years). Each patient

had bilateral implantation of STN for treatment of their parkinsonism (mean time since surgery 2.6 years, range 4 months to 9 years), using previously described techniques (section 2.1.2).

Intraoperative electrode localization was tested by macro-stimulation in all patients. 14 patients had post-operative MRI. Post-operative imaging was consistent with the placement of at least one macroelectrode contact in the STN (see figure 2.2).

5.2.2 Protocol

All patients were assessed after overnight withdrawal of antiparkinsonian drugs. For convenience this will be termed the off medication state, although it is acknowledged that patients were only likely to have been partially withdrawn from the effects of dopaminergic therapy after overnight abstinence (see section 2.1.1).

All patients were studied off medication at the clinically effective frequency and when the stimulator was switched off. For convenience, this will be termed the 0 Hz condition.

The median clinically effective stimulation frequency was 130 Hz (see Table 5.1) and henceforth such stimulation will be termed '130 Hz'.

In ten subjects (cases 1, 4, 5, 7, 8, 10, 11, 13, 14, 15) stimulation was also performed at 5, 10, 15, 20, 25 and 30 Hz (i.e. with single shocks repeated every 200 ms, 100 ms, 67 ms, 50 ms, 40 ms and 33 ms), whilst still off medication. Case 11 was unable to perform the task with the right hand due to severe tremor, so off drug assessments

were obtained from 19 sides. Stimulation contacts, duration intensity and pulse duration were the same as utilised for therapeutic high frequency stimulation in each subject (Table 5.1).

In all 17 patients assessment of 0 and 130 Hz stimulation off medication was followed by treatment with 1.5 x each subject's standard morning dose of levodopa or 200 mg of levodopa in dispersible form (whichever was the greater) and then stimulation at 0, 5, 10, 15, 20, 25, 30 and 130 Hz, whilst on medication. For convenience this will be termed the on medication state. Case 6 was unable to perform the task with the left hand due to severe tremor, so on drug assessments were obtained from 33 sides. More patients were studied on than off medication as in the former state motor function was not necessarily completely stable over time as stimulation at different frequencies was started half an hour to an hour after medication and lasted for about an hour (Figure 5.1). Thus to compensate for the possibility of a non-stable baseline over the course of the drug response, stimulation was evaluated at the eight different frequencies in random order over a large sample of patients.

On and off medication studies in the same patients were performed on different days, separated by a minimum of 1 month, except in case 1 who was assessed both off and on medication on the same day.

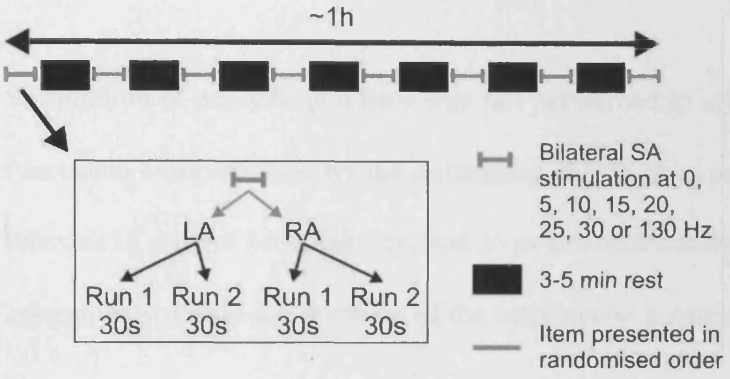

Figure 5.1 Timeline of experimental protocol. Two runs of a 30 s tapping test, were made with left (LA) and right hand (RA) after bilateral stimulation of the subthalamic area (SA) at 0, 5, 10, 15, 20, 25, 30, 130 Hz, in a randomised order across subjects. The waiting period after resetting frequency parameters was 3-5 mins.

Bradykinesia was assessed with the BRAIN TEST (see section 2.4.2). Rapid finger movement was performed by the subject between two keys on a keyboard completed over 30 seconds and repeated for each arm. Two runs were made at each stimulation frequency (including 0 Hz) per hand. The order of testing of different frequencies was randomised across subjects. The mean kinesia time (KT) for each side (right and left) was used as the measure of bradykinesia. This is the average time between consecutive taps in milliseconds so that the longer the KT the worse the performance. For each frequency both stimulators were programmed to the new frequency and testing commenced 3-5 minutes later. Patients were not told the new stimulation frequency. Right and left sides were counter balanced across subjects. Hemibody scores were assessed following medication and before stimulation trials to establish

the onset of drug response. Drug response was defined as a $\geq$ 20% improvement in motor hemibody scores during the experiment.

Stimulation of one side at a time was not performed in order to avoid possible functional compensation by the unstimulated side, to expedite assessment in the interests of patient acceptability, and so as to accommodate on medication assessments within the duration of the response to a single dose of levodopa.

5.2.3 Statistical analysis

A Kolmogorov Smirnov test showed the raw KT data to be normally distributed. Accordingly, analyses utilised repeated measures general linear models, incorporating, where necessary, a Huynh-Feldt correction for non-sphericity. Post-hoc Student's t-tests were two-tailed and Bonferroni corrected for multiple comparisons.

KT data were also normalised to performance without stimulation, but prior to this the linear dependency of KT on stimulation frequency off medication was removed. This dependency was estimated in each subject by linear regression of KT at all the stimulation frequencies in that subject. Normalised KT data were not normally distributed and differences between stimulation frequency on and off medication were analysed by serial Mann-Whitney tests, Bonferroni corrected for multiple comparisons. Means are given together with their standard error.

Case	Drugs (daily dose in mg)	Side of studied STN	Electrode contact - all monopolar	Amplitude (V)	Pulse width (μs)	Frequency (Hz)	Location of contacts used for stimulation
1	150 L-dopa 1 Pergolide	RT LT	1 2	2.5 2.3	60 60	130 130	STN Border STN/ RAPL
2	250 L-dopa 5 Cabergoline	RT LT	1 2	3.5 3.0	60 60	185 185	STN ZI
3	500 L-dopa 4 Cabergoline	RT LT	2 1	2.9 3.9	60 60	185 145	STN/ZI STN
4	250 L-dopa 2 Pergolide	RT LT	1 1	4.2 4.1	60 60	130 130	Border STN/ RAPL STN
5	400 L-dopa	RT LT	1 1	2.8 3.0	60 60	130 130	STN STN
6	850 L-dopa 100 Amantadine	LT	1	4.1	90	130	STN
7	750 L-dopa 1200 Entacapone 12.5 Clozapine	RT LT	1 1	4.0 4.0	60 60	130 130	STN STN
8	300 L-dopa	RT LT	0 1	3.8 3.7	60 60	145 145	N/A N/A
9	900 L-dopa 3 Pergolide	RT LT	1 1	3.6 3.6	60 60	180 180	STN STN
10	800 L-dopa	RT LT	2 01	4.0 4.1	60 60	180 180	N/A N/A
11	500 L-dopa 80 Sotalol	RT LT	12 12	3.0 3.7	60 60	130 130	STN Border STN/ RAPL
12	500 L-dopa 0.72 Pramipexole	RT LT	1 1	3.1 2.7	90 90	130 130	STN STN
13	400 L-dopa	RT LT	2 1	3.2 3.5	60 60	130 130	STN ZI/ RAPL
14	500 L-dopa 600 Entacapone 300 Amantadine 25 Clozapine	RT LT	1 1	2.4 3.0	90 60	130 130	N/A N/A
15	500 L-dopa	RT LT	1 1	4.7 4.8	60 60	130 130	STN STN
16	800 L-dopa 600 Entacapone	RT LT	2 1	3.2 3.3	60 60	130 130	ZI STN
17	1400 L-dopa 1200 Entacapone	RT LT	0 1	2.5 2.0	90 90	130 130	ZI ZI

Table 5.1 Stimulation parameters at the time of evaluation.

Patients 1-4 and 5-17 were from the surgical centres in London and Berlin, respectively. RT = Right; LT= Left; N/a = not available; RT = Right; LT= Left; STN = subthalamic nucleus; RAPL = prelemnscal radiations; ZI = zona incerta (see figure 2.3).

5.3 Results

Patients derived a mean 40.5 $\pm$ 4.7 % reduction in OFF treatment motor UPDRS scores with levodopa and 41.5 $\pm$ 3 % with therapeutic stimulation of the subthalamic area (SA). Two of the patients studied after drug treatment failed to turn on, or turned off again before all stimulation frequencies could be tested. These patients have not been included in the above demographics, table or on drug data.

The mean KT of patients while off stimulation differed on (644.8 $\pm$ 27.4 ms, n=33) and off (896.8.7 $\pm$ 57.3 ms, n=32) medication ($p<0.0001$). The mean KT of patients while off medication also differed with (678.3 $\pm$ 22.3 ms, n=33) and without (896.8 $\pm$ 57.3 ms) high frequency stimulation ($p<0.0001$). Thus patients were levodopa responsive and the tapping task sensitive to clinical change.

Figure 5.2 shows the mean effect of stimulation through the subthalamic macroelectrodes at different frequencies on and off medication. The off medication curve shows two peaks at 5-10 Hz and 20-25 Hz, superimposed on a trend for KT to progressively reduce as stimulation frequency increased. The on medication curve was flatter, but nevertheless there was a small trough at 20 Hz.

Data were further analysed using repeated measures general linear models with frequency of stimulation (0, 5, 10, 15, 20, 25, 30, 130 Hz) as the main factor. The 33 sides stimulated on medical treatment and 19 sides stimulated off medical treatment were analysed separately.

On medication multivariate tests showed a significant main effect for frequency ($F=2.886$, $p=0.023$). Polynomial contrasts showed a significant fourth order effect ($F_{[1,32]}=4.959$, $p=0.033$) for frequency. Thus the curve could be fitted by a polynomial with three turning points (the trough at 20 Hz and the shoulders either side). Post-hoc tests corrected for multiple comparisons demonstrated that the KT with stimulation at 20 Hz was smaller than with 5 Hz ($p=0.041$).

In the off drug condition there was a significant main effect for frequency ($F_{[2.79, 50.21]}=7.41$, $p<0.0001$). Polynomial contrasts showed linear ($F_{[1,18]}=16.09$, $p=0.001$) and fifth order effects ($F_{[1,18]}=4.76$, $p=0.043$) for frequency. Corrected post-hoc comparisons demonstrated the following differences between KTs: 130 Hz KT < 0, 10, 25, 30 Hz KT ($p=0.005$, $p=0.023$, $p=0.038$, $p=0.043$, respectively).

Polynomial contrasts indicated that the stimulation-response curve in the off drug state could be fitted by a polynomial with four turning points (corresponding to the two peaks at 5 and 20 Hz, the meeting point of the shoulders of the two peaks at 15 Hz and a further turning point at 30 Hz). A general linear model omitting 130 Hz also confirmed that the linear effect ($F_{[1,18]}=8.548$, $p=0.009$) was still seen over stimulation frequencies of 0-30 Hz in addition to a fourth order effect ($F_{[1,18]}=4.717$, $p=0.043$), so that local maxima and minima were superimposed upon the general trend for KT to decrease in proportion to the frequency of stimulation even at lower frequencies.

Finally, it was determined whether the local maxima and minima with stimulation $\leq$ 30 Hz differed in their pattern in the off and on drug states. To this end, the linear effect of stimulation upon KT in the off drug state and the effect of 0 Hz stimulation

in both drug states were removed, and then the KTs in the off and on drug states normalised by division by the respective KT without stimulation (0 Hz). Figure 5.3 summarises these data and serves to stress two points. First, the mean percentage changes in KT induced by stimulation at frequencies ≤ 30 Hz were small ($\leq \pm 7$ %), regardless of whether stimulation was performed on or off medication. Second, the figure suggests that the patterns of the normalised curves differ on and off medication, with the biggest difference being seen with stimulation frequencies of 20 Hz ($p = 0.036$, Mann-Whitney test corrected for multiple comparisons; other frequencies NS). Individual frequency response curves are illustrated in Figure 5.4.

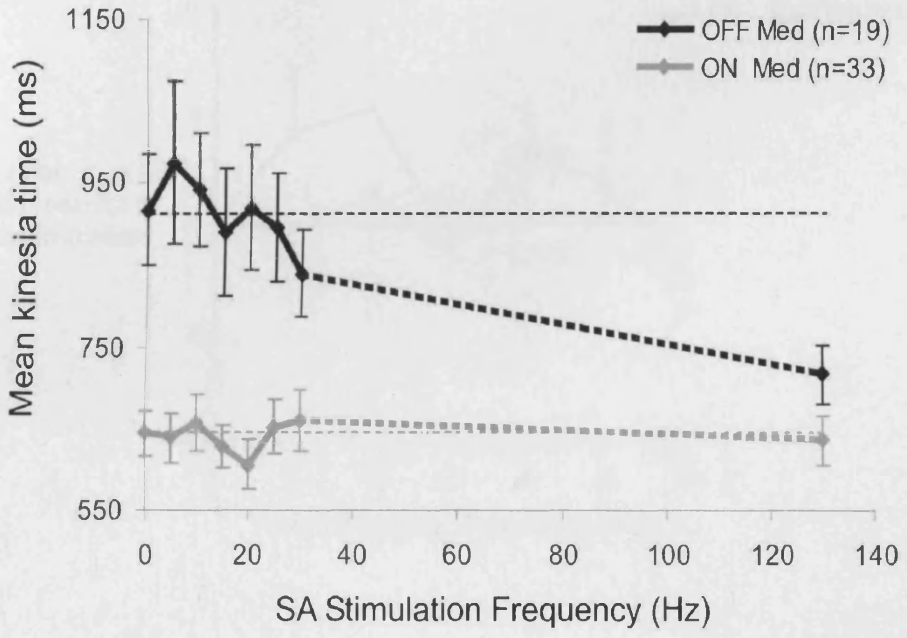

Figure 5.2 The effect of subthalamic area (SA) stimulation frequency on mean kinesia time (KT) after overnight withdrawal of antiparkinsonian medication (OFF – average of 19 sides) and after administration of antiparkinsonian medication (ON – average of 33 sides). OFF medication note the KT local maxima of slower performance at stimulation frequencies of 5-10 Hz and 20-25 Hz, together with the general trend for increasing frequency of stimulation to reduce KT. ON medication the stimulus-response curve is much flatter, although there is a local minimum at 20 Hz. Bars = standard errors of mean. Black and gray horizontal dotted lines are the mean KT with no stimulation (0 Hz) off and on medication, respectively.

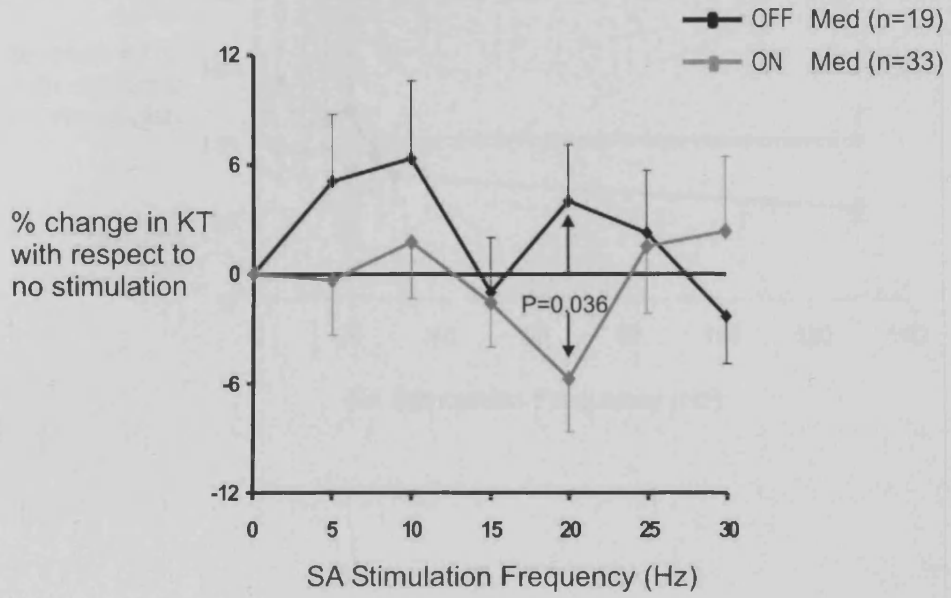

Figure 5.3 The effect of subthalamic area (SA) stimulation frequency on the percentage change in mean kinesia time (KT) normalised to unstimulated performance. The linear effect of frequency upon KT was first removed in OFF drug data. Note that effects of stimulation were small, but differed at 20 Hz in the ON and OFF medication states (see arrows: Mann-Whitney test, Bonferroni corrected for multiple comparisons). Bars = standard errors of mean.

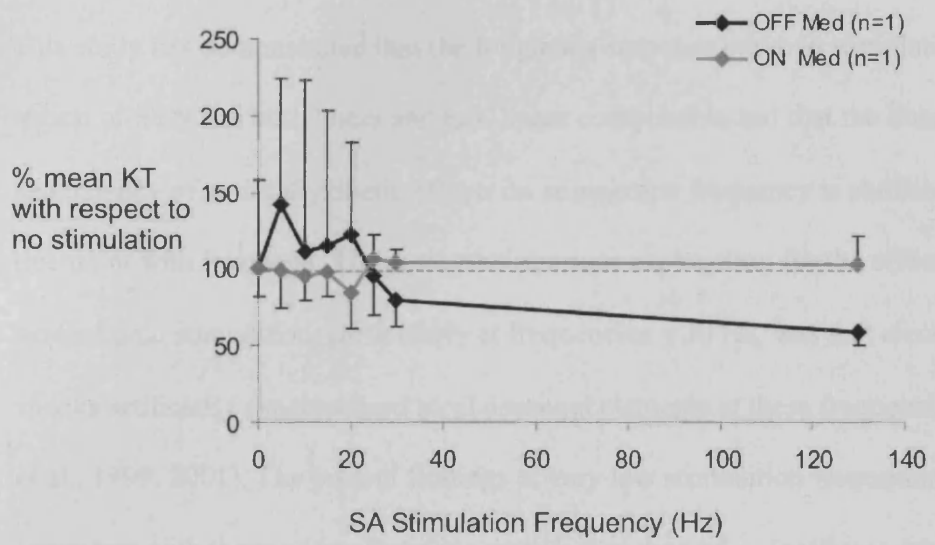

Figure 5.4 Individual frequency response curves. The effect of subthalamic area (SA) stimulation frequency on mean kinesia time normalised to unstimulated performance of the right hand in case 14 after an overnight withdrawal of antiparkinsonian medication (OFF) and of the right hand in case 10 after reinstitution of antiparkinsonian medication (ON). Bars = standard deviations. Gray horizontal dotted line is the normalised KT with no stimulation (0 Hz).

5.4 Discussion

This study has demonstrated that the frequency-response curve to stimulation in the region of STN has both linear and non-linear components and that the linear dependency of antibradykinetic effects on stimulation frequency is abolished by treatment with levodopa. The most parsimonious explanation for the effects of subthalamic stimulation, particularly at frequencies ≤ 30 Hz, was that electrical shocks artificially synchronised local neuronal elements at these frequencies (Ashby et al., 1999, 2001). The present findings at very low stimulation frequencies are consistent with those of two previous reports that showed a significant decrement in hand tapping performance with 5 Hz stimulation of STN (Moro et al. 2002) and significant worsening of akinesia with STN stimulation at 10 Hz (Timmermann et al., 2004), with respect to no stimulation in the unmedicated state. These and other studies (Limousin et al. 1995; Rizzone et al., 2001) have also demonstrated significant improvement in the off medication state with very high frequency stimulation.

5.4.1 Experimental limitations

As with all experimental studies of function in PD patients with deep brain electrodes, placement of macroelectrodes in STN can only be considered presumptive without histological verification of electrode site (section 2.1.3). In the present study the intended surgical coordinates, the clinical effects of intra-operative and post-operative stimulation and post-operative imaging were consistent with placement of at least one macroelectrode contact in the STN.

In addition, the results were probably compromised by fluctuations in tapping performance due to fatigue, practice effects and, in the on state, the time-course of the response to medication. Even though stimulation on medication was only performed while patients were improved, drug induced improvement in motor response was unlikely to afford a stable baseline. In an attempt to limit the effects of these sources of variance, the order of stimulation at different frequencies was randomised to prevent any systematic bias, and a large cohort of patients was studies in the on medication state.

Another very important consideration is the small scale of the effects of stimulation at low frequencies. The differential effects of stimulation at 5-10 Hz and 20-25 Hz off medication and of 20 Hz on medication were certainly modest in comparison to the effects of levodopa or high frequency stimulation. There may be several explanations for this.

First, non-linearities in the frequency response curve may reflect aspects of the basal ganglia response to stimulation that are of relatively little, if any functional significance. Nevertheless, it seems unlikely that the apparent non-linearities in the response to low-frequency stimulation arose by chance. Frequency as a main effect and higher order polynomial contrasts emerged as consistent features in ANOVAs on and off medication, and whether or not stimulation at 130 Hz was included. Moreover, the findings at very low stimulation frequencies were consistent with those of two previous reports showing a significant increase in bradykinesia with 5 Hz and 10 Hz stimulation of STN in the off medication condition (Moro et al., 2002; Timmermann et al., 2004).

Second, it is possible that increases in KT were limited by ceiling effects in the untreated drug state. Compensatory processes may exist that limit the effects of excessive synchronisation in vivo, given that cortico-basal ganglia loops are chronically exposed to rhythmic activity in these pass bands.

Third, a waiting period of only 3-5 minutes was used after switching stimulation settings, thereby failing to obtain the full effect of stimulation (Lopiano et al., 2003; Temperli et al., 2003). Conversely, effects persisting beyond cessation of stimulation may have tended to obscure differences between stimulation regimens. However, the duration of the study period had to be limited in the interests of patient comfort, to limit fatigue effects, and also so to try and contain the study period within the on medication phase. Other studies of motor performance at low stmulation frequencies, perhaps for similar reasons, have also used similar time intervals of $\leq$ 10 minutes (Moro et al., 2002; Timmermann et al., 2004).

Fourth, some of the variability in the effects of stimulation between subjects may reflect variation in the precise placement of macroelectrode contacts and in the choice of which contacts to stimulate. Some of this variability may have been limited by the use of more than one parameter of motor function, but this would have again prolonged the study duration.

Fifth, it is possible that the task used in this study was not sensitive enough to pick up significant changes in motor performance. Indeed a recent report demonstrated that a related tapping task was not responsive to L-dopa and was not suitable for the assessment of bradykinesia in PD (Kraus et al., 2005). However, the more complex

motor task used in the present study was L-dopa responsive and has also been validated as a reliable measure of bradykinesia in PD patients (Giovanni et al., 1999; Homann et al., 2000).

Finally, perhaps the most important limitation in the present study is the extent to which direct stimulation of the subthalamic area at frequencies < 30 Hz can be considered an effective synchronising influence upon local neurons or fibres of passage. Electrical stimulation is characterised by an artificial square waveform and may have been relatively ineffective at mimicking physiological patterns of synchronisation as it is likely to indiscriminately excite local neuronal systems with diverse and even contrasting function in the region of STN (Dostrovsky and Lozano, 2002; Ashby et al., 2001). Moreover, the synchronisation caused by electrical stimulation at frequencies $\leq$ 30 Hz is likely to involve the simple superimposition of the respective rhythm upon existing spontaneous neuronal activity, whereas physiological synchronisation involves the modulation of spontaneous neural activity, which in the case of the STN is of higher frequency and has an intrinsic tendency to bursting in the parkinsonian state (Bevan et al., 2002). In other words, single square-waveform pulses of stimulation repeated at periods of 100-200 ms (5-10 Hz) or 40-50 ms (20-25 Hz) may not parallel patterns of spontaneous synchronisation if these involve bursts of high frequency discharges repeated at similar intervals. Thus in natural circumstances there may be more than one discharge to each beat of the synchronising rhythm, thereby improving the efficacy of any rhythmic drive through temporal summation.

5.4.2 Non-linearities in the response to SA stimulation at frequencies ≤ 30 Hz

Off medication, there was a strong linear relationship between stimulation frequency and decrement in KT, which could be considered in terms of a simple relationship between 'dose' and response, where dose is the number of stimuli delivered per second. This suggests that the response to stimulation at increasing frequencies may be achieved through direct activation rather than depolarising block, as the latter is most unlikely at the lower frequencies of stimulation used in this study (Dostrovsky and Lozano, 2002; Garcia et al., 2003; Maurice et al., 2003). However, stimulation-response curves also showed small relative increases in KT with 5-10 Hz and 20-25 Hz stimulation in the off drug state and a relative decrease in KT with stimulation at 20 Hz in the medicated state. The explanation for these complex non-linearities in the frequency response curve is unclear, as, indeed, is the general mechanism of action of high frequency stimulation (Dostrovsky and Lozano, 2002). Their presence, however, suggests that the response to stimulation may not be simply modelled as a linear dose-response curve.

The frequencies of local maxima and minima correspond to those of peaks in spontaneous LFP power in the theta-alpha and beta bands observed within and between several levels of the basal ganglia (and related cortical areas), including STN, and believed to be indicative of local neuronal synchronisation in these frequency ranges in the healthy monkey (Courtemanche et al., 2003) and parkinsonian patient (Brown et al., 2001; Williams et al., 2002; Brown, 2003; Silberstein et al, 2003, Kühn et al., 2005; chapter 3). As such, non-linearities in the response to SA stimulation may result from an interaction between stimulation and the properties of local networks,

which preferentially oscillate in certain frequency bands. One possibility is that stimulation at low frequency tends to locally synchronise neuronal discharge at, or near to, the frequency of stimulation. Synchronisation here is considered in probabilistic terms, so that the discharges of neurons firing at high rates are more likely to coincide at the stimulation frequency than any other frequency. Some degree of synchronisation of local neuronal activity during STN stimulation is suggested by direct recordings from GPi (Brown et al., 2004) and from effects evoked in cerebral cortex and muscle (Ashby et al., 1999, 2001). Non-linearities in the frequency response curve would then imply that extrinsically driven synchronisation is more likely to occur and/or be propagated at certain frequencies, as dictated by the properties of local neural networks at the point of stimulation and at subsequent projection sites. A similar effect has recently been shown in the degree of oscillatory synchronisation in GPi upon stimulation of STN at different frequencies (Brown et al., 2004). This study found that stimulation in STN was most effective in changing oscillatory synchronisation in GPi when it occurred at frequencies comparable to those of spontaneous oscillations in GPi.

5.4.3 Differences in the frequency-response curve off and on medication

The most remarkable change in the frequency-response curve off and on levodopa was the loss of the linear effect of increasing stimulation frequencies upon KT. This was most evident in the attenuation of the response to stimulation at *ca* 130 Hz following levodopa, relative to the untreated state. Nutt et al. (2001) also found that peak dose levodopa and high frequency stimulation of the STN did not have additive effects on tapping speed. Even where assessments have involved the complete motor

section of the UPDRS, the effect of STN stimulation upon the on drug state has been either non-significant (Krack et al., 2003) or modest (Limousin et al., 1998; The deep-brain stimulation for Parkinson's disease study group, 2001), although these observations are only likely to be relevant in those cases with optimal targeting of STN. One possible explanation for the absence of algebraically additive effects when the two treatment modalities are combined is that the pathophysiological process antagonised by high frequency stimulation is also reversed by levodopa, so that high frequency stimulation becomes relatively ineffective in the on medication state. For example, it has been suggested that high frequency stimulation may serve to suppress spontaneous 'antikinetic' beta band synchronisation (Brown, 2003; see chapter 4). Such synchronisation is also attenuated by levodopa (Brown, 2003).

Differences between stimulation-response curves on and off medication were also seen at frequencies below 30 Hz. Not only did levodopa treatment cancel the linear effect of stimulation frequency in this range, but it also reversed the effect of stimulation at 20 Hz. Off medication, stimulation at this frequency lead to a relative increase in bradykinesia, whereas on medication the same stimulation tended to improve bradykinesia. These collective changes in the stimulation-response curve following levodopa suggest that dopaminergic input may radically change the network properties of the basal ganglia, something that also finds support in the major shifts in the nature of spontaneous oscillatory synchronisation following levodopa (Brown et al., 2001; Levy et al., 2002; Priori et al., 2002; Williams et al., 2002, chapter 4).

5.5 Summary of key points

- The study demonstrated that the effects of stimulation in the region of the STN in patients with PD do not simply increase as stimulation frequency increases, but that there are local maxima and minima in the frequency-response curve at low frequencies.
- These peaks and troughs correspond to the previously identified oscillatory activities of the local neuronal population.
- Non-linearities in the response to subthalamic stimulation may result from an interaction between stimulation and the properties of local networks, whereby extrinsically driven synchronisation is more likely to occur and/or be propagated at certain frequencies.
- Changes in the nature of the frequency-response curve following treatment with levodopa suggest that network resonances may be modulated according to the prevailing level of dopaminergic activity.

CHAPTER 6: Discussion

In this final chapter I will start by summarizing the results of the studies in this thesis. I will then discuss the general limitations of the methodologies in this thesis before continuing to discuss the significance of the results.

The major results of the studies will be discussed from six different angles. These will attempt to explore the significance of the findings with regards to the different activities identified (sections 6.3-6.5), the possible implications of the findings in understanding the role of the basal ganglia (section 6.6), the pathophysiology of PD (section 6.7), and the nature of the basal ganglia circuitry (section 6.8).

Finally I will conclude by suggestions of further studies that can expand the findings in the present thesis.

6.1 Summary of results

6.1.1 Chapter 3

Findings from the study in chapter 3 show that there is a strong coupling between LFP activities recorded with MEs in the SA and cortical EEG over a wide range of frequencies in the untreated parkinsonian patient. This coupling was greatest in the alpha and upper beta bands, and not at rest tremor frequencies. In addition, coherent subcortico-cortical loops of different frequency were not only topographically organised at the cortex, but also characterised by differences phase relationships between EEG and SA LFPs. These findings suggest that there are several functional sub-loops between the subthalamic area and cerebral cortical motor regions, distinguished by their frequency, cortical topography and temporal relationships.

6.1.2 Chapter 4

LFP activity in the 5-32 Hz band was significantly negatively correlated with that in the 65-85 Hz band in the treated parkinsonian patient. Negative correlations were relatively selective for interactions between these frequency bands and occurred over time epochs of as little as 40 s. They occurred around the time that peak plasma L-dopa levels would be expected, and were associated with concurrent dyskinesias. The spontaneous negative correlations suggest a reciprocal relationship between population synchrony in the high and low frequency ranges and raise the possibility that spontaneous fluctuations in the balance between these activities may contribute to levodopa-induced dyskinesias.

6.1.3 Chapter 5

Frequency-response curves to subthalamic deep brain stimulation in PD patients, demonstrated small local maxima and minima in kinesia time at different frequencies over 5-30 Hz. In addition, there was a differential effect of stimulation at the clinically effective frequency in the presence and absence of dopaminergic therapy.
The frequency of local maxima and minima in the frequency-response curve corresponded to the previously identified oscillatory activities in the parkinsonian basal ganglia (Brown, 2003). The results provide direct evidence that synchronisation of local neuronal activity in the region of the STN may have some functional consequences, that these consequences vary according to the frequency of synchronisation and are modulated according to the prevailing level of dopaminergic activity. The size of the effects demonstrated was, however, small.

6.2 General experimental limitations

The main limitation of all the studies in this thesis is that of the verification of the localization of the macroelectrodes in the patients as discussed in section 2.1.3. The approaches that were used included evaluation of post-operative MRI where available, determining clinical efficacy of stimulation, and providing evidence of polarity reversal of relevant activities at ME contacts. The combination of these approaches should give reasonable evidence for localization of the ME in the subthalamic area.

LFP activity recorded in chapters 3 and 4 were recorded bipolarly and are thus likely to be focally generated. In addition, evidence of polarity reversal points to a local dipole or dipoles for both the beta and gamma band activities. Previously published data suggest that the generator of these activities is the subthalamic nucleus itself in the case of activities below 30 Hz (Brown et al., 2001; Kühn et al., 2004; Priori et al., 2004; Doyle et al., 2005; Sharott et al., 2005; Kühn et al., 2005), and chapter 4 supports this conclusion with respect to LFP oscillations in the 65-85 Hz band.

Furthermore, the SA-ME LFP activities reported in the studies in this thesis, as coherent with EEG have been reported in other studies of neuronal synchronisation within the STN of the parkinsonian human, where targeting has been supported by microelectrode recordings and/or post-operative imaging, or within the STN of the parkinsonian rat or monkey, where placement has been confirmed histologically (Bergman et al., 1994; Levy et al., 2000; Marsden et al., 2001; Brown et al., 2001; Levy et al., 2001; Cassidy et al., 2002; Levy et al., 2002a,b; Priori et al., 2002; Williams et al., 2002; Kühn et al., 2004; Sharott et al., 2005). In particular findings

from microelectrode recordings in Kühn et al. (2005) and chapter 4 of this thesis have shown that beta and gamma frequency band LFP activities are focal to the STN.

6.3 Low frequency activity at 4 – 32 Hz

The studies in this thesis give further evidence of the pathological nature of low frequency activity in the basal ganglia (see section 1.5.2), specifically in the subthalamic area.

The prominent coherence of SA low frequency activity (4-32 Hz) with the cortical EEG, in the dopaminergic depleted state (chapter 3) and the reciprocal relationship between these low frequency activities and 'prokinetic' high frequency activity in the gamma range (chapter 4), may provide possible mechanisms for the 'antikinetic' nature of these low frequency activities (Brown, 2003). Synchronisation at these frequencies seems to have direct bradykinetic effects in PD patients, as demonstrated by low frequency stimulation of the subthalamic region (chapter 5).

6.4 Low frequency activity below 30 Hz – not a homogeneous band

The studies in this thesis provide evidence for the heterogeneous nature of activities in the low frequency range.

First, evidence suggests that there are several activities in the subthalamic area. These activities are distinct and distinguished by their frequency (theta, alpha, lower beta,

upper beta), and have different patterns of cortical topography and direction of drive (chapter 3).

Second, the response to stimulation in the subthalamic region is non-linear specifically at frequencies $\leq$ 30 Hz. Peaks of deterioration in motor performance in the depleted dopaminergic state corresponded to the alpha and upper beta peaks observed from LFP activity recorded from the parkinsonian basal ganglia (see section 1.5.2), and the prominent coherence peaks observed in chapter 3. This suggests that the pattern of synchronisation evident within and between nodes of the basal ganglia and linked cortical areas in parkinsonian humans may have functional significance, and that the role of synchronisation at different frequencies may differ.

Third, the negative correlations of low frequency activity with the high frequency gamma range seems to cluster around two major activities, one in the theta-alpha range and the second in the beta range (see figure 4.2).

In general, the evidence indicates the existence of several distinct activities below 30 Hz. These may have different functional and pathological significance (see section 6.7).

6.5 High frequency activity at 65-85 Hz

Chapter 4 provides further evidence for the prokinetic nature of subthalamic area high frequency activity in the gamma range. This activity was evident only in recordings of PD patients treated with antiparkinsonian medication. Furthermore, gamma activity showed a reciprocal relationship with activities that are characteristic of the parkinsonian antikinetic state.

One of the characteristics that has emerged from the study is that of the elusive nature of gamma activity, in comparison to the consistent findings of low frequency activity from SA LFPs. Gamma activity is less common and evidence from the study in chapter 4 suggests that this is due to its dynamic nature in relation to level of dopaminergic activity, and spontaneous fluctuations associated with involuntary movements such as dyskinesias.

In addition, microelectrode recordings have shown LFP gamma activity to be focally generated in upper STN and in the bordering cells above STN, such as ZI and Field of Forel.

6.6 Pathological or physiological exaggeration?

The recordings in this thesis were performed in patients with PD and therefore the findings should be viewed in the context of the disease rather than normal function. As such it is difficult to determine whether the findings are unique to PD patients or whether we see an exaggeration of physiological properties of basal ganglia activity.

With regards to the coherence between the subthalmic area and the motor cortex, one would expect less coherence in this loop in healthy subjects, as this is decreased after dopaminergic therapy in PD patients (Cassidy et al., 2002; Williams et al., 2002). In addition, although it is difficult to be categorical, there is the suggestion that in the healthy brain the subthalamic – cortical loops are even more segregated than is observed in PD (Filion et al., 1994; Nini et al., 1995; Bergman et al., 1998; Levy et al., 2000). Thus, the partial functional segregation observed in chapter 3 in PD patients is likely to be physiological, the pathology being a degradation of the functional segregation.

Synchronisation at low frequencies (specifically beta) has been recorded from the intact basal ganglia primates and humans (Courtemanche et al., 2003; Sochurkova and Rektor, 2003). STN synchronisation at these frequencies is suppressed in PD patients after administration of L-dopa (Levy et al., 2000; Cassidy et al., 2002; Williams et al., 2002) and is relatively weak in healthy primates (Wichmann et al., 1994a,b). Thus, excessive synchronisation in the subthalamic area is likely to be a pathological exaggeration of physiological activity.

Importantly, findings from chapter 5 indicate that the network properties of the subthalamic region change after administration of dopaminergic medication. This suggests that in healthy humans the network properties of the basal ganglia may be significantly different than those in the parkinsonian state, probably to an even greater extent than the difference observed between the untreated and treated states in chapter 5.

The reciprocal relationship observed in chapter 4 between low frequency activity and high frequency gamma activity in the subthalamic region is likely to also exist in healthy humans. Here, recordings were performed in PD patients after the administration of L-dopa, so were in a relatively 'normal' state. However, it is predicted that this reciprocal relationship is likely to be much more dynamic in healthy humans and would probably be associated with periodic episodes of motor planning.

6.7 Pathological significance in PD

Excessive low frequency coherence between the subthalamic area and the cortex may be important in understanding the pathophysiological mechanism of PD. Excessive coherence suggests that the basal ganglia and relevant areas in the cortex are locked together at low frequency activity, preventing dynamic changes of activity in the loop and in turn the processing of relevant motor information.

Prominent coherence at upper beta frequencies of the SA with the SMA is of relevance in the context of the disease as the SMA deficits are specifically associated with PD (Samuel et al., 1997).

One of the disadvantages of the study in chapter 3 is that it is not possible to determine whether the seemingly functionally distinct low frequency activities are also responsible or associated with different parkinsonian motor symptoms such as bradykinesia and tremor. However, the existence of some functional segregation

suggests that even though this may be impaired in the parkinsonian state, it is still preserved, at least on a coarse scale, in the patients studied here.

In chapter 5, direct low frequency stimulation of the subthalamic area in the depleted dopaminergic state showed relative, if modest, deterioration in tapping performance. This was consistent with the theory that synchronisation at low frequency contributes to bradykinesia in PD. This is of significance since it is direct evidence for the relationship between oscillatory activity in the basal ganglia and a motor symptom of the disease.

In addition, the relevance of the study outlined in chapter 5, is in the comparison of the OFF and ON medication states. Both states were characterised by non-linearities in the frequency range below 30 Hz. However, local maxima and minima were significantly different, as well as the response to the clinically effective frequency of stimulation. Thus, the dopaminergic level also has a significant effect on the network properties of the subthalamic region. Thus, the medicated states of the PD patient are not only different clinically but also at the level of the local networks, and any comparison between the two conditions should be viewed in this light.

The pathological significance of the negative correlations between gamma and low frequencies, observed in the study of chapter 4, is their association with symptoms of dyskinesia. This may be of importance in the understanding of the mechanism of levodopa-induced dyskinesias. There is a suggestion that both the dyskinesias and negative correlations occur around the time that the dopaminergic deficit is reversed, reflecting a bistable state in which the SA is characterised by fluctuations between

states of synchronisation at high and low frequencies. These fluctuations may underlie the mechanism of dyskinesias, which are hypothesised to occur due to an imbalance between pathways in the basal ganglia loop (Baas, 2002; Vitek and Giroux, 2000). Indeed, inverse relationships between low frequency activity (<30 Hz) and high frequency activity (65-85 Hz) in GP and levels of dyskinetic EMG have recently been reported (Silberstein et al., 2005).

6.8 Circuit loops in the subthalamic area

What additional insights do the studies in this thesis provide us about the nature of the basal ganglia circuitry?

First, it is suggested that multiple oscillatory circuits exist between the subthalamic area and cerebral motor areas, characterised by frequency, cortical topography and direction of drive in the untreated PD state (chapter 3). The idea of multiple circuits within the basal ganglia – thalamocortical circuitry has already been suggested (Joel and Weiner, 1997). Thus, the Albin-DeLong 'motor circuit' model (Albin et al., 1989; DeLong, 1990) may consist of several functional sub-loops coupling basal ganglia and cortical activities. However, in this thesis, some degree of overlap is still evident in cortical topography and temporal relationship, between the sub-loops. Thus, frequency may possibly be the only reliable way of marking the different sub-loops, and providing a means of preserving information relayed through multiple levels across the circuit (Kimpo et al., 2003). Indeed, the excessive synchronisation in low frequency bands may be a way to compensate for the loss of cortical segregation hypothesised to occur in the parkinsonian state.

Second, the network properties of the basal ganglia both off and on antiparkinsonian medication have non-linear properties at frequencies below 30 Hz (chapter 5). In the OFF medication state, local peaks of deterioration in motor performance correspond to previously identified spontaneous network resonances manifest in the population activity of the basal ganglia. Thus, it is possible that there are preferred activity patterns of subthalamic neuronal populations, which were revealed through the interaction of relevant stimulation frequencies and thus shape the effects of stimulation at low frequencies. The local resonant properties of the network seem to change, especially at 20 Hz, according to the ambient dopaminergic state.

In summary the findings of chapters 3 and 5, both point towards a tendency for neuronal populations in the subthalamic area to resonate at specific frequencies, specifically at the alpha and upper beta frequency range in the off medicated state in PD.

Third, the negative correlations observed in chapter 4, reveal that even in the dopaminergic therapeutic state of PD, two reciprocal patterns exist in the SA. This pharmacological state is also characterised by a bistability and a tendency to fluctuate between the two functionally distinct states. The suggestion here is that the depleted dopaminergic state is characterised by more robust patterns of activity in the basal ganglia, and may be a possible explanation for the 'effective' locking of basal ganglia activity. The dopaminergic state on the other hand, is characterised by more dynamic patterns of activity, which may be associated with motor fluctuations and dyskinesia of the ON medicated state in PD, or may be indicative of the possibly even more dynamic state of the basal ganglia in the healthy human. This bistability has been

implicated in computational models of the STN (Gillies and Willshaw, 2004) and may be essential for dynamic motor control processes to occur.

6.9 Future directions

It would be of importance to determine whether distinct activities in the parkinsonian basal ganglia, identified specifically in chapter 3, have different functional and pathophysiological roles in the various symptoms of PD.

Studies exploring in greater detail the temporal relation between dyskinesia onset and high frequency activity and its negative correlation with low frequency activity would be of great interest, with prospective, simultaneous recordings of subthalmic LFPs, plasma levodopa levels and electromyographic or accelerometric assessments of dyskinesias throughout the off-on-off treatment cycle. This would be of importance in the investigation of possible mechanisms of involuntary levodopa-induced dyskinesias, which remain largely unknown.

Finally, the impairment of tapping performance was modest with trains of single pulses in chapter 5. Further studies are warranted in patients in the peri-operative period to determine whether stimulation with trains at 5-10 Hz and 20-25 Hz are more effective in compromising motor performance if repetitive stimuli consist of several pulses at high frequency rather than single shocks. These more efficient methods of mimicking synchronisation in the basal ganglia would be highly beneficial in exploring the direct link between different frequencies and the effect on specific motor symptoms in PD such as bradykinesia and tremor.

REFERENCES

Abeles M, Gerstein GL (1988) Detecting spatiotemporal firing patterns among simultaneously recorded single neurons. J Neurophysiol 60: 909-924.

Albin RL, Young AB, Penney JB (1989) The functional anatomy of basal ganglia disorders. Trends Neurosci 12: 366-375.

Alexander GE, Crutcher MD (1990) Functional architecture of basal ganglia circuits: neural substrates of parallel processing. Trends Neurosci 13: 266-271.

Alexander GE, and DeLong MR (1992) Central mechanisms of initiation and control of movement In. Diseases of the nervous system. Clinical Neurobiology. 2nd ed (Ashby AK, McKahn GM, McDonald WI, eds), pp.285-308. Philadelphia, Pennsylvania. W.B. Saunders Company, Harcourt Brace Jovanovich Inc.

Allers KA, Kreiss DS, Walters JR (2000) Multisecond oscillations in the subthalamic nucleus: Effects of apomorphine and dopamine cell lesion. Synapse 38: 38-50.

Ashby P, Kim YJ, Kumar R, Lang AE, Lozano AM (1999) Neurophysiological effects of stimulation through electrodes in the human subthalamic nucleus. Brain 122: 1919-1931.

Ashby P, Paradiso G, Saint-Cyr JA, Chen R, Lang AE, Lozano AM (2001) Potentials recorded at the scalp by stimulation near the human subthalamic nucleus. Clin Neurophysiol 112: 431-437.

Ashkan K, Wallace B, Bell BA, Benabid AL (2004) Deep brain stimulation of the subthalamic nucleus in Parkinson's disease 1993-2003: where are we 10 years on? Br J Neurosurg 18: 19-34.

Aziz TZ, Peggs D, Sambrook MA, Crossman AR (1991) Lesions of the subthalamic nucleus for the alleviation of 1-methyl-4-phenyl-1,2,3,6-tetrahydropyridine (MPTP)-induced parkinsonism in the primate. Mov Disord 6: 288-292.

Baas H (2000) Dyskinesia in Parkinson's disease. Pathophysiology and clinical risk factors. J Neurol 247 (Suppl 4): IV/12 – IV/16.

Bekisz M, Wróbel A (2003) Attention-dependent coupling between beta activities recorded in the cat's thalamic and cortical representations of the central visual field. Eur J Neurosci 17: 421-426.

Benabid AL, Benazzouz A, Pollak P (2002) Mechanisms of deep brain stimulation. Commentary. Mov Disord 17 (Suppl 3): S73-S74.

Benazzouz A, Gross C, Feger J, Boraud T, Bioulac B (1993) Reversal of rigidity and improvement in motor performance by subthalamic high-frequency stimulation in MPTP-treated monkeys. Eur J Neurosci 5: 382-389.

Benazzouz A, Hallett M (2000) Mechanism of action of deep brain stimulation. Neurology 55 (Suppl 6): S13-S16.

Bergman H, Deuschl GD (2002) Pathophysiology of Parkinson's disease: from clinical neurology to basic neuroscience and back. Mov Disord 17 (Suppl 3): S28-S40.

Bergman H, Feingold A, Nini A, Raz A, Slovin H, Abeles M, Vaadia E (1998) Physiological aspects of information processing in the basal ganglia of normal and parkinsonian primates. Trends Neurosci 21: 32-38.

Bergman H, Wichmann T, DeLong MR (1990) Reversal of experimental parkinsonism by lesions of the subthalamic nucleus. Science 249: 1436-1438.

Bergman H, Wichmann T, Karmon B, DeLong MR (1994) The primate subthalamic nucleus. II. Neuronal activity in the MPTP model of Parkinsonism. J Neurophysiol 72: 507-520.

Berke JD, Okatan M, Skurski J, Eichenbaum HB (2004) Oscillatory entrainment of striatal neurons in freely moving rats. Neuron 43: 883-896.

Bernat JL, and Vincent FM, eds. (1987a) Tremor In. Neurology, pp. 170-178. Oradell, New Jersey, Medical Economics Books.

Bernat JL, and Vincent FM, eds. (1987b) Movement disorders In. Neurology, pp. 337-348. Oradell, New Jersey, Medical Economics Books.

Bevan MD, Magill PJ, Terman D, Bolam JP, Wilson CJ (2002) Move to the rhythm: oscillations in the subthalamic nucleus-external globus pallidus network. Trends Neurosci 25: 525-531.

Birkmayer W, and Hornykiewicz O, eds. (1976) Advances in Parkinsonism: Biochemistry, Physiology, Treatment. Fifth international symposium on Parkinson's disease (Vienna). Basel: Roche.

Blanchet PJ, Boucher R, Bedard PJ (1994) Excitatory lateral pallidotomy does not relieve L-dopa induced dyskinesias in MPTP parkinsonian monkeys. Brain Res 650: 32-39.

Blin O (2003) The pharmacokinetics of pergolide in Parkinson's disease. Curr Opin Neurol 16 (Suppl 1): S9-S12.

Brown P (2003) Oscillatory nature of human basal ganglia activity: relationship o the pathophysiology of Parkinson's disease. Mov Disord 18: 357-363.

Brown P, Marsden CD (1998) What do the basal ganglia do? Lancet 351: 1801-1804.

Brown P, Marsden CD (1999) Bradykinesia and impairment of EEG desynchronisation in Parkinson's disease. Mov Disord 14: 423-429.

Brown P, Kupsch A, Magill PJ, Sharott A, Harnack D, Meissner W (2002a) Oscillatory local field potentials recorded from the STN of the alert rat. Exp Neurol 177: 581-585.

Brown P, Salenius S, Rohwell JC, Hari R (1998) Cortical correlate of the piper rhythm in humans. J Neurophysiol 80: 2911-2917.

Brown P, Williams D, Aziz T, Mazzone P, Oliviero A, Insola A, Tonali P, Di Lazzaro V (2002b) Pallidal activity recorded in patients with implanted electrodes predictively correlates with eventual performance in a timing task. Neurosci Lett 330: 188-192.

Brown P, Mazzone P, Oliviero A, Altibrandi MG, Pilato F, Tonali PA, Di Lazzaro V (2004) Effects of stimulation of the subthalamic area on oscillatory pallidal activity in Parkinson's disease. Exp Neurol 188:480-490.

Brown P, Oliviero A, Mazzone P, Insola A, Tonali P, Di Lazzaro V (2001) Dopamine dependency of oscillations between subthalamic nucleus and pallidum in Parkinson's disease. J Neurosci 21: 1033-1038.

Brillinger DR (1981) Time series - data analysis and theory (2^{nd} edn). San Francisco: Holden Day.

Buzsáki G, Bickord RG, Ponomareff G, Thal LJ, Mandel R, Gage FH (1988) Nucleus basalis and thalamic control of neocortical activity in the freely moving rat. J Neurosci 8: 4007-4026.

Buzsáki G, Draguhn A. (2004) Neuronal oscillations in cortical networks. Science 304: 1926-1929.

Carlsson A (1959) The occurrence, distribution and physiological role of catecholamines in the nervous system. Pharmacol Rev 11: 490-493.

Cassidy M, Mazzone P, Oliviero A, Insola A, Tonali P, Di Lazzaro V, Brown P (2002) Movement-related changes in synchronisation in the human basal ganglia. Brain 125: 1235-1246.

Chang HT, Kita H, Kitai ST (1983) The fine structure of the rat subthalamic nucleus: an electron microscopic study. J Comp Neurol 221: 113-123.

Classen J, Gerloff C, Honda M, Hallett M (1998) Integrative visuomotor behavior is associated with interregionally coherent oscillations in the human brain. J Neurophysiol 79: 1567-1573.

Contin M, Riva R, Martinelli P, Albani F, Avoni P, Baruzzi A (2001) Levodopa therapy monitoring in patients with Parkinson Disease: a kinetic-dynamic approach. Ther Drug Monit 23: 621-629.

Côté LJ, Crutcher MD (1991) The Basal Ganglia In. Principles of neural science. 3rd ed. (Kandel ER, Schwartz JH, Jessel TM eds), pp. 647-659. EnglewoodCliffs, new Jersey, Prentice-Hal International Inc.

Courtemanche R, Fujii N, Graybiel AM (2003) Synchronous, focally modulated β-band oscillations characterize local field potential activity in the striatum of awake behaving monkeys. J Neurosci 23: 11741-11752.

Creutzfeldt OD, Watanabe S, Lux HD (1966) Relations between EEG phenomena and potentials of single cortical cells. I. Evoked responses after thalamic and epicortical stimulation. Electroenceph clin Neurophysiol 20: 1-18.

Crone NE, Miglioretti DL, Gordon B, Lesser RP (1998) Functional mapping of human sensorimotor cortex with electrocorticographic spectral analysis II. Event-related synchronisation in the gamma band. Brain 121: 2301-2315.

DeLong MR (1990) Primate models of movement disorders of basal ganglia origin. Trends Neurosci 13: 281-285.

DeLong MR (2000) The Basal Ganglia. In. Principles of neural science. 4th ed. (Kandel ER, Schwartz JH, Jessel TM eds), pp. 853-867. The McGraw-Hill Companies, Inc.

DeLong MR, Crutcher MD, Georgopoulos AP (1985) Primate globus pallidus and subthalamic nucleus: functional organization. J Neurophysiol 53: 530-543.

Devos D, Labyt E, Cassim F, Bourriez JL, Reyns N, Touzet G, Blond S, Guieu JD, Derambure P, Destee A, Defebvre L (2003) Subthalamic stmulation influences postmovement cortical somatosensory processing in Parkinson's disease. Eur J Neurosci 18: 1884-1888.

Devos D, Labyt E, Derambure P, Bourriez JL, Cassim F, Reyns N, Blond S, Guieu JD, Destee A, Defebvre L (2004) Subthalamic nucleus stimulation modulates motor cortex oscillatory activity in Parkinson's disease. Brain 127: 408-419.

Dimpfel W, Spüler M, Wessel K (1992) Different neuroleptics show common dose and time dependent effects in quantitative field potential analysis in freely moving rats. Psychopharmacology 107: 195-202.

Dostrovsky JO, Lozano AM (2002) Mechanisms of deep brain stimulation. Mov Disord 17 (Suppl 3): S63-S68.

Doyle LMF, Kühn AA, Hariz M, Kupsch A, Schneider G-H, Brown P (2005) Levodopa-induced modulation of subthalamic beta oscillations during self-paced movements in patients with Parkinson's disease. Eur J Neurosci 21: 1403-1412.

Engel AK, Fries P, Singer W (2001) Dynamic predictions: oscillations and synchrony in top-down processing. Nat Rev Neurosci 2: 704-716. Review.

Esselink RAJ, de Bie RMA, de Haan RJ, Lenders MWPM, Nijssen PCG, Sraal MJ, Smeding, HMM, Schuurman PR, Bosch DA, Speelman JD (2004) Unilateral pallidotomy versus bilateral subthalamic nucleus stimulation in PD. Neurology 62: 201-207.

Fahn S, Elton RL, Members of the UPDRS development committee (1987) Unified Parkinson's Disease Rating Scale. In. Recent Developments in Parkinson's Disease. (Fahn S, Marsden CD, Calne DB, Goldstein M, eds.), Vol 2, pp. 153-163, 293-304. Florham Park, NJ, Macmillan Health Care Information.

Filion M, Tremblay L (1991) Abnormal spontaneous activity of globus pallidus neurons in monkeys with MPTP-induced parkinsonism. Brain Res 547: 142-151.

Filion M, Tremblay L, Matsumura M, Richard H (1994) Dynamic focusing of informational convergence in basal ganglia. Rev Neurol (Paris) 150:627-633.

Foffani G, Priori A, Egidi M, Rampini P, Tamma F, Caputo E, Moxon K A, Cerutti S, Barbieri S (2003) 300-Hz subthalamic oscillations in Parkinson's disease. Brain 126: 2153-2163.

Fogelson N, Kühn AA, Silberstein P, Dowsey Limousin P, Hariz M, Trottenberg T, Kupsch A, Brown P (2005a) Frequency dependent effects of subthalamic nucleus stimulation in Parkinson's Disease. Neurosci Lett 382: 5-9 .

Fogelson N, Pogosyan A, Kühn AA, Kupsch A, van Bruggen G, Speelman H, Tjissen M, Quartone A, Insola A, Mazzone P, Di Lazzaro V, Limousin P, Brown P (2005b) Reciprocal interactions between oscillatory activities of different frequencies in the subthalmic region of patients with Parkinson's disease. Eur J Neurosci 22: 257-266.

Fogelson N, Williams D, Tijssen M, van Bruggen G, Speelman H, Brown P (2005c) Different functional loops between cerebral cortex and the subthalamic area in Parkinson's disease. Cereb Cortex, doi:10.1093/cercor/bhi084.

Garcia L, Audin J, D'Alessandro G, Bioulac B, Hammond C (2003) Dual effect of high-frequency stimulation on subthalamic neuron activity. J Neurosci 23: 8743-8751.

Gazzaniga MS, Ivry RB, Mangun GR (eds) (1998) Motor control. In. Cogitive Neuroscience. The biology of the mind, pp.371-421. New York, W.W. Norton & Company, Inc.

Gerfen CR (1995) Dopamine receptor function in the basal ganglia. Clin Neuropharmacol 18 (Suppl 1): S162-S177.

Gerloff C, Richard J, Hadley J, Schulman AE, Honda M Hallet M (1998) Functional coupling and regional activation of human cortical motor areas during simple, internally paced and externally paced finger movements. Brain 121: 1513-1531.

Gillies A, Willshaw D (2004) Models of the subthalamic nucleus. The importance of intranuclear connectivity. Med Eng Phys 26: 723-732.

Giovanni G, van Schalkwyk J, Fritz VU, Lees AJ (1999) The Bradylinesia Akinesia Inco-orination Test (BRAIN TEST): an objective computerized assessment of upper limb motor function. J Neurol Neurosurg Psychiatry 67: 624-629.

Goldberg JA, Boraud T, Maraton S, Haber SN, Vaadia E, Bergman H (2002) Enhanced synchrony among primary motor cortex neurons in the 1-methyl-4-phenyl-1,2,3,6-tetrahydropyridine primate model of Parkinson's disease. J Neurosci 22: 4639-4653.

Goldberg JA, Rokni U, Boraud T, Vaadia E, Bergman H (2004) Spike synchronisation in the cortex-basal ganglia networks of Parkinsonian primates reflects global dynamics of the local field potentials. J Neurosci 24: 6003-6010.

Gotman J (1983) Measurement of small time differences between EEG channels: method and application to epileptic seizure propagation. Electroencephalogr Clin Neurophysiol 56: 501-514.

Gotman J (1990) The use of computers in analysis and display of EEG and evoked potentials. In. Current practice of clinical electroencephalography. 4th ed. (Daly AA and Pedley A, eds.), pp.51-83. New York, Raven Press.

Goto Y and O'Donnell P (2001) Network synchrony in the nucleus accumbens in vivo. J Neurosci 21: 4498-4504.

Greenstein B, Greenstein A (eds.) (2000) The motor cortex. In. Color Atlas of Neuroscience Neuroanatomy and Neurophysiology, pp. 178-179. Stuttgart, New York: Thieme.

Grosse P, Cassidy MJ, Brown P (2002) EEG-EMG, MEG-EMG and EMG-EMG frequency analysis: physiological principles and clinical applications. Clin Neurophysiol 113: 1523-1531.

Gurney K, Prescott TJ, Wickens JR, Redgrave P (2004) Computational models of the basal ganglia: from robots to membranes. Trends Neurosci 27: 453-459.

Halliday DM, Conway BA, Farmer SF, and Rosenberg JR (1999) Load-independent contributions from motor-unit synchronisation to human physiological tremor. J Neurophysiol 82: 664-675.

Halliday DM, Rosenberg JR, Amjad AM, Breeze P, Conway BA, Farmer SF (1995) A framework for the analysis of mixed time series/point process data - theory and application to the study of physiological tremor, single motor unit discharges and electromyograms. Prog Biophys Mol Biol 64: 237-278.

Hamani C, Saint-Cyr JA, Fraser J, Kaplitt M, Lozano AM (2004) The subthalmic nucleus in the context of movement disorders. Brain 127: 4-20.

Hellwig B, Haussler S, Lauk M, Guschlbauer B, Koster B, Kristeva-Feige R, Timmer J, Lücking CH (2000) Tremor-correlated cortical activity detected by electroencephalography. Clin Neurophysiol 111: 806-809.

Herrmann CS, Munk MJH, Engel AK (2004) Cognitive functions of gamma-band activity: memory match and utilization. Trends Cogn Sci 8: 347-355.

Homann CK, Suppan K, Wenzel K, Giovannoni G, Ivanic G, Horner S, Ott E, Hartung HP (2000) The bradykinesia akinesia incoordination test (BRAIN TEST), an objective and user-friendly means to evaluate patients with parkinsonism. Mov Disord 15: 641-647.

Hornykiewicz O (1966) Metabolism of brain dopamine in human parkinsonism: Neurochemical and clinical aspects. In biochemistry and pharmacology of the basal ganglia. (Costa E, Côté LJ, Yahr MD eds), pp. 171-185. New York: Raven Press.

Hurtado JM, Gray CM, Tamas LB, Sigvardt KA (1999) Dynamics of tremor-related oscillations in the human globus pallidus: a single study. Proc. Natl. Acad. Sci. USA 96: 1674-1679.

Hurtado JM, Lachaux J-P, Beckley DJ, Gray CM, Sigvardt KA (2000) Inter- and intralimb oscillator coupling in parkinsonian tremor. Mov Disord 15: 683-691.

Hutchison WD, Dostrovsky JO, Lozano AM (2003) Movement disorders surgery: microelectrode recording from deep brain nuclei In. Movement Disorders. Handbook of Clinical Neurophysiology (Hallett M, ed.), pp.417-435. Amsterdam, the Netherlands: Elsevier B.V.

Hutchison WD, Lozano AM, Tasker RR, Lang AE, Dostrovsky JO (1997) Identification and characterisation of neurons with tremor-frequency activity in human globus pallidus. Exp Brain Res 113: 557-563.

Hutchison WD, Allan RJ, Opitz H, Levy R, Dostrovsky JO, Lang AE, Lozano AM (1998) Neurophysiological identification of the subthalamic nucleus in surgery for Parkinson's disease. Ann neurol 44: 622-628.

Jenkins IH, Jahanshani M, Jueptner M, Passingham RE, Brooks DJ (2000) Self-initiated versus externally triggered movements II. The effect of movement predictability on regional cerebral blood flow. Brain 123: 1216-1228.

Joel D, Weiner I (1977) The connections of the primate subthalamic nucleus: indirect pathways and the open-interconnected scheme of basal ganglia – thalamocortical circuitry. Brain Res Rev 23: 62-78.

John ER (2002) The neurophysics of consciousness. Brain Res Brain Res Rev 39: 1-28. Review.

Kimpo RR, Theunissen FE, Doupe AJ (2003) Propogation of correlated activity through multiple stages of a neural circuit. J Neurosci 23: 5750-5761.

Klimesch W, Doppelmayr M, Russegger H, Pachinger J, Schwaiger J (1998) Induced alpha band power changes in the human EEG and attention. Neurosci Lett 244: 73-76.

Knox CK (1981) Detection of neuronal interactions using correlation analysis. Trends Neurosci 4: 222-225.

Kocsis B, Bragin A, and Buzsáki G (1999) Interdependence of multiple theta generators in the hippocampus: a partial coherence analysis. J Neurosci 19: 6200-6212.

König P, Schillen TB (1991) Stimulus-dependent assembly formation of oscillatory responses: I. Synchronisation. Neural Comp 3: 155-166.

Krack P, Batir A, Van Blercom N, Chabardes S, Fraix V, Ardouin C, Koudsie A, Dowsey Limousin P, Benazzouz A, LeBas JF, Benabid A-L, Pollak P (2003) Five-Year follow-up of bilateral stimulation of the subthalamic nucleus in advanced Parkinson's disease. N Engl J Med 349: 1925-1934.

Krakauer J, Ghez C (2000) Voluntary movement. In. Principles of neural science. 4th ed. (Kandel ER, Schwartz JH, Jessel TM eds), pp. 756-779. The McGraw-Hill Companies, Inc.

Kraus PH, Klotz P, Hoffman A, Lewe J, Przuntek H (2005) Analysis of the course of Parkinson's disease under dopaminergic therapy: performance of "fast tapping" is not a suitable parameter. Mov Disord 20: 348-354.

Kühn AA, Williams D, Kupsch A, Limousin P, Hariz M, Schneider G-H, Yarrow K, Brown P (2004) Event-related beta synchronisation in human subthalamic nucleus correlates with motor performance. Brain 127: 735-746.

Kühn AA, Trottenberg T, Kivi A, Kupsch A, Schneider G-H, Brown P (2005) The relationship between local field potential and neuronal discharge in the subthalamic nucleus of patients with Parkinson's disease. Exp Neurol 194: 212-220.

Lance JW, Schwab RS, Peterson EA (1963) Action tremor and the cogwheel phenomenon in Parkinson's disease. Brain 86: 95-110.

Limousin P, Krack P, Pollak P, Benazzouz A, Ardouin C, Hoffmann D, Benabid A-L (1998) Electrical stimulation of the subthalamic nucleus in advanced Parkinson's disease. N Engl J Med 339: 1105-1111.

Limousin P, Greene J, Pollak P, Rothwell J, Benabid A-L, Frackowiak R (1997) Changes in cerebral activity pattern due to subthalamic nucleus or internal pallidum stimulation in Parkinson's disease. Ann Neurol 42: 283-291.

Limousin P, Pollak P, Benazzouz A, Hoffmann D, Le Bas J-F, Broussolle E, Perret JE, Benabid A-L (1995) Effect on parkinsonian signs and symptoms of bilateral subthalamic nucleus stimulation. Lancet 345: 91-95.

Levy R, Ashby P, Hutchison WD, Lang AE, Lozano AM, Dostrovsky JO (2002a) Dependence of subthalamic nucleus oscillations on movement and dopamine in Parkinson's disease. Brain 125:1196-1209.

Levy R, Dostrovsky JO, Lang AE, Sime E, Hutchinson WD, Lozano AM (2001) Effects of apomorphine on subthalamic nucleus and globus pallidus internus neurons in patients with Parkinson's disease. J Neurophysiol 86: 249-260.

Levy R, Hutchison WD, Lozano AM, Dostrovsky JO (2000) High-frequency synchronisation of neuronal activity in the subthalamic nucleus of parkinsonian patients with limb tremor. J Neurosci 20: 7766-7775.

Levy R, Hutchison WD, Lozano AM, Dostrovsky JO (2002b) Synchronized neuronal discharge in the basal ganglia of parkinsonian patients is limited to oscillatory activity. J Neurosci 22: 2855-2861.

Llinás R, Ribary U (1993) Coherent 40-Hz oscilation characterizes dream state in humans. Proc Natl Acad Sci USA 90: 2078-2081.

Llinás RR, Ribary U, Jeanmonod D, Kronberg E, Mitra PP (1999) Thalamocortical dysrhythmia: a neurological and neuropsychiatric syndrome characterized by magnetoencephalography. Proc Natl Acad Sci USA 96: 15222–15227.

Lopes da Silva F (1991) Neural mechanisms underlying brain waves: from neural membranes to networks. Electroenceph Clin Neurophysiol 79: 81-93. Review.

Lopes da Silva F, van Rotterdam A (2005) Biophysical aspects of EEG and magnetoencephalogram generation In. Electroencephalography. Basic principles, clinical applications, and related fields. 5th edition (Niedermeyer E, Lopes da Silva F, eds), pp. 107-125. Philadelphia, Pennsilvania. Lippincott Williams & Willkins.

Lopes da Silva FH, Vos JE, Mooibroek JN, and Van Rotterdam A (1980) A partial coherence analysis of thalamic and cortical alpha rhythms in dog – a contribution towards a general model of cortical organisation of rhythmic activity. In: Event Related Changes in Cortical Rhythmic Activities - Behavioural Correlates (Pfurtscheller G, ed.), pp. 33-59. Amsterdam: Elsevier/North-Holland Biomedical Press.

Lopiano L, Torre E, Benedetti F, Bergamasco B, Perozzo P, Pollo A, Rizzone M, Tavella A, Lanotte M (2003) Temporal changes in movement time during the switch of the stimulators in Parkinson's disease patients treated by subthalamic nucleus stimulation. Eur Neurol 50: 94-99.

Lorente de No R (1947) Analysis of the distribution of action currents of nerve in a volume conductor. Stud Rockefeller Inst Med Res 132: 384-477.

Louis ED, Levy G, Cote LJ, Meija H, Fahn S, Marder K (2001) Clinical correlates of action tremor in Parkinson's disease. Arch Neurol 58: 1630-1634.

Lozano AM (2001) Deep brain stimulation for Parkinson's disease. Parkinsonism Relat Disord 7: 199-203.

MacDonald BK, Cockerell OC, Sander JWAS, Shorvon SD (2000) The incidence and prevalence of neurological disorders in a prospective community-based study in the UK. Brain 123: 665-676.

Magarinos-Ascone CM, Figueiras-Mendez R, Riva-Meana C, Cordoba-Fernandez A (2000) Subthalamic neuron activity related to tremor and movement in Parkinson's disease. Eur J Neurosci 12: 2597-2607.

Magarinos-Ascone C, Pazo JH, Macadar O, Buno W (2002) High-frequency stimulation of the subthalamic nucleus silences subthalamic neurons: a possible cellular mechanism in Parkinson's disease. Neuroscience 115: 1109-1117.

Magill PJ, Sharott A, Bevan MD, Brown P, Bolam JP (2004a) Synchronous unit activity and local field potentials evoked in the subthalamic nucleus by cortical stimulation. J Neurophysiol 92: 700-714.

Magill PJ, Sharott A, Bolam JP, Brown P. (2004b) Brain state-dependence of coherent oscillatory activity in the cerebral cortex and basal ganglia of the rat. J Neurophysiol 92: 2122-2136.

Magnin M, Morel A, Jeanmond D (2000) Single unit analysis of the pallidum, thalamus and subthalamic nucleus in parkinsonian patients. Neuroscience 96: 549-564.

Magnani G, Cursi M, Leocani L, Volonte MA, Locatelli T, Elia A, Comi G (1998) Event-related desynchronisation to contigent negative variation and self paced movement paradigms in Parkinson's disease. Mov Disord 13: 653-660.

Marsden CD (1992) Motor dysfunction and movement disorders In. Diseases of the nervous system. Clinical Neurobiology. 2nd ed (Ashby AK, McKahn GM, McDonald WI, eds), pp.309-318. Philadelphia, Pennsylvania. W.B. Saunders Company, Harcourt Brace Jovanovich Inc.

Marsden CD and Obeso JA (1994) The functions of the basal ganglia and the paradox of stereotaxic surgery in Parkinson's disease. Brain 117: 877-897. Review.

Marsden JF, Limousin-Dowsey P, Ashby P, Pollak, Brown P (2001) Subthalamic nucleus, sensorimotor cortex and muscle interrelationships in Parkinson's disease. Brain 124: 378-388.

Martin JH (1991) The collective electrical behavior of cortical neurons: the electroenecephalogram and the mechanism of epilepsy In. Principles of neural science. 3rd ed. (Kandel ER, Schwartz JH, Jessel TM eds), pp. 777-791. EnglewoodCliffs, new Jersey, Prentice-Hal International Inc.

Masimore B, Kakalios J, Redish AD (2004) Measuring fundamental frequencies in local field potentials. J Neurosci Methods 138: 97-105.

Maurice N, Thierry A-M, Glowinski J, Deniau J-M (2003) Spontaneous and evoked activity of substantia nigra pars reticulate neurons during high-frequency stimulation of the subthalamic nucleus. J Neurosci 23: 9929-9936.

Miltner WHR, Braun C, Arnold M, Witte H, Taub E (1999) Coherence of gamma-band EEG activity as a basis for associative learning. Nature 397: 434-436.

Mima T, Matsuoka T, Hallett M (2000a) Functional coupling of human right and left cortical motor areas demonstrated with partial coherence analysis. Neurosci Lett 287: 93-96.

Mima T, Steger J, Schulman AE, Gerloff C, Hallett M (2000b) Electroencephalographic measurement of motor cortex control of muscle activity in humans. Clin Neurophysiol 111: 326-337.

Mink JW (1996) The basal ganglia: focused selection and inhibition of competing motor programs. Prog Neurobiol 50: 381-425.

Moll L, Kuypers HGJM (1977) Premotor cortical ablations in monkeys: contralateral changes in visually guided reaching behavior. Science 198: 317-319.

Moro E, Esselink RJA, Xie J, Hommel M, Benabid AL, Pollak P (2002) The impact on Parkinson's disease of electrical parameter settings in STN stimulation. Neurology 59: 706-713.

Mulholland T (1995) Human EEG, behavioural stillness and biofeedback. Int J Psychophysiol 19: 263-279.

Nambu A, Tokuno H, Hamada I, Kita H, Imanishi M, Akazawa T, Ikeuchi Y, Hasegawa N (2000) Excitatory cortical inputs to pallidal neurons via the subthalamic nucleus in the monkey. J Neurophysiol 84: 289-300.

Neufeld MY, Blumen S, Aitkin I, Parmet Y, Korczyn AD (1994) EEG frequency analysis in demented and nondemented parkinsonian patients. Dementia 5: 23-28.

Neufeld MY, Inzelberg R, Korczyn AD (1988) EEG in demented and non-demented parkinsonian patients. Acta Neurol Scand 78: 1-5.

Neuper C, Pfurtscheller G (2001a) Event-related dynamics of cortical rhythms: frequency-specific features and functional correlates. Int J Psychophysiol 43: 41-58.

Neuper C, Pfurtscheller G (2001b) Evidence for distinct beta resonance frequencies in human EEG related to specific sensorimotor cortical areas. Clin Neurophysiol 112: 2084-2097.

Niedermeyer E (2005) The normal EEG of the waking adult. In. Electroencephalography. Basic principles, clinical applications, and related fields. 5th edition (Niedermeyer E, Lopes da Silva F, eds), pp. 167-191. Philadelphia, Pennsilvania. Lippincott Williams & Willkins.

Nini A, Feingold A, Slovin H, Bergman H (1995) Neurons in the globus pallidus do not show correlated activity in the normal monkey, but phase-locked oscillations appear in the MPTP model of parkinsonism. J Neurophysiol 74:1800-1805.

Norman GR, Streiner DL (2000a) The normal distribution. In. Biostatistics. The bare essentials. 2nd edition (Norman GR, Streiner DL, eds.), pp. 27-32. Hamilton, Ontario. B.C. Decker Inc.

Norman GR, Streiner DL (2000b) Comparing two groups. The t-test. In. Biostatistics. The bare essentials. 2nd edition (Norman GR, Streiner DL, eds.), pp. 62-67. Hamilton, Ontario. B.C. Decker Inc.

Norman GR, Streiner DL (2000c) Elements of statistical inference. In. Biostatistics. The bare essentials. 2nd edition (Norman GR, Streiner DL, eds.), pp. 42-56. Hamilton, Ontario. B.C. Decker Inc.

Norman GR, Streiner DL (2000d) Repeated measures ANOVA. In. Biostatistics. The bare essentials. 2nd edition (Norman GR, Streiner DL, eds.), pp. 94-102. Hamilton, Ontario. B.C. Decker Inc.

Norman GR, Streiner DL (2000e) More than two groups. One-way ANOVA. In. Biostatistics. The bare essentials. 2nd edition (Norman GR, Streiner DL, eds.), pp. 68-78. Hamilton, Ontario. B.C. Decker Inc.

Nutt JG, Rufener SL, Carter JH, Andreson VC, Pahwa R, Hammerstad JP, Burchiel KJ (2001) Interactions between deep brain stimulation and levodopa in Parkinson's disease. Neurology 57: 1835-1842.

Obeso JA, Rodriguez MC, DeLong MR (1997) Basal Ganglia Pathophysiology; a critical review. Adv Neurol 74: 3-18.

Obeso JA, Rodriguez-Oroz MC, Rodriguez M, Lanciego JL, Artieda J, Gonzalo N, Olanow CW (2000) Pathophysiology of the basal ganglia in Parkinson's disease. Trends Neurosci 23: S8-S19. Review.

Pantev C, Makeig S, Hoke M, Galambos R, Hamson S, Gallen C (1991) Human auditory evoked gamma-band magnetic fields. Proc Natl Acad Sci USA 88: 8996-9000.

Parent A, Hazrati L-N (1995) Functional anatomy of the basal ganglia. II. The place of subthalamic nucleus and external pallidum in basal ganglia circuitry. Brain Res Rev 20: 128-154.

Pfurtsceller G (1989) Spatiotemporal analysis of alpha frequency components with the ERD technique. Brain Topogr 2: 3-8.

Pfurtscheller G (1992) Event-related synchronisation (ERS): an electrophysiological correlate of cortical areas at rest. Electroenceph Clin Neurophysiol 83: 62-69.

Pfurtscheller G, Lopes da Silva FH (1999) Event-related EEG/MEG synchronisation and desynchronisation: basic principles. Clin Neurophysiol 110: 1842-1857.

Pfurtscheller G, Pichler-Zalaudek K, Ortmayr B, Diez J, Reisecker F (1998) Postmovement beta synchronisation in patients with Parkinson's disease. J Clin Neurophysiol 15: 243-250.

Pfurtscheller G, Stancak A Jr., Edlinger G (1997) On the existence of different types of central beta rhythms below 30 Hz. Electroenceph Clin Neurophysiol 102: 316-325.

Pfurtscheller G, Woertz M, Supp G, Lopes da Silva FH (2003) Early onset of post-movement beta electroencephalogram synchronisation in the supplementary motor area during self-paced finger movement in man. Neurosci Lett 339: 111-114.

Plaha P, Patel NK, Gill SS (2004) Stimulation of the subthalamic region for essential tremor. J Neurosurg 101: 48-54.

Priori A, Foffani G, Pesenti A, Bianchi A, Chiesa V, Baselli G, Caputo E, Tamma F, Rampini P, Egidi M, Locatelli M, Barbieri S, Scarlato G (2002) Movement-related modulation of neural activity in human basal ganglia and its L-DOPA dependency: recordings from deep brain stimulation electrodes in patients with Parkinson's disease. Neurol Sci 23: S101-S102.

Priori A, Foffani G, Pesenti A, Tamma F, Bianchi A, Pellegrini M, Locatelli M, Moxon KA, Villani RM (2004) Rhythm-specific pharmacological modulation of subthalamic activity in Parkinson's disease. Exp Neurol 189: 369-379.

Raz A, Feingold A, Zelanskaya V, Vaadia E, Bergman H (1996) Neuronal synchronisation of tonically active neurons in the striatum of normal and parkinsonian primates. J Neurophysiol 76:2083-2088.

Raz A, Vaadia E, Bergman H (2000) Firing patterns and correlations of spontaneous discharge of pallidal neurons in the normal and the tremulous 1-methyl-4-phenyl-1,2,3,6-tetrahydropyridine vervet model of parkinsonism. J Neurosci 20:8559-8571.

Raz A, Frechter-Mazar V, Feingold A, Abeles M, Vaadia E, Bergman H (2001) Activity of pallidal and striatal tonically active neurons is correlated in MPTP-treated monkeys but not in normal monkeys. J Neurosci 21:RC128.

Reilly EL (2005) EEG recordings and operation of apparatus. In. Electroencephalography. Basic principles, clinical applications, and related fields. 5th edition (Niedermeyer E, Lopes da Silva F, eds), pp. 139-159. Philadelphia, Pennsilvania. Lippincott Williams & Willkins.

Rinne UK, Bracco F, Chouza C, Dupont E, Gershanik O, Marti Masso JF, Montastruc JL, Marsden CD, Dubini A, Orlando N, Grimaldi R (1997) Cabergoline in the treatment of early Parkinson's disease: results of the first year of treatment in a double-blind comparison of cabergoline and levodopa. The PKDS009 Collaborative Study Group. Neurology 48: 363-368.

Rizzone M, Lanotte M, Bergamasco B, Tavella A, Torre E, Faccani G, Melcarne A, Lopiano L (2001) Deep brain stimulation of the subthalamic nucleus in Parkinson's disease: effects of variation in stimulation parameters. J Neurol Neurosurg Psychiatry 71: 215-219.

Roland PE, Larsen B, Lassen NA, Skinhøj E (1980) Supplementary motor area and other cortical areas in organization of voluntary movement in man. J of Neurophysiol 43: 118-136.

Rothwell JC (2003) Diseases and treatments: Parkinson's disease In. Movement Disorders. Handbook of Clinical Neurophysiology (Hallett M, ed.), pp.417-435. Amsterdam, the Netherlands: Elsevier B.V.

Rosenberg JR, Amjad AM, Breeze P, Brillinger DR, Halliday DM (1989) The Fourier approach to the identification of functional coupling between neuronal spike trains. Prog Biophys Mol Biol 53: 1-31.

Rosenberg JR, Halliday DM, Breeze P, and Conway BA (1998) Identification of patterns of neuronal activity; partial spectra, partial coherence, and neuronal interactions. J Neurosci Methods 83: 57-72.

Ruskin DN, Bergstrom DA, Walters JR (1999) Multisecond oscillations in firing rate in the basal ganglia: robust modulation by dopamine receptor activation and anesthesia. J Neurophysiol 81: 2046-2055.

Ruskin DN, Bergstrom DA, Tierney PL, Walters JR (2003) Correlated multisecond oscillations in firing rate in the basal ganglia: Modulation by dopamine and the subthalamic nucleus. Neuroscience 117: 427-438.

Saint-Cyr JA, Hoque T, Pereira LC, Dostrovsky JO, Hutchison WD, Milkulis DJ, Abosch A, Sime E, Lang AE, Lozano AM (2002) Localisation of clinically effective stimulating electrodes in the human subthalamic nucleus on magnetic resonance imaging. J Neurosurg 97:1152-1166.

Salenius S, Avikainen S, Kaakkola S, Hari R, Brown P (2002) Defective cortical drive to muscle in Parkinson's disease and its improvement with levodopa. Brain 125: 491-500.

Salenius S, Salmelin R, Neuper C, Pfurtscheller G, Hari R (1996) Human cortical 40 Hz rhythm is closely related to EMG rhythmicity. Neurosci Lett 213: 75-78.

Samuel M, Ceballos-Baumann AO, Blin J, Uema T, Boecker H, Passingham RE, Brooks DJ (1997) Evidence for lateral premotor and parietal overactivity in Parkinson's disease during sequential and bimanual movements. A PET study. Brain 120: 963-76.

Samthein J, Morel A, von Stein A, Jeanmonod D (2003) Thalamic theta field potentials and EEG: high thalamocortical coherence in patients with neurogenic pain, epilepsy and movement disorders. Thalamus and related systems 2: 231-238.

Sharott A, Magill PJ, Harnack D, Kupsch A, Meissner W, Brown P (2005) Dopamine depletion increases the power and coherence of β-oscillations in the cerebral cortex and subthalamic nucleus of the awake rat. Eur J Neurosci 21: 1413-1422.

Shimohama S, Sawada H, Kitamura Y, Taniguchi T (2003) Disease model: Parkinson's disease. Trends Mol Med 9: 360-365.

Silberstein P, Kühn AA, Kupsch A, Trottenberg T, Krauss J, Wöhrle JC, Mazzone P, Insola A, Di Lazzaro V, Oliviero A, Aziz T, Brown P (2003) There is a difference in patterning of globus pallidus local field potentials between PD and dystonia. Brain 126, 2597-2608.

Silberstein P, Oliviero A, Di Lazzaro V, Insola A, Mazzone P, Brown P (2005) Oscillatory pallidal local field potential activity inversely correlates with limb dyskinesias in Parkinson's disease. Exp Neurol 194: 523-529.

Singer W (1993) Synchronisation of cortical activity and its putative role in information processing and learning. Annu Rev Physiol 55: 349-374.

Sochurkova D, Rektor I (2003) Event-related desynchronisation/synchronisation in the putamen. An SEEG case study. Exp Brain Res 149: 401-404.

Soikkeli R, Partanen J, Soininen H, Paakkonen A, Riekkinen Sr. P (1991) Slowing of EEG in Parkinson's disease. Electroencephalogr Clin Neurophysiol 79: 159-165.

Spauschus A, Marsden J, Halliday DM, Rosenberg JR, and Brown P (1999) The origin of ocular microtremor in man. Exp Brain Res 126: 556-562.

Spehlman R (ed.) (1981a) The source of the EEG. In: EEG Primer, pp.7-19. Amsterdam: Elsevier/North-Holland Biomedical Press.

Spehlman R (ed.) (1981b) Recording strategy. In: EEG Primer, pp.63-81. Amsterdam: Elsevier/North-Holland Biomedical Press.

Spehlman R (ed.) (1981c) Localized and lateralized changes of amplitude: asymmetries. In: EEG Primer, pp.406-408. Amsterdam: Elsevier/North-Holland Biomedical Press.

Starr PA, Vitek JL, Bakay RAE (1998) Ablative surgery and deep brain stimulation for Parkinson's disease. Neurosurgery 43: 989-1015.

Steiner H, Kitai ST (2001) Unilateral striatal dopamine depletion: time-dependent effects on cortical function and behavioural correlates. Eur J Neurosci 14: 1390-1404.

Steriade M (2005) Cellular substrates of brain rhythms In. Electroencephalography. Basic principles, clinical applications, and related fields. 5th edition (Niedermeyer E, Lopes da Silva F, eds), pp. 31-83. Philadelphia, Pennsilvania. Lippincott Williams & Willkins.

Steriade M, Gloor P, Llinás RR. Lopes da Silva FH, Mesulam M-M (1990) Basic mechanisms of cerebral rhythmic activities. Electroenceph Clin Neurophysiol 1990; 76: 481-508.

Steriade M, McCormick DA, Senjowski TJ (1993) Thalamocortical oscillations in the sleeping and aroused brain. Science 262: 679-685.

Taha JM, Favre J, Baumann TK, Burchiel KJ (1997) Tremor control after pallidotomy in patients with Parkinson's disease: correlation with microrecording findings. J Neurosurg 86: 642-647.

Tallon-Baudry C, Bertrand O (1999) Oscillatory gamma activity in humans and its role in object representation. Trends Cogn Sci 3: 151-162.

Temperli P, Ghika J, Villemure J-G, Burkhard PR, Bogousslavsky J, Vingerhoets FJG (2003) How do parkinsonian signs return after discontinuation of subthalamic DBS? Neurology 60: 78-81.

The deep-brain stimulation for Parkinson's disease study group (2001) Deep-brain stimulation of the subthalamic nucleus or the pars interna of the globus pallidus in Parkinson's disease. N Engl J Med 345: 956-963.

Timmermann L, Gross J, Dirks M, Volkmann J, Freund-Hans J, Schnitzler A (2003) The cerebral oscillatory network of parkinsonian resting tremor. Brain 126 : 199-212.

Timmermann L, Wojtecki L, Gross J, Lehrke R, Voges J, Maarouf M, Treuer H, Sturm V, Schnitzler A (2004) Ten-Hertz stimulation of subthalamic nucleus deteriorates motor symptoms in Parkinson's disease. Mov Disord 19: 1328-1333.

Verheul MH, Geuze RH (2004) Inter-limb coupling in bimanual rhythmic coordination in Parkinson's disease. Hum Mov Sci 23: 503-525.

Vitek JL and Giroux M (2000) Physiology of hypokinetic and hyperkinetic movement disorders: model for dyskinesia. Ann Neurol 47 (Suppl 1): S131-S140.

Voges J, Volkman J, Allert N, Lehrke R, Koulousakis A, Freund HJ, Sturm V (2002) Bilateral high-frequency stimulation in the subthalamic nucleus for treatment of Parkinson disease: correlation of therapeutic effect with anatomical electrode position. J Neurosurg 96: 269-279.

Volkmann J, Joliot M, Mogilner A, Ioannides AA, Lado F, Fazzini E, Ribary U, Llinas R (1996) Central motor loop oscillations in Parkinsonian resting tremor revealed by magnetoencephalography. Neurology 46: 1359-1370.

von der Malsburg C (1995) Binding in models of perception and brain function. Curr Opin Neurobiol 5: 520-526.

Vorobyov VV, Schibaev NV, Morelli M, Carta AR (2003) EEG modifications in the cortex and striatum after dopaminergic priming in the 6-hydroxydopamine rat model of Parkinson's disease. Brain Res 972: 177-185.

Wang H-C, Lees AJ, Brown P (1999) Impairement of EEG desynchronisation before and during movement and its relation to bradykinesia in Parkinson's disease. J Neurol Neurosurg Psychiatry 66: 442-446.

Wennberg RA, Pohlmann-Eden B, Chen R, Lozano A (2002) Combined scalp-thalamic recording in sleep and epilepsy. Clin Neurophysiol 113: 1867-1871.

Wennberg RA and Lozano AM (2003) Intracranial volume conduction of cortical spikes and sleep potentials recorded with deep brain stimulating electrodes. Clin Neurophysiol 114: 1403-1418.

Wichmann T, Bergman H, DeLong MR (1994a) The primate subthalamic nucleus. I. Functional properties in intact animals. J Neurophysiol 72: 494-506.

Wichmann T, Bergman H, and DeLong MR. The primate subthalamic nucleus (1994b) III. Changes in motor behavior and neuronal activity in the internal pallidum induced by subthalamic inactivation in the MPTP model of parkinsonism. J Neurophysiol 72: 521-530.

Wichmann T, DeLong MR (1996) Functional and pathophysiological models of the basal ganglia. Curr Opin Neurobiol 6: 751-758.

Williams D, Kühn A, Kupsch A, Tijssen M, van Bruggen G, Speelman H, Hotton G, Yarrow K, Brown P (2003) Behavioural cues are associated with modulations of synchronous oscillations in the human subthalamic nucleus. Brain 126: 1975-1985.

Williams D, Tijssen M, van Bruggen G, Bosch A, Insola A, Di Lazzaro V, Mazzone P, Oliviero A, Quartarone A, Speelman H, Brown P (2002) Dopamine-dependent changes in the functional connectivity between basal ganglia and cerebral cortex in humans. Brain 125: 1558-1569.

Yelnik J, Percheron G, Francois C (1984) A golgi analysis of the primate globus pallidus. II. Quantitative morpjology and spatial orientation of dendritic arborizations. J Comp Neurol 227: 200-213.

Yurek DM, Randall PK (1991) Striatal depth EEG reveals postsynaptic activity of striatal neurons following dopamine receptor stimulation and blockade. J Neurosci Methods 37: 81-91.